Westinghouse Non-Proprietary Class 3

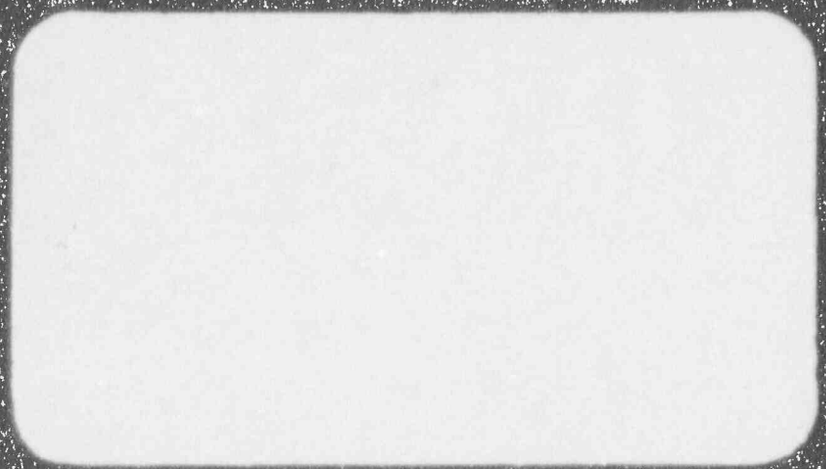

Westinghouse Energy Systems

Westinghouse Non-Proprietary Class 3

Westinghouse Energy Systems

WCAP-14315

ANALYSIS OF CAPSULE U FROM THE TEXAS UTILITIES ELECTRIC COMPANY COMANCHE PEAK STEAM ELECTRIC STATION UNIT NO. 2 REACTOR VESSEL RADIATION SURVEILLANCE PROGRAM

R. Auerswald
J. M. Lynde
J. F. Williams

July 1995

Work Performed Under Shop Order WFTP-106

Prepared by Westinghouse Electric Corporation
for the Texas Utilities Electric Company

Approved by: B A Bishop for
R. D. Rishel, Manager
Metallurgical & NDE Analysis

WESTINGHOUSE ELECTRIC CORPORATION
Nuclear Technology Division
P.O. Box 355
Pittsburgh, Pennsylvania 15230-0355

PREFACE

This report has been technically reviewed and verified.

	Reviewer:	
Sections 1 through 5, 7, 8 and Appendix A	P. A. Peter	P. A. Peter
Section 6	S. L. Anderson	S. L. Anderson

TABLE OF CONTENTS

LIST OF TABLES

LIST OF TABLES (CONTINUED)

LIST OF TABLES (CONTINUED)

LIST OF ILLUSTRATIONS

LIST OF ILLUSTRATIONS (CONTINUED)

SECTION 1.0
SUMMARY OF RESULTS

The analysis of the reactor vessel materials contained in surveillance capsule U, the first capsule to be removed from the Texas Utilities Electric Company (TU Electric) Comanche Peak Steam Electric Station (CPSES) Unit No. 2 reactor pressure vessel, led to the following conclusions:

- The capsule received an average fast neutron fluence (E > 1.0 MeV) of 3.28×10^{18} n/cm^2 after 0.904 effective full power years (EFPY) of plant operation.

- Irradiation of the reactor vessel intermediate shell plate R3807-2 Charpy specimen, oriented with the longitudinal axis of the specimen parallel to the major rolling direction of the plate (longitudinal orientation), to 3.28×10^{18} n/cm^2 (E > 1.0 MeV) resulted in a 30 ft-lb transition temperature shift of 0°F and a 50 ft-lb transition temperature shift of 0°F. This results in an irradiated 30 ft-lb transition temperature of -5°F and an irradiated 50 ft-lb transition temperature of 35°F for the longitudinally-oriented specimens.

- Irradiation of the reactor vessel intermediate shell plate R3807-2 Charpy specimen, oriented with the longitudinal axis of the specimen normal to the major rolling direction of the plate (transverse orientation), to 3.28×10^{18} n/cm^2 (E > 1.0 MeV) resulted in a 30 ft-lb transition temperature increase of 25°F and a 50 ft-lb transition temperature increase of 20°F. This results in an irradiated 30 ft-lb transition temperature of 15°F and an irradiated 50 ft-lb transition temperature of 75°F for transversely-oriented specimens.

- Irradiation of the weld metal Charpy specimens to 3.28×10^{18} n/cm^2 (E > 1.0 MeV) resulted in a 30 ft-lb transition temperature shift of 0°F and a 50 ft-lb transition temperature shift of 0°F. This results in an irradiated 30 ft-lb transition temperature of -45°F and an irradiated 50 ft-lb transition temperature of 5°F.

- Irradiation of the weld Heat-Affected-Zone (HAZ) metal Charpy specimens to 3.28×10^{18} n/cm^2 (E > 1.0 MeV) resulted in a 30 ft-lb transition temperature shift of 0°F and a 50 ft-lb transition temperature shift of 0°F. This results in an irradiated 30 ft-lb transition temperature of -105°F and an irradiated 50 ft-lb transition temperature of -50°F.

- The average upper shelf energy of the intermediate shell plate R3807-2 (longitudinal orientation) resulted in an average energy *increase* of 3 ft-lb after irradiation to 3.28 x 10^{18} n/cm^2 (E > 1.0 MeV). This results in an irradiated average upper shelf energy of 118 ft-lb for the longitudinally oriented specimen. (Since neutron irradiation is expected to decrease the upper shelf energy, this does not represent a measurable change.)

- The average upper shelf energy of the intermediate shell plate R3807-2 (transverse orientation) resulted in an average energy *increase* of 4 ft-lb after irradiation to 3.28 x 10^{18} n/cm^2 (E > 1.0 MeV). This results in an irradiated average upper shelf energy of 88 ft-lb for the transversely-oriented specimens. (Since neutron irradiation is expected to decrease the upper shelf energy, this does not represent a measurable change.)

- The average upper shelf energy of the weld metal Charpy specimens resulted in an average energy decrease of 9 ft-lb after irradiation to 3.28 x 10^{18} n/cm^2 (E > 1.0 MeV). This results in an irradiated average upper shelf energy of 85 ft-lb for the weld metal specimens.

- The average upper shelf energy of the weld HAZ metal resulted in an average energy *increase* of 11 ft-lb after irradiation to 3.28 x 10^{18} n/cm^2 (E > 1.0 MeV). This results in an irradiated average upper shelf energy of 127 ft-lb for the weld HAZ metal. (Since neutron irradiation is expected to decrease the upper shelf energy, this does not represent a measurable change.)

- A comparison of the CPSES Unit No. 2 Surveillance Capsule U test results with the Regulatory Guide 1.99, Revision 2[1], predictions led to the following conclusions:

  - All measured 30 ft-lb transition temperature shift values are less than the Regulatory Guide 1.99, Revision 2, predictions (Table 5-10).

  - All surveillance capsule material measured upper shelf energy decreases are less than the Regulatory Guide 1.99, Revision 2, predictions (Table 5-10).

- All beltline materials exhibit a more than adequate upper shelf energy level for continued safe plant operation and are expected to maintain an upper shelf energy of no less than 50 ft-lb throughout the life of the vessel (32 EFPY) as required by 10 CFR 50, Appendix G[2].

- The calculated end-of-life (32 EFPY) maximum neutron fluence (E > 1.0 MeV) for the CPSES Unit No. 2 reactor vessel is as follows:

  Vessel inner radius* = 2.836×10^{19} n/cm^2

  Vessel 1/4 thickness = 1.512×10^{19} n/cm^2

  Vessel 3/4 thickness = 3.063×10^{18} n/cm^2

  * Clad/base metal interface

SECTION 2.0
INTRODUCTION

This report presents the results of the examination of Capsule U, the first capsule to be removed from the reactor in the continuing surveillance program which monitors the effects of neutron irradiation on the TU Electric CPSES Unit No. 2 reactor pressure vessel materials under actual operating conditions.

The surveillance program for CPSES Unit No. 2 was designed and recommended by the Westinghouse Electric Corporation. A description of the surveillance program and the preirradiation mechanical properties of the reactor vessel materials is presented in WCAP-10684, "Texas Utilities Generating Company Comanche Peak Unit No. 2 Reactor Vessel Radiation Surveillance Program"[3]. The surveillance program was planned to cover the 40-year design life of the reactor pressure vessel and was based on ASTM E185-82, "Standard Practice for Conducting Surveillance Tests for Light-Water Cooled Nuclear Power Reactor Vessels." Capsule U was removed from the reactor after 0.904 EFPY of exposure and shipped to the Westinghouse Science and Technology Center Hot Cell Facility, where the postirradiation mechanical testing of the Charpy V-notch impact and tensile surveillance specimens was performed.

This report summarizes the testing of and the postirradiation data obtained from surveillance capsule U removed from the TU Electric CPSES Unit No. 2 reactor vessel and discusses the analysis of the data.

SECTION 3.0
BACKGROUND

The ability of the large steel pressure vessel containing the reactor core and its primary coolant to resist fracture constitutes an important factor in ensuring safety in the nuclear industry. The beltline region of the reactor pressure vessel is the most critical region of the vessel because it is subjected to significant fast neutron bombardment. The overall effects of fast neutron irradiation on the mechanical properties of low alloy, ferritic pressure vessel steels such as A533 Grade B Class 1 (base material of the CPSES Unit No. 2 reactor pressure vessel beltline) are well documented in the literature. Generally, low alloy ferritic materials show an increase in hardness and tensile properties and a decrease in ductility and toughness during high-energy irradiation.

A method for performing analyses to guard against fast fracture in reactor pressure vessels has been presented in "Protection Against Nonductile Failure," Appendix G to Section III of the ASME Boiler and Pressure Vessel Code[4]. The method uses fracture mechanics concepts and is based on the reference nil-ductility transition temperature (RT_{NDT}).

RT_{NDT} is defined as the greater of either the drop weight nil-ductility transition temperature (NDTT per ASTM E-208[5]) or the temperature 60°F less than the 50 ft-lb (and 35-mil lateral expansion) temperature as determined from Charpy specimens oriented normal (transverse) to the major working direction of the plate or forging. The RT_{NDT} of a given material is used to index that material to a reference stress intensity factor curve (K_{IR} curve) which appears in Appendix G to the ASME Code[4]. The K_{IR} curve is a lower bound of dynamic, crack arrest, and static fracture toughness results obtained from several heats of pressure vessel steel. When a given material is indexed to the K_{IR} curve, allowable stress intensity factors can be obtained for this material as a function of temperature. Allowable operating limits can then be determined using these allowable stress intensity factors.

RT_{NDT} and, in turn, the operating limits of nuclear power plants can be adjusted to account for the effects of radiation on the reactor vessel material properties. The changes in mechanical properties of a given reactor pressure vessel steel, due to irradiation, can be monitored by a reactor surveillance program, such as the CPSES Unit No. 2 reactor vessel radiation surveillance program[3], in which a surveillance capsule is periodically removed from the operating nuclear reactor and the encapsulated specimens tested. The increase in the average Charpy V-notch 30 ft-lb temperature (ΔRT_{NDT}) due to irradiation is added to the initial RT_{NDT} to adjust the RT_{NDT} (ART) for radiation embrittlement. This ART (initial RT_{NDT} + ΔRT_{NDT}) is used to index the material to the K_{IR} curve and, in turn, to set

operating limits for the nuclear power plant which take into account the effects of irradiation on the reactor vessel materials.

SECTION 4.0
DESCRIPTION OF PROGRAM

Six surveillance capsules for monitoring the effects of neutron exposure on the CPSES Unit 2 reactor pressure vessel core region (beltline) materials were inserted in the reactor vessel prior to initial plant start-up. The six capsules were positioned in the reactor vessel between the thermal shield and the vessel wall as shown in Figure 4-1. The vertical center of the capsules is opposite the vertical center of the core. The capsules contain specimens made from the intermediate shell plate R3807-2 and weld metal fabricated with 3/16-inch Mil B-4 weld filler wire (heat number 89833, Linde 124 flux, and lot number 1061) which is identical to that used in the actual fabrication of the intermediate to lower shell girth weld seam of the reactor pressure vessel.

Capsule U was removed after 0.904 effective full power years (EFPY) of plant operation. This capsule contained Charpy V-notch, tensile and compact fracture mechanics specimens made from intermediate shell plate R3807-2 and submerged arc weld metal identical to the closing girth weld seam. In addition, this capsule contained Charpy V-notch specimens from the weld Heat-Affected-Zone (HAZ) of plate R3807-2.

Test material obtained from the intermediate shell plate (after the thermal heat treatment and forming of the plate) was taken at least one plate thickness from the quenched ends of the plate. All test specimens were machined from the 1/4 and 3/4-thickness location of the plate after performing a simulated postweld, stress-relieving treatment on the test material and also from weld and heat-affected-zone metal of a stress-relieved weldment joining intermediate shell plate R3807-2 and adjacent lower shell plate R3816-2. All heat-affected-zone specimens were obtained from the weld heat-affected-zone of lower shell plate R3807-2.

Charpy V-notch impact specimens corresponding to ASTM 370 Type A were machined from intermediate shell plate R3807-2 in both the longitudinal orientation (longitudinal axis of specimen parallel to major rolling direction) and transverse orientation (longitudinal axis of specimen normal to major rolling direction). The core region weld Charpy impact specimens were machined from the weldment such that the long dimension of the Charpy specimen was normal to the weld direction. The notch was machined such that the direction of crack propagation in the specimen was in the welding direction.

The chemical composition and heat treatment of the surveillance material is presented in Tables 4-1 through 4-4. The data in Tables 4-1 through 4-4 was obtained from Appendix A of the unirradiated surveillance program, WCAP-10684[3].

Capsule U contained dosimeter wires of pure copper, iron, nickel, and aluminum-0.15 weight percent cobalt (cadmium-shielded and unshielded). In addition, cadmium-shielded dosimeters of neptunium (Np^{237}) and uranium (U^{238}) were placed in the capsule to measure the integrated flux at specific neutron energy levels.

The capsule contained thermal monitors made from two low-melting-point eutectic alloys and sealed in Pyrex tubes. These thermal monitors were used to define the maximum temperature attained by the test specimens during irradiation. The composition of the two eutectic alloys and their melting points are as follows:

2.5% Ag, 97.5% Pb	Melting Point: 579°F (304°C)
1.5% Ag, 1.0% Sn, 97.5% Pb	Melting Point: 590°F (310°C)

The arrangement of the various mechanical specimens, dosimeters and thermal monitors contained in Capsule U is shown in Figure 4-2.

TABLE 4-1				
Chemical Composition (wt%) of the CPSES Unit No. 2 Reactor Vessel Intermediate Shell Plate[3]				
Element	Intermediate Shell Plate R3807-1[a]	Intermediate Shell Plate R3807-2[a,b]	Intermediate Shell Plate R3807-2[a,b,c]	Intermediate Shell Plate R3807-3[a]
C	.21	.22	.22	.22
Mn	1.42	1.40	1.36	1.30
P	.006	.007	.014	.007
S	.015	.016	.014	.009
Si	.25	.24	.25	.19
Ni	.64	.64	.62	.60
Mo	.60	.59	.58	.58
Cr	.05	.04	.06	.06
Cu	.06	.06	.065	.05
Al	.020	.025	.018	.023
Co	.012	.013	.014	.009
Pb	< .001	< .001	.002	< .001
W	< .01	< .01	< .01	< .01
Ti	< .01	< .01	.004	< .01
Zr	< .001	< .001	< .002	< .001
V	.002	.003	< .002	.002
Sn	.003	.004	.002	.003
As	.004	.005	.004	.005
Cb	< .01	< .01	< .002	< .01
N_2	.009	.010	.008	.007
B	< .001	< .001	< .001	< .001

NOTES:

a. Chemical Analysis by Combustion Engineering, Inc.

b. Surveillance program test plate.

c. Chemical Analysis by Westinghouse.

TABLE 4-2

Chemical Composition (wt%) of the CPSES Unit No. 2 Reactor Vessel Lower Shell Plate[a]

Element	Lower Shell Plate R3816-1	Lower Shell Plate R3816-2	Lower Shell Plate R3816-3
C	.23	.23	.22
Mn	1.48	.148	1.50
P	.001	.002	.008
S	.004	.012	.008
Si	.19	.21	.19
Ni	.59	.65	.63
Mo	.49	.50	.52
Cr	.03	.03	.04
Cu	.05	.03	.04
Al	.026	.026	.018
Co	.02	.012	.012
Pb	< .001	< .001	< .001
W	< .01	< .01	< .01
Ti	< .01	< .01	< .01
Zr	< .001	< .001	< .001
V	.003	.003	.003
Sn	.001	.001	.002
As	.009	.011	.015
Cb	< .01	< .01	< .01
N_2	.028	.014	.014
B	< .001	< .001	< .001

NOTE:

a. Chemical Analysis by Combustion Engineering, Inc.

TABLE 4-3

Chemical Composition (wt%) of the CPSES Unit No. 2 Reactor Vessel Weld Metal

Element	Intermediate and Lower Shell Longitudinal Weld Seams		Closing Girth Weld Seam	Surveillance Weldment (Identical to the Closing Girth Seam Weld)[c]
	Wire Flux Test Weld Sample[a]	Sample Production Weld[a][b] Seam No. 101-142A	Wire Flux Test Weld Sample[a]	
C	.16	.16	.088	.11
Mn	1.32	1.24	1.33	1.37
P	.005	.004	.004	.011
S	.011	.009	.010	.014
Si	.16	.19	.51	.49
Ni	.05	.08	.03	.072
Mo	.54	.59	.54	.59
Cr	.02	.02	.03	.058
Cu	.07	.05	.05	.030
Al	--	.004	--	.006
Co	--	.011	--	.008
Pb	--	< .001	--	.001
W	--	.01	--	< .01
Ti	--	< .01	--	.002
Zr	--	.001	--	< .002
V	.004	.005	.003	< .002
Sn	--	.003	--	.003
As	--	.021	--	.018
Cb	--	< .01	--	< .002
N_2	--	.007	--	.008
B	--	.001	--	.001

NOTES:

a. Chemical Analyses by Combustion Engineering, Inc.

b. Actual Beltline production weld chemistry (Lower Shell plate Seam No. 101-142A).

c. Chemical Analysis by Westinghouse of the Surveillance Program Test Weldment (Test Plate "D") supplied by Combustion Engineering, Inc. (Analysis results contain an error band of +/- 10%. Standards are traceable to the National Institute of Standards & Technology and are run with each group of samples.)

TABLE 4-4

Heat Treatment of the CPSES Unit No. 2 Reactor Vessel Beltline Region Surveillance Material

Material	Temperature (°F)	Time[a] (hr)	Cooling
Intermediate Shell Plates R3807-1 and R3807-2 R3807-3	Austenitizing: 1600 ± 25 (871°C)	4	Water-quenched
	Tempered: 1225 ± 25 (663°C)	4	Air-cooled
	Stress Relief: 1150 ± 50 (621°C)	19.25[b]	Furnace-cooled
Lower Shell Plates R3816-1 and R3816-2 R3816-3	Austenitizing: 1600 ± 25 (871°C)	4	Water-Quenched
	Tempered: 1225 ± 25 (663°C)	4	Air-Cooled
	Stress Relief: 1150 ± 50 (621°C)	14.5[b]	Furnace-Cooled
Intermediate Shell Longitudinal Seam Welds	Stress Relief: 1150 ± 50 (621°C)	19.25[b]	Furnace-cooled
Lower Shell Longitudinal Seam Welds		14.5[b]	Furnace-cooled
Intermediate to Lower Shell Girth Seam Weld	Local Stress Relief: 1150 ± 50 (621°C)	8.0	Furnace-cooled
Surveillance Program Test Material			
Surveillance Program Weldment Test Plate "D" (Representative of closing Girth Seam)	Post Weld Stress Relief: 1150 ± 50 (621°C)	8.5[c]	Furnace-cooled

NOTES:

a. Lukens Steel Company, Marrel Freres and Combustion Engineering, Inc. Certification Reports.

b. Stress Relief includes the Intermediate to Lower Shell Closing Girth Seam Post Weld Heat Treatment.

c. The Stress Relief Heat Treatment received by the Surveillance Test Weldment has been simulated.

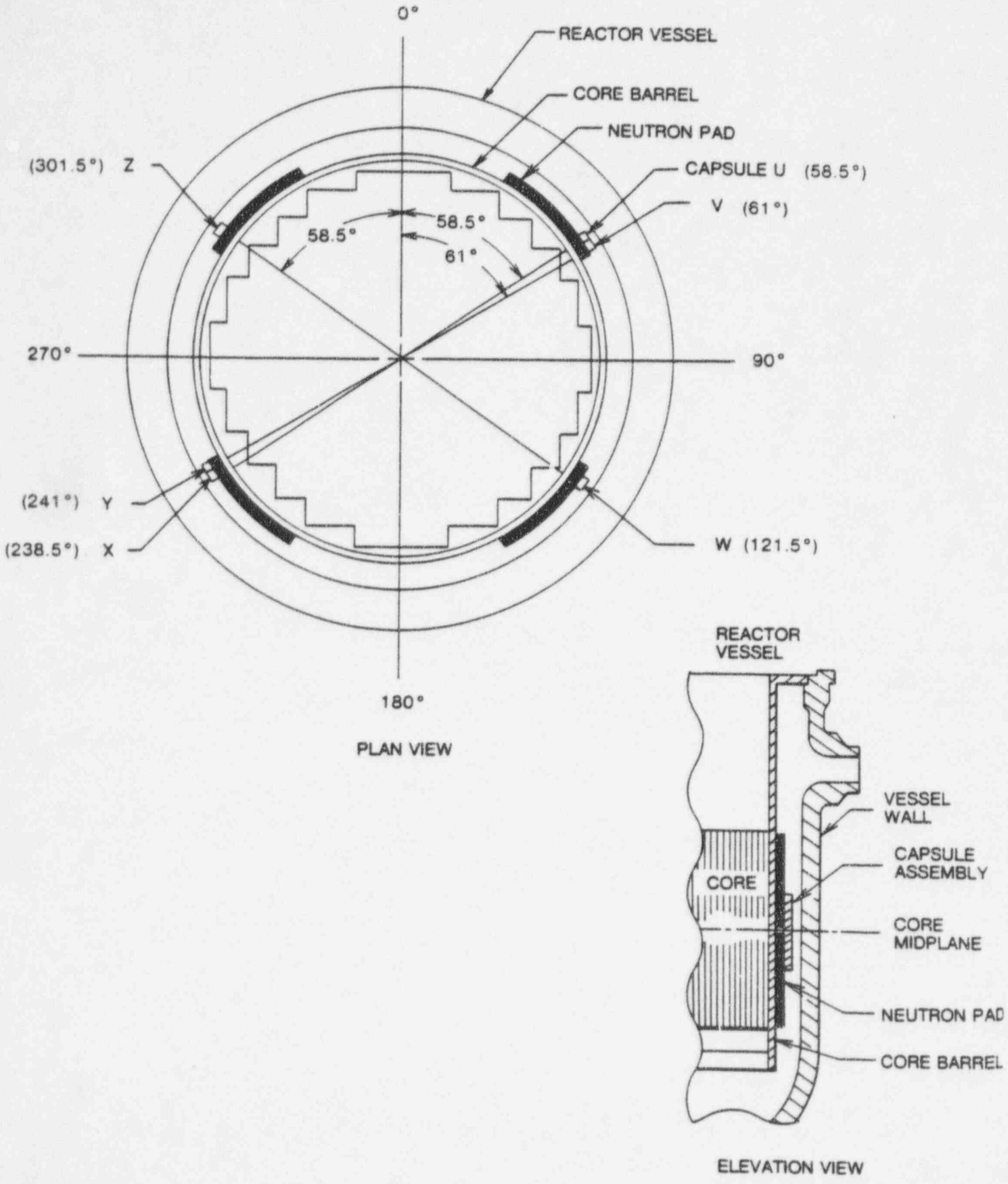

Figure 4-1 Arrangement of Surveillance Capsules in the CPSES Unit No. 2 Reactor Vessel

LEGEND: CL - INTERMEDIATE SHELL PLATE R3807-2 (LONGITUDINAL)
CT - INTERMEDIATE SHELL PLATE R3807-2 (TRANSVERSE)
CW - WELD METAL
CH - HEAT-AFFECTED-ZONE MATERIAL

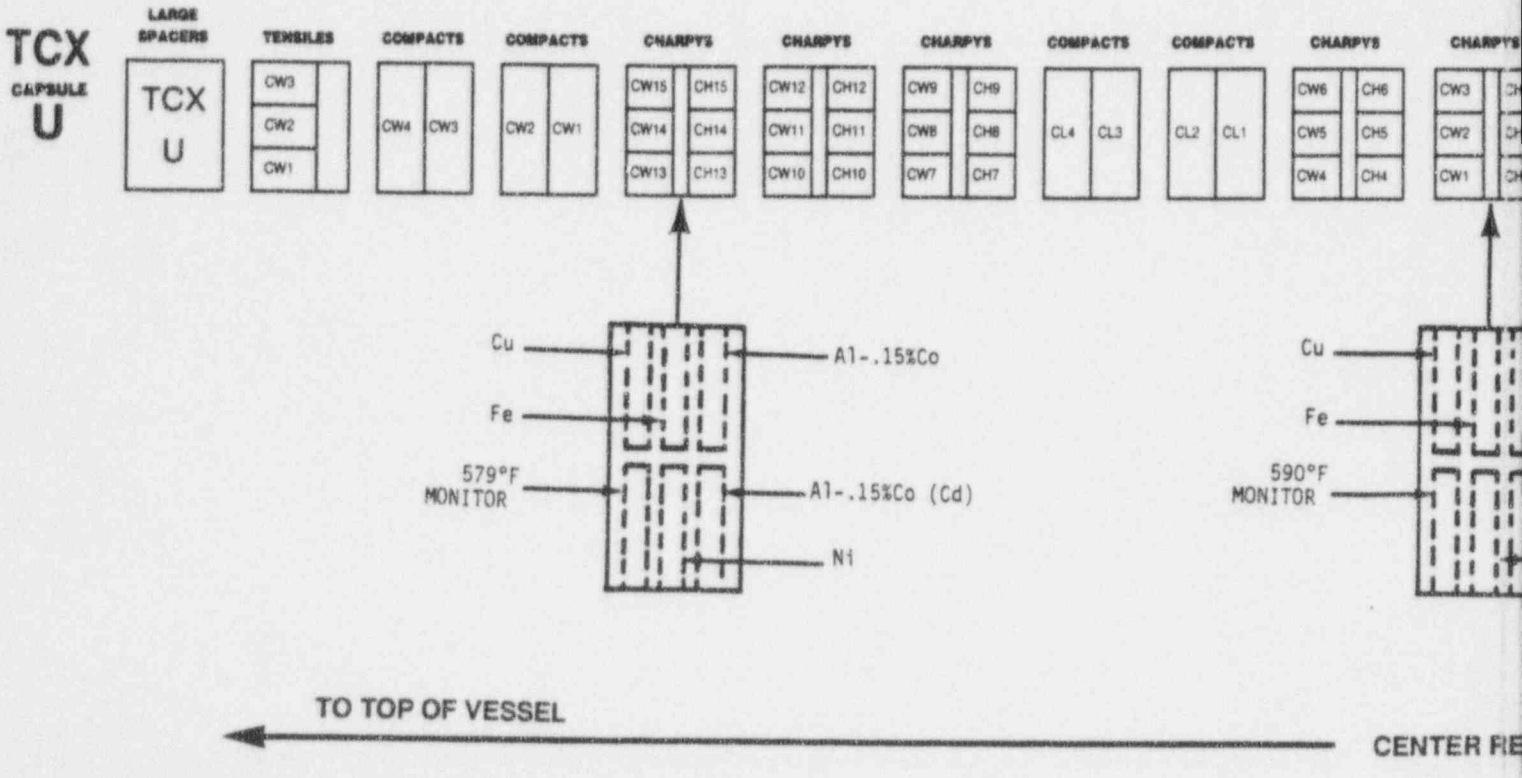

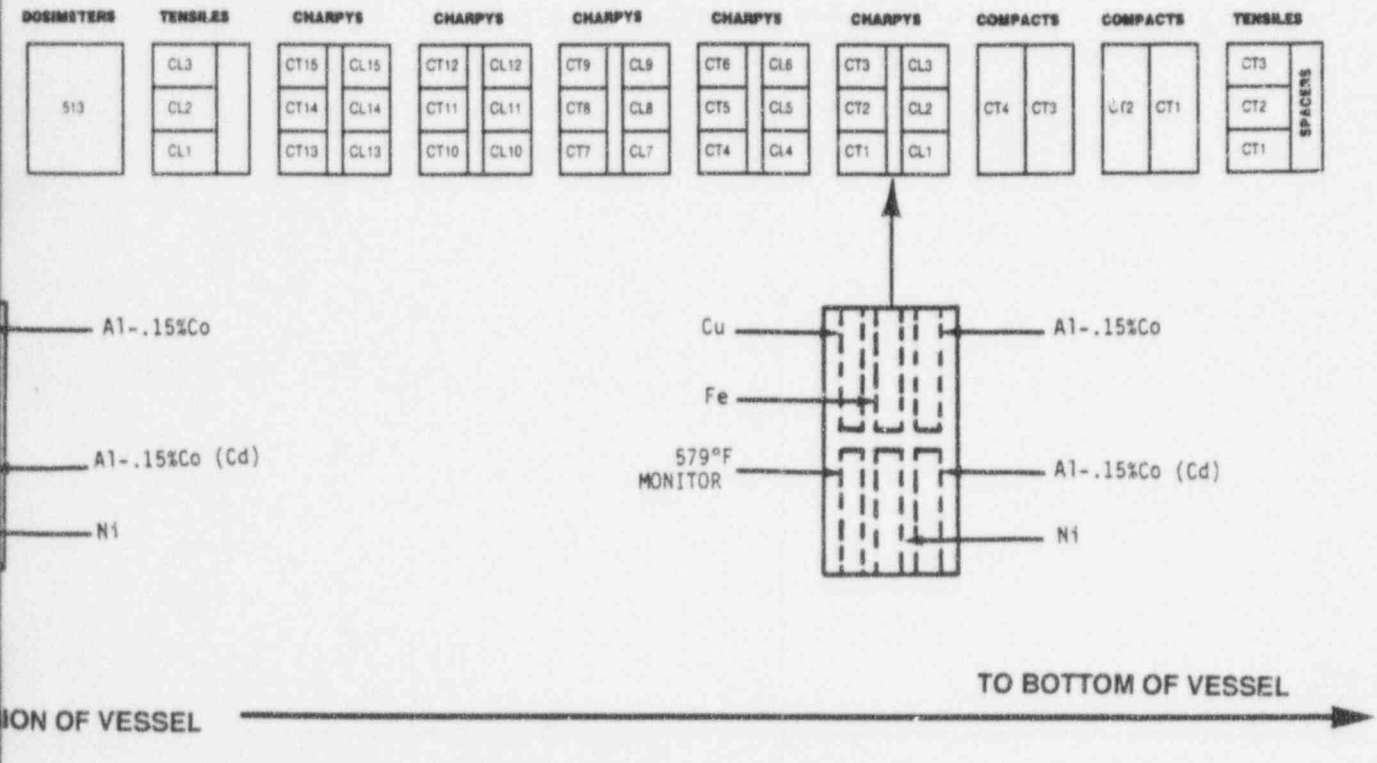

Figure 4-2 Capsule U Diagram Showing the Location of Specimens, Thermal Monitors, and Dosimeters

SECTION 5.0
TESTING OF SPECIMENS FROM CAPSULE U

5.1 Overview

The post-irradiation mechanical testing of the Charpy V-notch impact specimens and tensile specimens was performed in the Remote Metallographic Facility at the Westinghouse Science and Technology Center. Testing was performed in accordance with 10 CFR 50, Appendix H[6], ASTM Specification E185-82[7] and Westinghouse Procedure MHL 8402, Revision 2 as modified by Westinghouse RMF Procedure 8102, Revision 1, and 8103, Revision 1.

Upon receipt of the capsule at the hot cell laboratory, the specimens and spacer blocks were carefully removed, inspected for identification number, and checked against the master list in WCAP-10684[3]. No discrepancies were found.

Examination of the two low-melting point 579°F (304°C) and 590°F (310°C) eutectic alloys indicated no melting of either type of thermal monitor. Based on this examination, the maximum temperature to which the test specimens were exposed was less than 579°F (304°C).

The Charpy impact tests were performed per ASTM Specification E23-93a[8] and RMF Procedure 8103, Revision 1, on a Tinius-Olsen Model 74, 358J machine. The tup (striker) of the Charpy impact test machine is instrumented with a GRC 830-I instrumentation system, feeding information into an IBM compatible 486 computer. With this system, load-time and energy-time signals can be recorded in addition to the standard measurement of Charpy energy (E_D). From the load-time curve (Appendix A), the load of general yielding (P_{GY}), the time to general yielding (t_{GY}), the maximum load (P_M), and the time to maximum load (t_M) can be determined. Under some test conditions, a sharp drop in load indicative of fast fracture was observed. The load at which fast fracture was initiated is identified as the fast fracture load (P_F), and the load at which fast fracture terminated is identified as the arrest load (P_A).

The energy at maximum load (E_M) was determined by comparing the energy-time record and the load-time record. The energy at maximum load is approximately equivalent to the energy required to initiate a crack in the specimen. Therefore, the propagation energy for the crack (E_p) is the difference between the total energy to fracture (E_D) and the energy at maximum load (E_M).

The yield stress (σ_Y) was calculated from the three-point bend formula having the following expression:

$$\sigma_Y = (P_{GY} * L) / [B * (W - a)^2 * C] \quad (1)$$

where: L = distance between the specimen supports in the impact machine
B = the width of the specimen measured parallel to the notch
W = height of the specimen, measured perpendicularly to the notch
a = notch depth

The constant C is dependent on the notch flank angle (ϕ), notch root radius (ρ) and the type of loading (ie. pure bending or three-point bending). In three-point bending, for a Charpy specimen in which $\phi = 45°$ and $\rho = 0.010$ inches, Equation 1 is valid with C = 1.21. Therefore (for L = 4W),

$$\sigma_Y = (P_{GY} * L) / [B * (W - a)^2 * 1.21] = (3.33 * P_{GY} * W) / [B * (W - a)^2] \quad (2)$$

For the Charpy specimen, B = 0.394 inches, W = 0.394 inches and a = 0.079 inches, Equation 2 then reduces to:

$$\sigma_Y = 33.3 * P_{GY} \quad (3)$$

where σ_Y is in units of psi and P_{GY} is in units of pound. The flow stress was calculated from the average of the yield and maximum loads, also using the three-point bend formula.

Symbol A in columns 4, 5, and 6 of Tables 5-5 through 5-7 is the cross-sectional area under the notch of the Charpy specimens.

$$A = B (W-a) + 0.1241 \text{ sq. in.} \quad (4)$$

Percent shear was determined from post-fracture photographs using the ratio-of-areas methods in compliance with ASTM Specification A370-92[9]. The lateral expansion was measured using a dial gage rig similar to that shown in the same specification.

Tensile tests were performed on a 20,000-pound Instron, split-console test machine (Model 1115) per ASTM Specification E8-93[10] and E21-92[11], and RMF Procedure 8102, Revision 1. The upper pull rod was connected through a universal joint to improve axiality of loading. The tests were conducted at a constant crosshead speed of 0.05 inches per minute throughout the test.

Extension measurements were made with a linear variable displacement transducer extensometer. The extensometer knife edges were spring-loaded to the specimen and operated through specimen failure. The extensometer gage length was 1.00 inch. The extensometer is rated as Class B-2 per ASTM E83-93[12].

Elevated test temperatures were obtained with a three-zone electric resistance split-tube furnace with a 9-inch hot zone. All tests were conducted in air.

Because of the difficulty in remotely attaching a thermocouple directly to the specimen, the following procedure was used to monitor specimen temperatures. Chromel-alumel thermocouples were positioned at center and each end of the gage section of a dummy specimen and in each grip. In the test configuration, with a slight load on the specimen, a plot of specimen temperature versus upper and lower grip and controller temperatures was developed over the range from room temperature to 550°F (288°C). The upper grip was used to control the furnace temperature. During the actual testing, the grip temperatures were used to obtain desired specimen temperatures. Experiments indicate that this method is accurate to $\pm$ 2°F.

The yield load, ultimate load, fracture load, total elongation, and uniform elongation were determined directly from the load-extension curve. The yield strength, ultimate strength, and fracture strength were calculated using the original cross-sectional area. The final diameter and final gage length were determined from post-fracture photographs. The fracture area used to calculate the fracture stress (true stress at fracture) and percent reduction in area was computed using the final diameter measurement.

5.2 Charpy V-Notch Impact Test Results

The results of the Charpy V-notch impact tests performed on the various materials contained in Capsule U, which was irradiated to 3.28 x 10^{18} n/cm^2 (E > 1.0 MeV), are presented in Tables 5-1 through 5-8 and are compared with unirradiated results[3] as shown in Figures 5-1 through 5-4. The transition temperature increases and upper shelf energy decreases for the Capsule U surveillance materials are summarized in Table 5-9.

Irradiation of the reactor vessel intermediate shell plate R3807-2 Charpy specimens oriented with the longitudinal axis of the specimen parallel to the major rolling direction of the plate (longitudinal orientation) to 3.28 x 10^{18} n/cm^2 (E > 1.0 MeV) (Figure 5-1) resulted in a 30 ft-lb transition temperature shift of 0°F and a 50 ft-lb transition temperature shift of 0°F. This results in an irradiated

30 ft-lb transition temperature of -5°F and an irradiated 50 ft-lb transition temperature of 35°F (longitudinal orientation).

The average upper shelf energy (USE) of the intermediate shell plate R3807-2 (longitudinal orientation) resulted in an energy increase of 3 ft-lb after irradiation to 3.28 x 10^{18} n/cm^2 (E > 1.0 MeV). This results in an irradiated average USE of 118 ft-lb (Figure 5-1).

Irradiation of the reactor vessel intermediate shell plate R3807-2 Charpy specimens, oriented with the longitudinal axis of the specimen normal to the major rolling direction of the plate (transverse orientation) to 3.28 x 10^{18} n/cm^2 (E > 1.0 MeV) (Figure 5-2) resulted in a 30 ft-lb transition temperature increase of 25°F and a 50 ft-lb transition temperature increase of 20°F. This results in an irradiated 30 ft-lb transition temperature of 15°F and an irradiated 50 ft-lb transition temperature of 75°F (transverse orientation). (The notch in the Charpy specimen of the "transverse" specimen is orientated such that the direction of crack propagation is in the rolling direction.)

The average upper shelf energy (USE) of the intermediate shell plate R3807-2 Charpy specimens (transverse orientation) resulted in an energy increase of 4 ft-lb after irradiation to 3.28 x 10^{18} n/cm^2 (E > 1.0 MeV). This results in an irradiated average USE of 88 ft-lb (Figure 5-2).

Irradiation of the surveillance weld metal Charpy specimens to 3.28 x 10^{18} n/cm^2 (E > 1.0 MeV) (Figure 5-3) resulted in a 30 ft-lb transition temperature shift of 0°F and a 50 ft-lb transition temperature shift of 0°F. This results in an irradiated 30 ft-lb transition temperature of -45°F and an irradiated 50 ft-lb transition temperature of 5°F.

The average USE of the surveillance weld metal resulted in an energy decrease of 9 ft-lb after irradiation to 3.28 x 10^{18} n/cm^2 (E > 1.0 MeV). This results in an irradiated average USE of 85 ft-lb (Figure 5-3).

Irradiation of the reactor vessel HAZ metal Charpy specimens to 3.28 x 10^{18} n/cm^2 (E > 1.0 MeV) (Figure 5-4) resulted in a 30 ft-lb transition temperature change of 0°F and a 50 ft-lb transition temperature change of 0°F. This results in an irradiated 30 ft-lb transition temperature of -105°F and an irradiated 50 ft-lb transition temperature of -50°F.

The average USE of the weld HAZ metal resulted in an energy increase of 11 ft-lb after irradiation to 3.28 x 10^{18} n/cm^2 (E > 1.0 MeV). This results in an irradiated average USE of 127 ft-lb (Figure 5-4).

The fracture appearance of each irradiated Charpy specimen from the various materials is shown in Figures 5-5 through 5-8 and show an increasingly ductile or tougher appearance with increasing test temperature.

A comparison of the CPSES Unit No. 2 reactor vessel beltline material test results with the Regulatory Guide 1.99, Revision 2, predictions (Table 5-10) led to the following conclusions:

- All measured 30 ft-lb transition temperature shift values of the surveillance materials are less than the Regulatory Guide 1.99, Revision 2, predictions.

- All measured upper shelf energy (USE) percent decreases are less than the Regulatory Guide 1.99, Revision 2, predictions.

All beltline materials exhibit a more than adequate upper shelf energy level for continued safe plant operation and are expected to maintain an upper shelf energy of no less than 50 ft-lb throughout the life of the vessel (32 EFPY) as required by 10 CFR 50, Appendix G[2].

The load-time records for individual instrumented Charpy specimen tests are shown in Appendix A.

5.3 Tensile Test Results

The results of the tensile tests performed on the various materials contained in Capsule U irradiated to 3.28×10^{18} n/cm^2 (E > 1.0 MeV) are presented in Table 5-11 and are compared with unirradiated results[3] as shown in Figures 5-9 through 5-11.

The results of the tensile tests performed on the intermediate shell plate R3807-2 (longitudinal orientation) indicated that irradiation to 3.28×10^{18} n/cm^2 (E > 1.0 MeV) caused a 2 to 7 ksi increase in the 0.2 percent offset yield strength and a 3 to 5 ksi increase in the ultimate tensile strength when compared to unirradiated data[3] (Figure 5-9).

The results of the tensile tests performed on the intermediate shell plate R3807-2 (transverse orientation) indicated that irradiation to 3.28×10^{18} n/cm^2 (E > 1.0 MeV) caused a 2 to 12 ksi increase in the 0.2 percent offset yield strength and a 3 to 5 ksi increase in the ultimate tensile strength when compared to unirradiated data[3] (Figure 5-10).

The results of the tensile tests performed on the surveillance weld metal indicated that irradiation to 3.28×10^{18} n/cm^2 (E > 1.0 MeV) caused a 3 to 7 ksi increase in the 0.2 percent offset yield strength and a 5 to 9 ksi increase in the ultimate tensile strength when compared to unirradiated data[3] (Figure 5-11).

The fractured tensile specimens for the intermediate shell plate R3807-2 material are shown in Figures 5-12 and 5-13, while the fractured specimens for the surveillance weld metal are shown in Figure 5-14.

The engineering stress-strain curves for the tensile tests are shown in Figures 5-15 through 5-20.

TABLE 5-1

Charpy V-Notch Impact Data for the CPSES Unit No. 2 Intermediate Shell Plate R3807-2 Irradiated to a Fluence of 3.28 x 10^{18} n/cm^2 (E > 1.0 MeV) (Longitudinal Orientation)

Sample	Temperature		Impact Energy		Lateral Expansion		Shear
Number	(°F)	(°C)	(ft-lb)	(J)	(mils)	(mm)	(%)
CL2	-75	-59	8	11	8	0.20	2
CL11	-50	-46	11	15	10	0.25	5
CL10	-25	-32	20	27	17	0.43	10
CL13	-10	-23	36	49	27	0.69	15
CL9	0	-18	41	56	30	0.76	15
CL5	10	-12	42	57	32	0.81	20
CL15	25	-4	42	57	32	0.81	25
CL3	50	10	58	79	46	1.17	35
CL4	72	22	85	115	61	1.55	40
CL14	100	38	88	119	65	1.65	45
CL6	125	52	106	144	71	1.80	60
CL7	150	66	115	156	80	2.03	100
CL8	200	93	116	157	81	2.06	100
CL1	250	121	116	157	77	1.96	100
CL12	300	149	127	172	84	2.13	100

TABLE 5-2

Charpy V-Notch Impact Data for the CPSES Unit No. 2 Intermediate Shell Plate R3807-2 Irradiated to a Fluence of 3.28×10^{18} n/cm^2 (E > 1.0 MeV) (Transverse Orientation)

Sample	Temperature		Impact Energy		Lateral Expansion		Shear
Number	(°F)	(°C)	(ft-lb)	(J)	(mils)	(mm)	(%)
CT3	-125	-87	6	8	6	0.15	0
CT5	-95	-71	4	5	5	0.13	0
CT12	-50	-46	20	27	14	0.36	5
CT9	-25	-32	22	30	16	0.41	10
CT15	-10	-23	29	39	24	0.61	10
CT2	0	-18	24	33	22	0.56	15
CT1	10	-12	26	35	20	0.51	15
CT11	50	10	35	47	35	0.89	20
CT13	72	22	66	89	50	1.27	30
CT10	100	38	48	65	46	1.17	25
CT7	125	52	73	99	54	1.37	30
CT8	150	66	85	115	67	1.70	100
CT6	200	93	87	118	70	1.78	100
CT14	250	121	86	117	67	1.70	100
CT4	300	149	96	130	69	1.75	100

TABLE 5-3

Charpy V-Notch Impact Data for the CPSES Unit No. 2 Surveillance Weld Metal Irradiated to a Fluence of 3.28×10^{18} n/cm^2 (E > 1.0 MeV)

Sample	Temperature		Impact Energy		Lateral Expansion		Shear
Number	(°F)	(°C)	(ft-lb)	(J)	(mils)	(mm)	(%)
CW11	-125	-87	3	4	8	0.20	5
CW5	-95	-71	11	15	9	0.23	5
CW15	-75	-59	7	9	9	0.23	10
CW1	-60	-51	32	43	24	0.61	10
CW4	-50	-46	38	52	29	0.74	15
CW3	-25	-32	40	54	31	0.79	15
CW9	-10	-23	48	65	38	0.97	25
CW2	0	-18	48	65	39	0.99	35
CW7	50	10	66	89	52	1.32	70
CW14	72	22	75	102	61	1.55	85
CW6	100	38	76	103	62	1.57	90
CW12	150	66	80	108	65	1.65	100
CW10	200	93	87	118	67	1.70	100
CW8	250	121	86	117	60	1.52	100
CW13	300	149	86	117	70	1.78	100

TABLE 5-4

Charpy V-Notch Impact Data for the CPSES Unit No. 2 Heat-Affected-Zone (HAZ) Metal Irradiated to a Fluence of 3.28×10^{18} n/cm^2 (E > 1.0 MeV)

Sample	Temperature		Impact Energy		Lateral Expansion		Shear
Number	(°F)	(°C)	(ft-lb)	(J)	(mils)	(mm)	(%)
CH9	-225	-143	7	9	2	0.05	5
CH8	-175	-115	16	22	8	0.20	5
CH3	-150	-101	20	27	9	0.23	10
CH2	-125	-87	40	54	21	0.53	15
CH7	-100	-73	23	31	13	0.33	10
CH5	-75	-59	90	122	44	1.12	50
CH10	-60	-51	59	80	37	0.94	30
CH11	-50	-46	35	47	26	0.66	30
CH4	-25	-32	52	71	29	0.74	60
CH12	0	-18	78	106	50	1.27	65
CH14	25	-4	90	122	59	1.50	65
CH15	72	22	124	168	75	1.91	100
CH13	150	66	104	141	71	1.80	100
CH1	200	93	154	209	74	1.88	100
CH6	200	93	*	*	*	*	*

* Specimen Alignment Error. Data is not valid.

TABLE 5-5

Instrumented Charpy Impact Test Results for the CPSES Unit No. 2 Intermediate Shell Plate R3807-2
Irradiated to a Fluence of 3.28 X 10^{18} n/cm^2 (E > 1.0 MeV) (Longitudinal Orientation)

Sample No.	Test Temp. (°F)	Charpy Energy E_D (ft-lb)	Normalized Energies (ft-lb/in^2)			Yield Load P_{GY} (lb)	Time to Yield t_{GY} (μsec)	Max. Load P_M (lb)	Time to Max. t_M (μsec)	Fast Fract. Load P_F (lb)	Arrest Load P_A (lb)	Yield Stress σ_Y (ksi)	Flow Stress (ksi)
			Charpy E_D/A	Max. E_M/A	Prop. E_P/A								
CL2	-75	8	64	37	27	3737	0.16	3737	0.16	3737	144	124	124
CL11	-50	11	89	46	42	3627	0.15	3808	0.17	3808	157	120	123
CL10	-25	20	161	120	41	3455	0.14	4209	0.31	4209	364	115	127
CL13	-10	36	290	242	47	3453	0.14	4520	0.54	4520	270	115	132
CL9	0	41	330	259	71	3454	0.14	4500	0.56	4486	229	115	132
CL5	10	42	338	292	46	3348	0.14	4534	0.63	4534	362	111	131
CL15	25	42	338	253	85	3250	0.14	4360	0.57	4360	725	108	126
CL3	50	58	467	313	154	3204	0.14	4392	0.69	4345	1457	106	126
CL4	72	85	684	319	365	3198	0.14	4441	0.69	3740	1668	106	127
CL14	100	88	709	310	398	3132	0.15	4324	0.69	3737	2019	104	124
CL6	125	106	854	305	549	3024	0.14	4323	0.69	3270	2052	100	122
CL7	150	115	926	303	623	2995	0.14	4218	0.69	N/A	N/A	99	120
CL8	200	116	934	295	639	2840	0.14	4124	0.69	N/A	N/A	94	116
CL1	250	116	934	289	645	2741	0.14	4026	0.7	N/A	N/A	91	112
CL12	300	127	1023	287	736	2703	0.14	3950	0.7	N/A	N/A	90	110

N/A - Fully ductile fracture. No arrest load.

TABLE 5-6

Instrumented Charpy Impact Test Results for the CPSES Unit No. 2 Intermediate Shell Plate R3807-2
Irradiated to a Fluence of 3.28 x 10^{18} n/cm^2 (E > 1.0 MeV) (Transverse Orientation)

Sample No.	Test Temp. (°F)	Charpy Energy E_D (ft-lb)	Normalized Energies (ft-lb/in^2)			Yield Load P_{GY} (lb)	Time to Yield t_{GY} (μsec)	Max. Load P_M (lb)	Time to Max. t_M (μsec)	Fast Fract. Load P_F (lb)	Arrest Load P_A (lb)	Yield Stress σ_Y (ksi)	Flow Stress (ksi)
			Charpy E_D/A	Max. E_M/A	Prop. E_P/A								
CT3	-125	6	48	29	20	3511	0.14	3511	0.14	3511	106	117	117
CT5	-95	4	32	16	16	2351	0.11	2351	0.11	2351	79	78	78
CT12	-50	20	161	116	45	3861	0.17	4242	0.31	4242	375	128	135
CT9	-25	22	177	125	52	3537	0.14	4244	0.32	4244	237	117	129
CT15	-10	29	234	189	45	3442	0.14	4368	0.44	4368	366	114	130
CT2	0	24	193	130	63	3431	0.14	4129	0.34	4129	489	114	126
CT1	10	25	209	141	69	3429	0.16	4159	0.36	4159	488	114	126
CT11	50	35	282	163	119	3165	0.14	4081	0.42	4081	1053	105	120
CT13	72	66	531	305	227	3229	0.16	4348	0.67	4152	1575	107	126
CT10	100	48	387	216	170	3096	0.14	4130	0.52	4130	2045	103	120
CT7	125	73	588	293	295	3090	0.14	4252	0.67	3917	2403	103	122
CT8	150	85	684	281	403	3045	0.14	4186	0.65	N/A	N/A	101	120
CT6	200	87	701	278	422	2932	0.14	4040	0.66	N/A	N/A	97	116
CT14	250	86	692	265	427	2715	0.14	3904	0.66	N/A	N/A	90	110
CT4	300	96	773	273	500	2672	0.14	3919	0.67	N/A	N/A	89	109

N/A - Fully ductile failure. No arrest load.

TABLE 5-7

Instrumented Charpy Impact Test Results for the CPSES Unit No. 2 Surveillance Weld Metal Irradiated to a Fluence of 3.28×10^{18} n/cm^2 (E > 1.0 MeV)

Sample No.	Test Temp. (°F)	Charpy Energy E_D (ft-lb)	Normalized Energies (ft-lb/in^2)			Yield Load P_{GY} (lb)	Time to Yield t_{GY} (μsec)	Max. Load P_M (lb)	Time to Max. t_M (μsec)	Fast Fract. Load P_F (lb)	Arrest Load P_A (lb)	Yield Stress σ_Y (ksi)	Flow Stress (ksi)
			Charpy E_D/A	Max. E_M/A	Prop. E_P/A								
CW11	-125	3	24	8	17	1353	0.09	1353	0.09	1353	86	45	45
CW5	-95	11	89	53	35	3816	0.15	4070	0.19	4070	137	127	131
CW15	-75	7	56	23	33	2958	0.13	2958	0.13	2958	126	98	98
CW1	-60	32	258	219	39	3716	0.17	4399	0.5	4399	246	123	135
CW4	-50	38	306	247	59	3541	0.14	4434	0.54	4414	113	118	132
CW3	-25	40	322	230	92	3493	0.14	4375	0.51	4268	579	116	131
CW9	-10	48	387	233	154	3479	0.14	4366	0.52	4150	442	116	130
CW2	0	48	387	234	152	3419	0.14	4318	0.53	4113	592	114	128
CW7	50	66	531	237	294	3160	0.14	4161	0.56	3214	1597	105	122
CW14	72	75	604	293	311	3109	0.15	4156	0.67	3160	2100	103	121
CW6	100	76	612	234	378	3116	0.14	4082	0.56	2464	1679	103	120
CW12	150	80	644	281	363	2970	0.14	3980	0.67	N/A	N/A	99	115
CW10	200	87	701	278	423	2817	0.14	3865	0.69	N/A	N/A	94	111
CW8	250	86	692	272	421	2756	0.14	3828	0.67	N/A	N/A	92	109
CW13	300	86	692	268	425	2675	0.14	3715	0.69	N/A	N/A	89	106

N/A - Fully ductile failure. No arrest load.

TABLE 5-8

Instrumented Charpy Impact Test Results for the CPSES Unit No. 2 Heat-Affected-Zone (HAZ) Metal Irradiated to a Fluence of 3.28×10^{18} n/cm^2 (E > 1.0 MeV)

Sample No.	Test Temp. (°F)	Charpy Energy E_D (ft-lb)	Normalized Energies (ft-lb/in^2)			Yield Load P_{GY} (lb)	Time to Yield t_{GY} (μsec)	Max. Load P_M (lb)	Time to Max. t_M (μsec)	Fast Fract. Load P_F (lb)	Arrest Load P_A (lb)	Yield Stress σ_Y (ksi)	Flow Stress (ksi)
			Charpy E_D/A	Max. E_M/A	Prop. E_P/A								
CH9	-225	7	56	33	23	4082	0.14	4082	0.14	4082	127	136	136
CH8	-175	16	129	87	42	5211	0.33	5211	0.33	5211	89	173	173
CH3	-150	20	161	107	54	4642	0.18	4778	0.26	4778	191	154	156
CH2	-125	40	322	270	52	4399	0.18	5183	0.53	5183	305	146	159
CH7	-100	23	185	152	33	4400	0.19	4849	0.35	4849	99	146	154
CH5	-75	90	725	348	376	4186	0.18	4910	0.67	4114	1670	139	151
CH10	-60	59	475	261	214	4056	0.17	4900	0.54	4699	1569	135	149
CH11	-50	35	282	180	102	4087	0.18	4621	0.41	4621	1599	136	145
CH4	-25	52	419	205	214	4099	0 17	4593	0.44	4297	2064	136	144
CH12	0	78	628	243	385	3614	0.14	4537	0.52	2902	1976	120	135
CH14	25	90	725	258	467	3486	0.15	4464	0.56	3622	2519	116	132
CH15	72	124	998	328	671	3461	0.15	4614	0.69	N/A	N/A	115	134
CH13	150	104	837	304	533	3214	0.14	4292	0.67	N/A	N/A	107	125
CH1	200	154	1240	395	845	3093	0.14	4355	0.86	N/A	N/A	103	124
CH6	200	*	*	*	*	*	*	*	*	*	*	*	*

* : Specimen Alignment Error. Data is not valid. N/A - Fully ductile failure. No arrest load.

TABLE 5-9

Effect of Irradiation to 3.28×10^{18} n/cm^2 (E > 1.0 MeV) on the Notch Toughness Properties of the CPSES Unit No. 2 Reactor Vessel Surveillance Materials

Material	Average 30 (ft-lb) [a] Transition Temperature (°F)			Average 35 mil Lateral [a] Expansion Temperature (°F)			Average 50 ft-lb [a] Transition Temperature (°F)			Average Energy Absorption [a] at Full Shear (USE) (ft-lb)		
	Unirrad.	Irradiated	ΔT	Unirrad.	Irradiated	ΔT	Unirrad.	Irradiated	ΔT	Unirrad.	Irradiated	Δ
Intermediate Shell Plate R3807-2 (Longitudinal)	-5	-5	0	30	30	0	35	35	0	115	118	+3
Intermediate Shell Plate R3807-2 (Transverse)	-10	15	25	45	45	0	55	75	20	84	88	+4
Weld Metal	-45	-45	0	-5	-5	0	5	5	0	94	85	-9
HAZ Metal	-105	-105	0	-35	-35	0	-50	-50	0	116	127	+11

(a) "Average" is defined as the value read from the curve fit through the data points of the Charpy tests (see Figures 5-1 through 5-4).

TABLE 5-10

Comparison of the CPSES Unit No. 2 Surveillance Material 30 ft-lb Transition Temperature Shifts and Upper Shelf Energy Decreases with Regulatory Guide 1.99, Revision 2 Predictions

Material	Capsule	Fluence (n/cm^2, E > 1.0 MeV)	30 ft-lb Transition Temperature Shift		Upper Shelf Energy Decrease	
			Predicted [a] (°F)	Measured (°F)	Predicted [a] (%)	Measured (%)
Intermediate Shell Plate R3807-2 (Longitudinal)	U	3.28×10^{18}	26.9	0	-14.5	+2.6
Intermediate Shell Plate R3807-2 (Transverse)	U	3.28×10^{18}	26.9	25	-14.5	+4.8
Weld Metal	U	3.28×10^{18}	20.0	0	-14.5	-9.6
HAZ Metal	U	3.28×10^{18}	-	0	-	+9.5

NOTE:

(a) Based on Regulatory Guide 1.99, Revision 2 methodology using Mean wt. % values of Cu and Ni

TABLE 5-11

Tensile Properties of the CPSES Unit No. 2 Reactor Vessel Materials Irradiated to a Fluence of 3.28×10^{18} n/cm^2 (E > 1.0 MeV)

Material	Sample Number	Test Temp. (°F)	0.2% Yield Strength (ksi)	Ultimate Strength (ksi)	Fracture Load (kip)	Fracture Stress (ksi)	Fracture Strength (ksi)	Uniform Elongation (%)	Total Elongation (%)	Reduction in Area (%)
Intermediate Shell Plate R3807-2 (Longitudinal)	CL1	70	71.3	91.7	3.00	184.5	61.1	11.3	25.2	67
	CL2	150	68.8	88.2	2.78	154.8	56.6	10.5	24.2	63
	CL3	550	62.4	89.0	2.90	166.8	59.1	11.3	24.2	65
Intermediate Shell Plate R3807-2 (Transverse)	CT1	25	72.8	96.8	3.40	152.8	69.3	12.8	25.2	55
	CTS	150	73.6	88.6	3.07	155.5	62.5	12.0	24.8	60
	CT3	550	61.9	89.0	3.25	175.3	66.2	11.3	21.9	62
Weld Metal	CW2	25	75.9	92.7	3.04	163.9	61.9	13.5	29.3	62
	CWI	150	73.3	87.6	2.85	169.4	58.1	12.0	29.6	66
	CW3	550	66.2	87.6	3.15	175.4	64.2	11.3	22.8	63

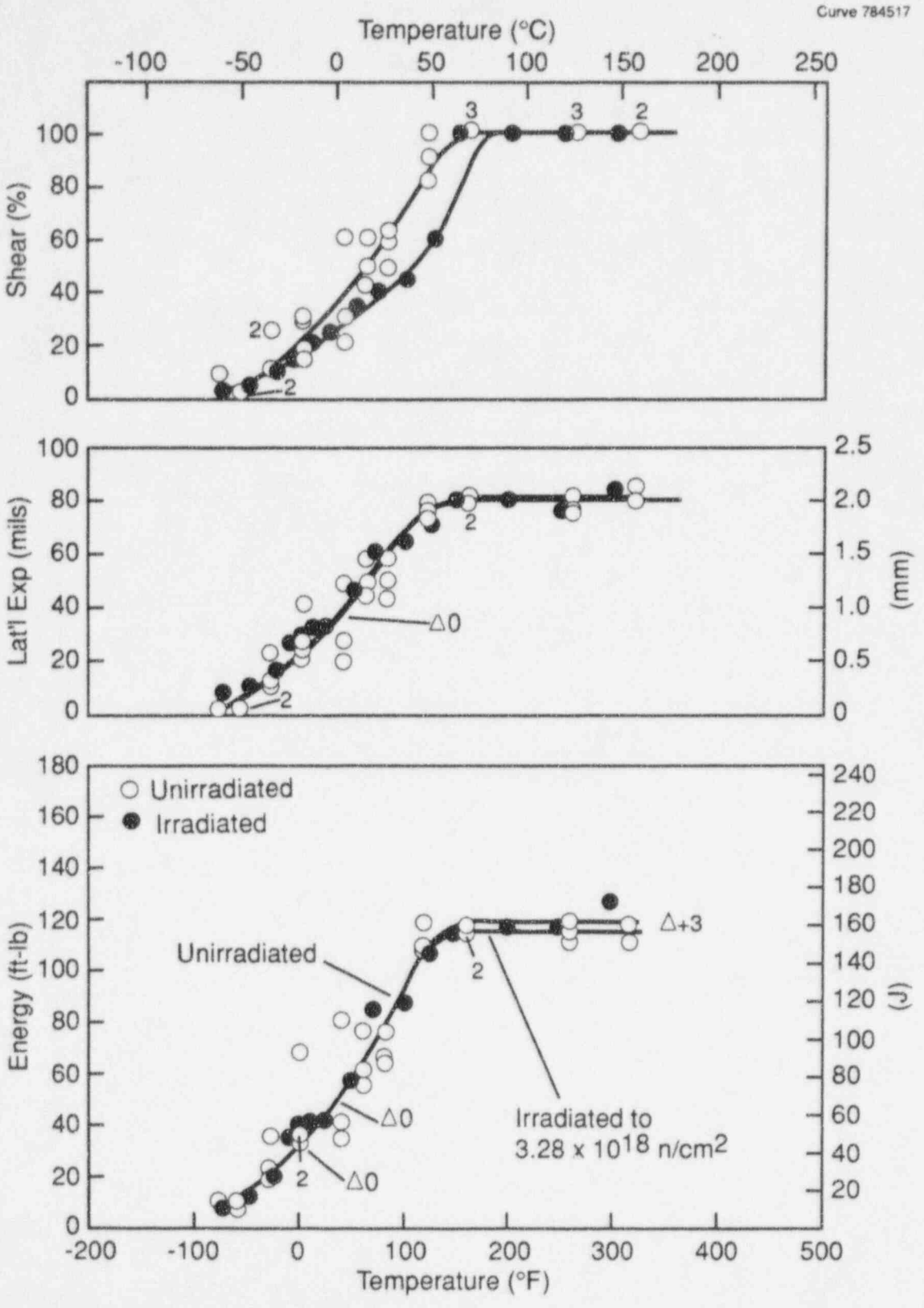

Figure 5-1 Charpy V-Notch Impact Properties for CPSES Unit No. 2 Reactor Vessel Intermediate Shell Plate R3807-2 (Longitudinal Orientation)

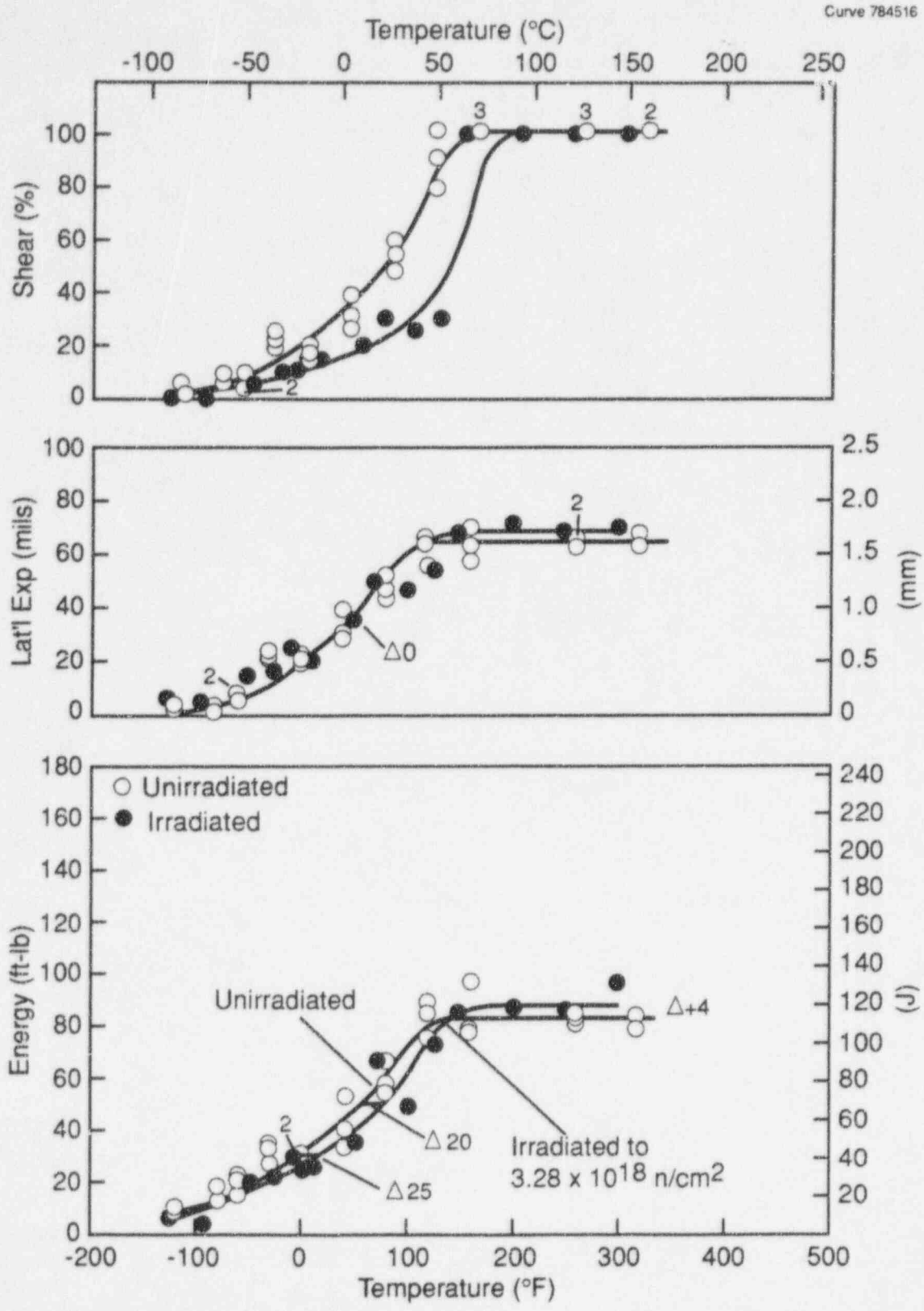

Figure 5-2 Charpy V-Notch Impact Properties for CPSES Unit No. 2 Reactor Vessel Intermediate Sheli Plate R3807-2 (Transverse Orientation)

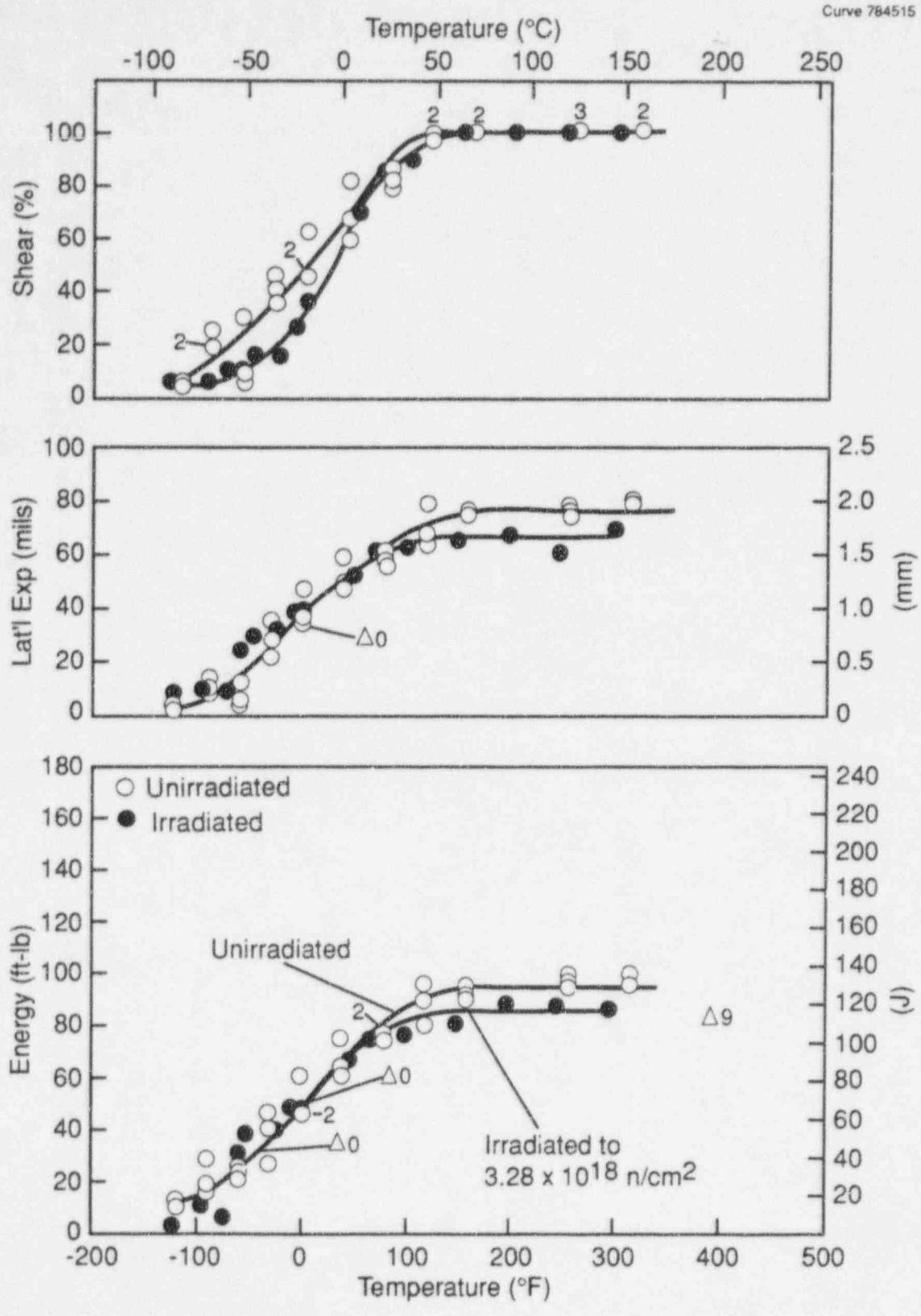

Figure 5-3 Charpy V-Notch Impact Properties for CPSES Unit No. 2 Reactor Vessel Weld Metal

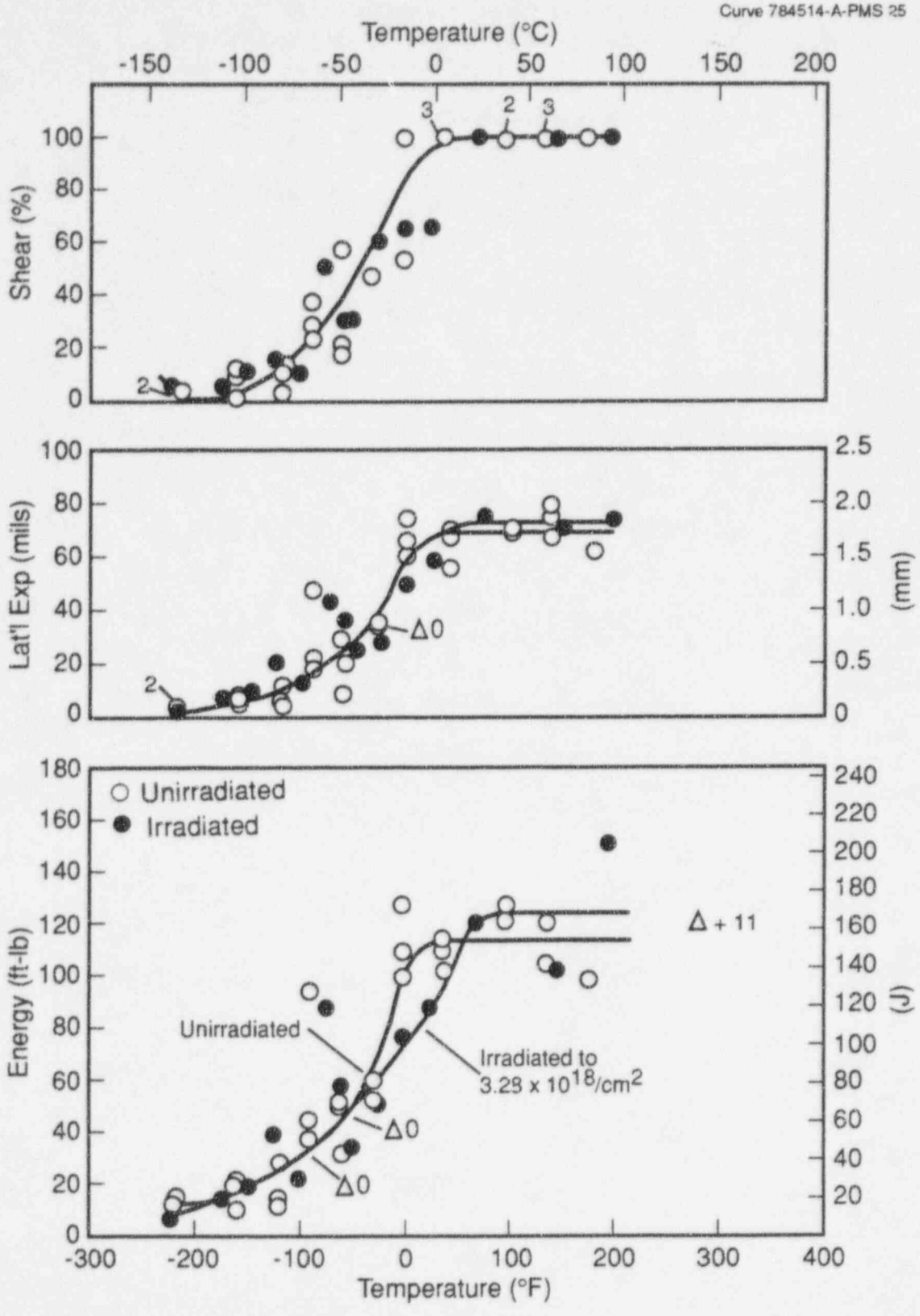

Figure 5-4 Charpy V-Notch Impact Properties for CPSES Unit No. 2 Reactor Vessel Heat-Affected-Zone (HAZ) Metal

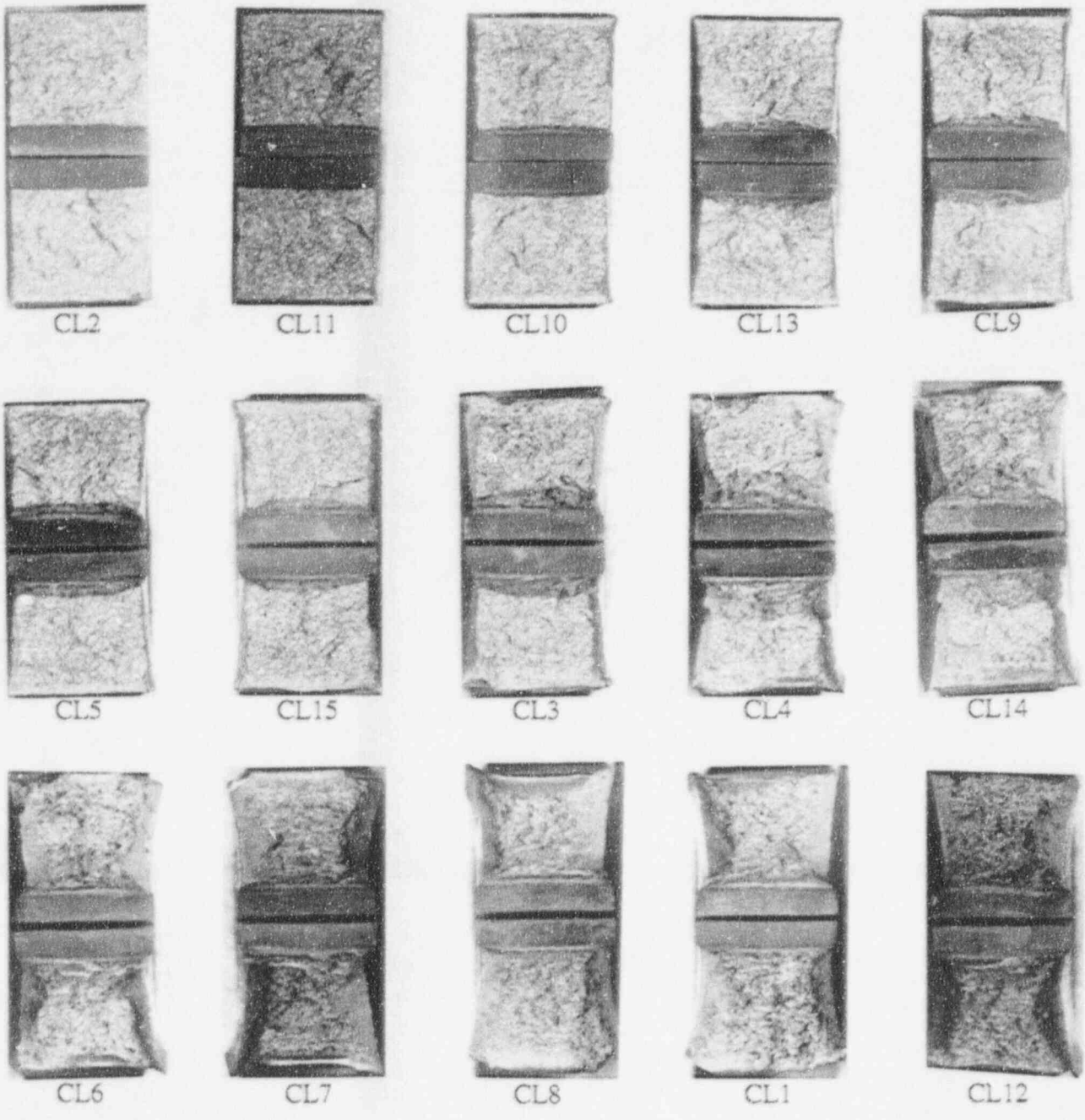

Figure 5-5 Charpy Impact Specimen Fracture Surfaces of the CPSES Unit No. 2 Reactor Vessel Intermediate Shell Plate R3807-2 (Longitudinal Orientation)

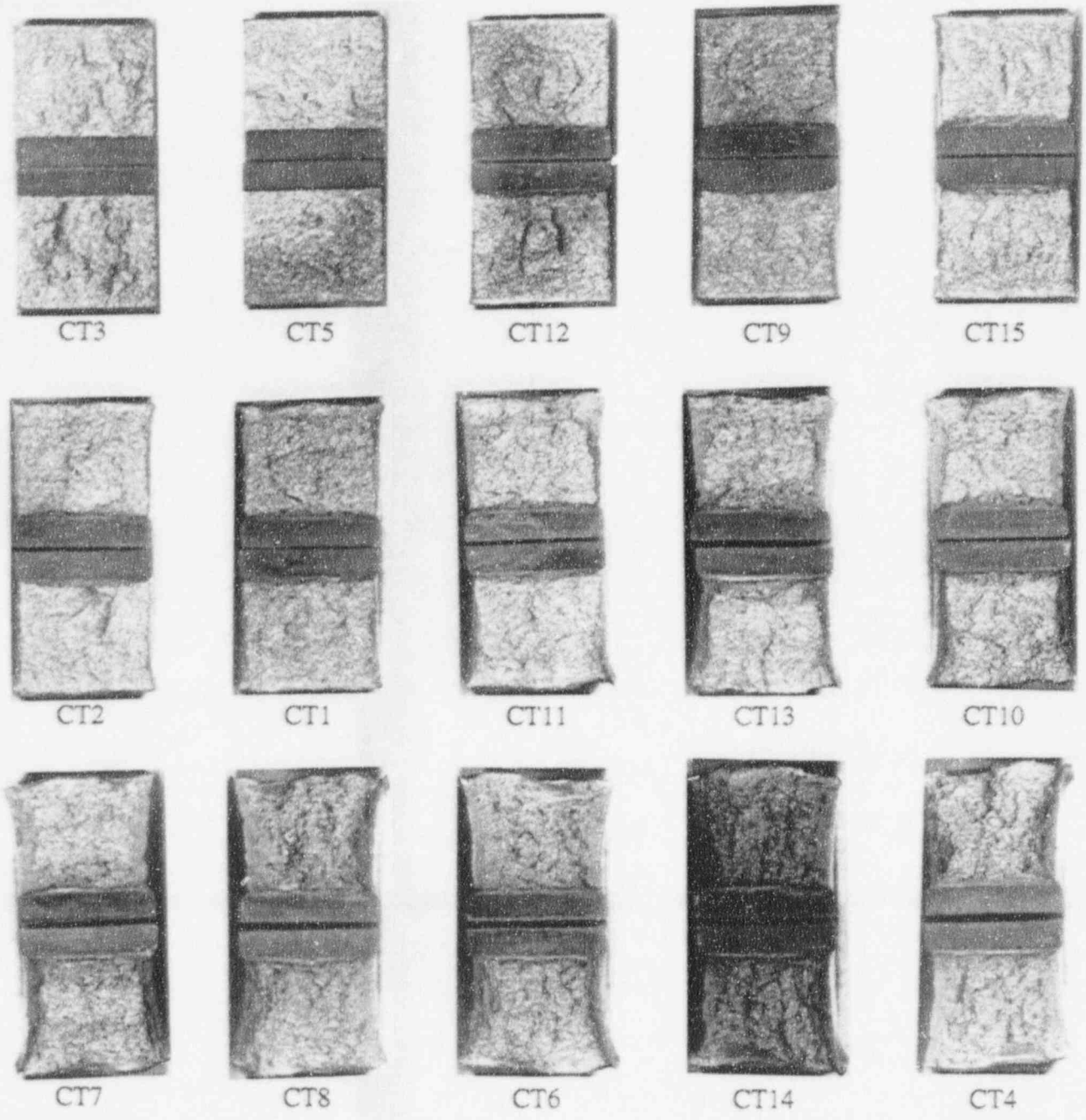

Figure 5-6 Charpy Impact Specimen Fracture Surfaces of the CPSES Unit No. 2 Reactor Vessel Intermediate Shell Plate R3807-2 (Transverse Orientation)

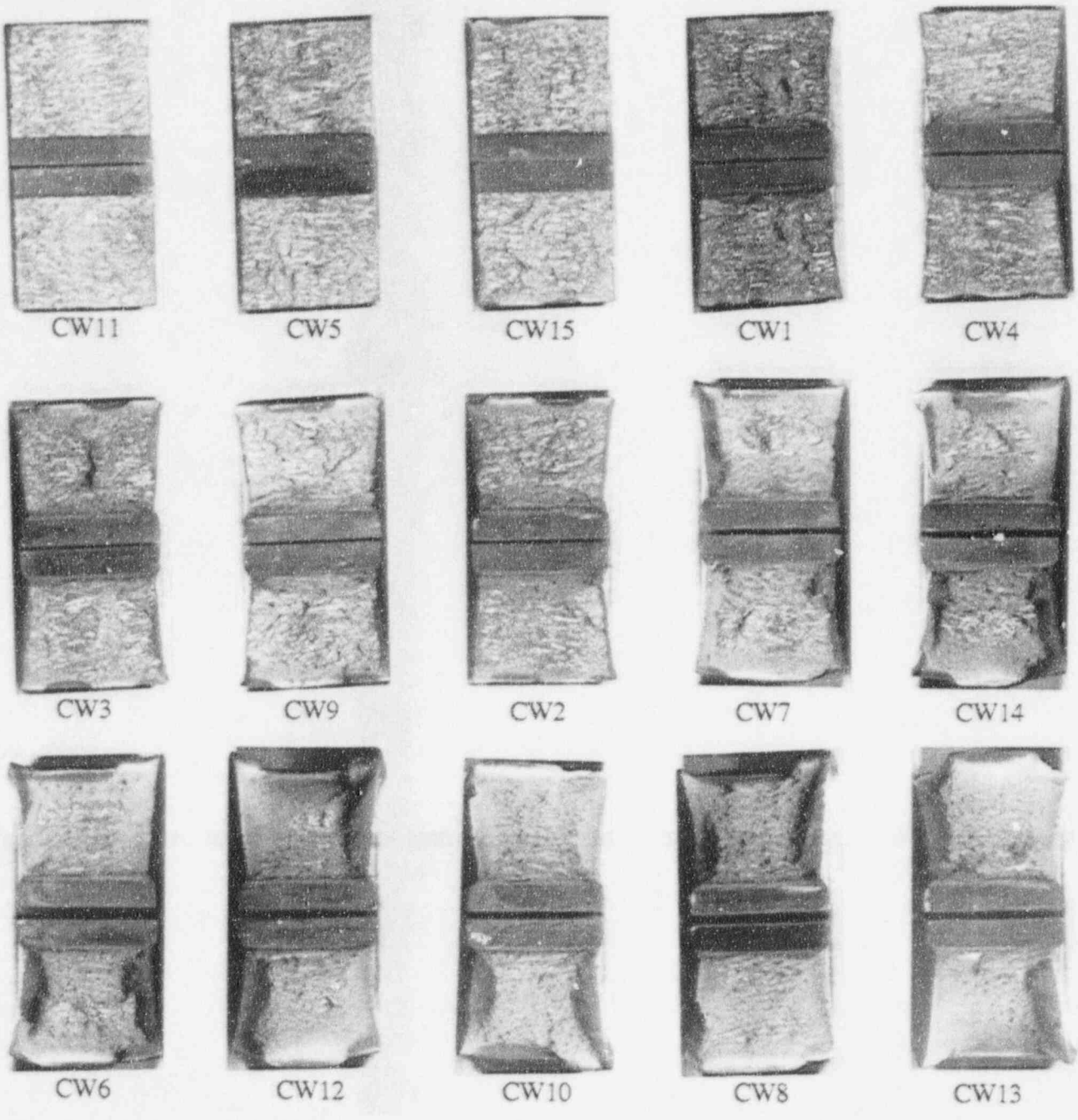

Figure 5-7 Charpy Impact Specimen Fracture Surfaces of the CPSES Unit No. 2 Reactor Vessel Weld Metal

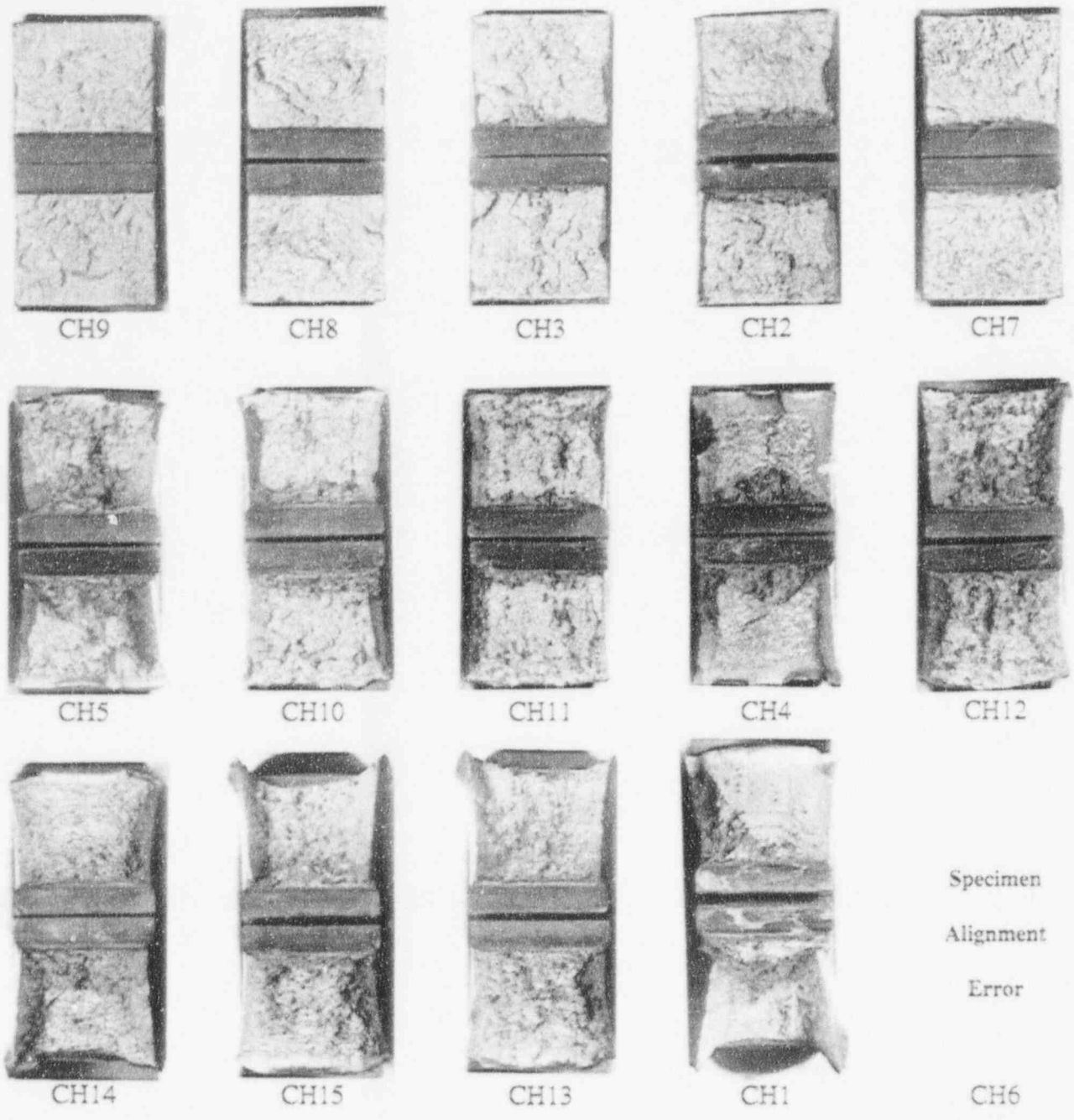

Figure 5-8 Charpy Impact Specimen Fracture Surfaces of the CPSES Unit No. 2 Reactor Vessel Heat-Affected-Zone (HAZ) Metal

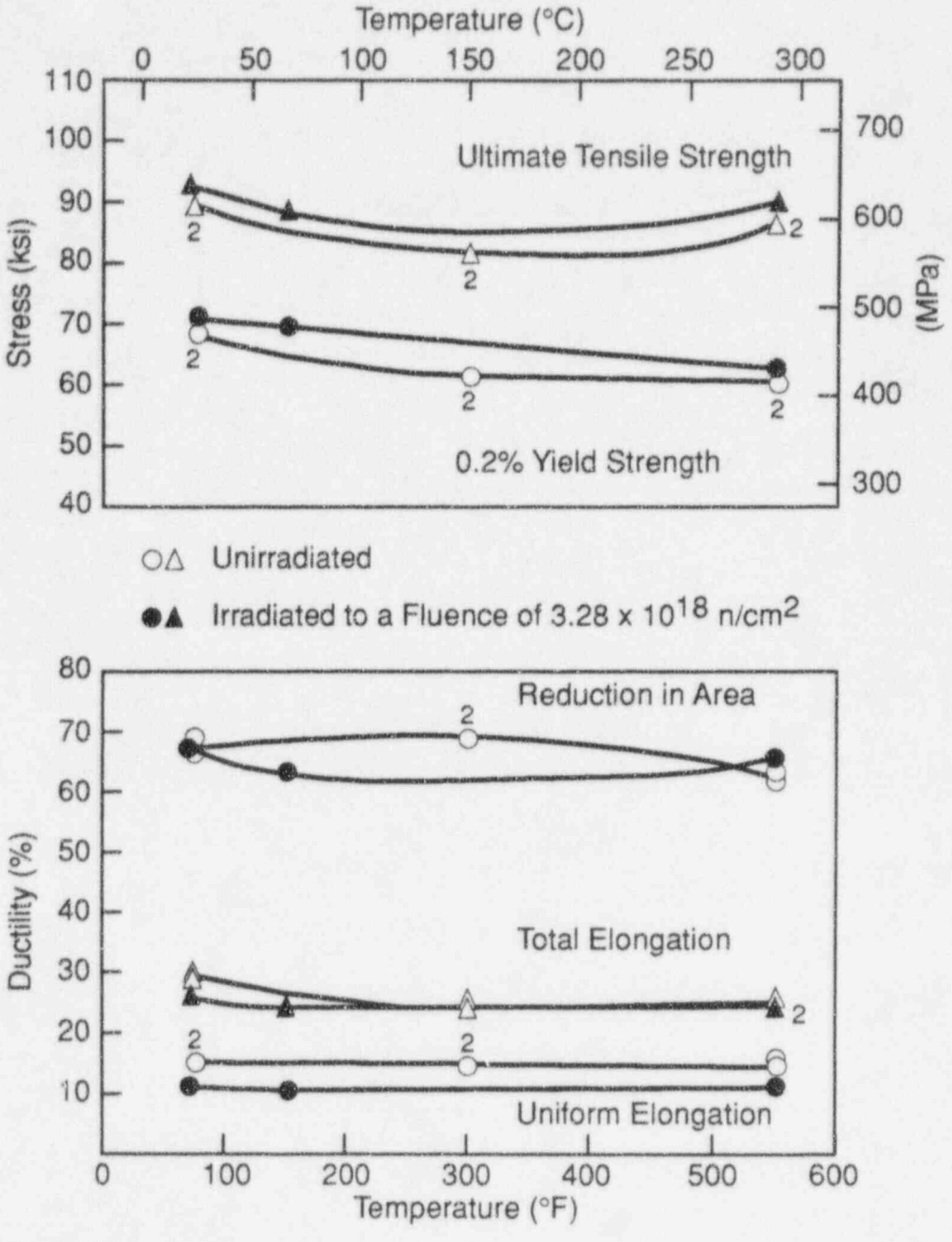

Figure 5-9 Tensile Properties for CPSES Unit No. 2 Reactor Vessel Intermediate Shell Plate R3807-2 (Longitudinal Orientation)

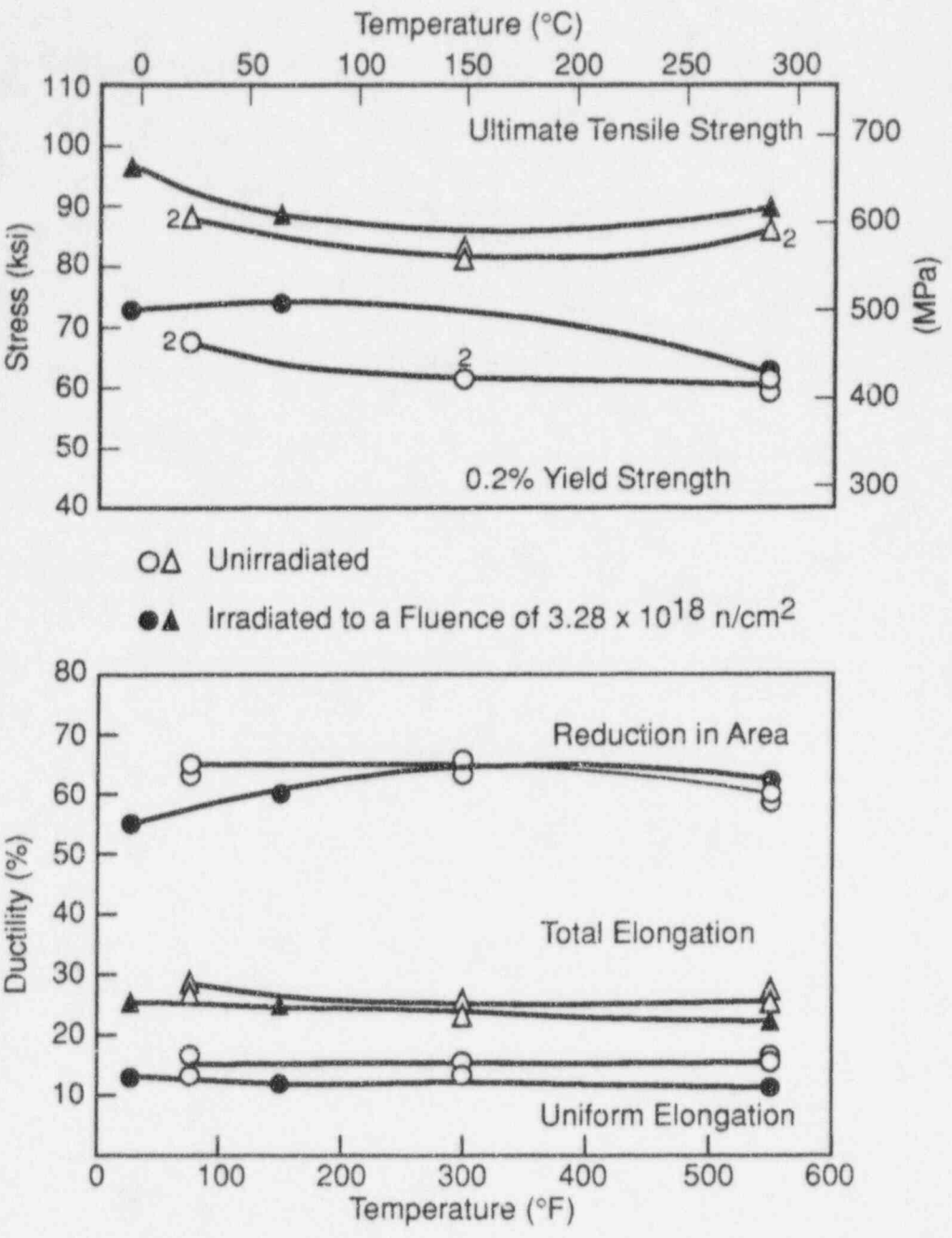

Figure 5-10 Tensile Properties for CPSES Unit No. 2 Reactor Vessel Intermediate Shell Plate R3807-2 (Transverse Orientation)

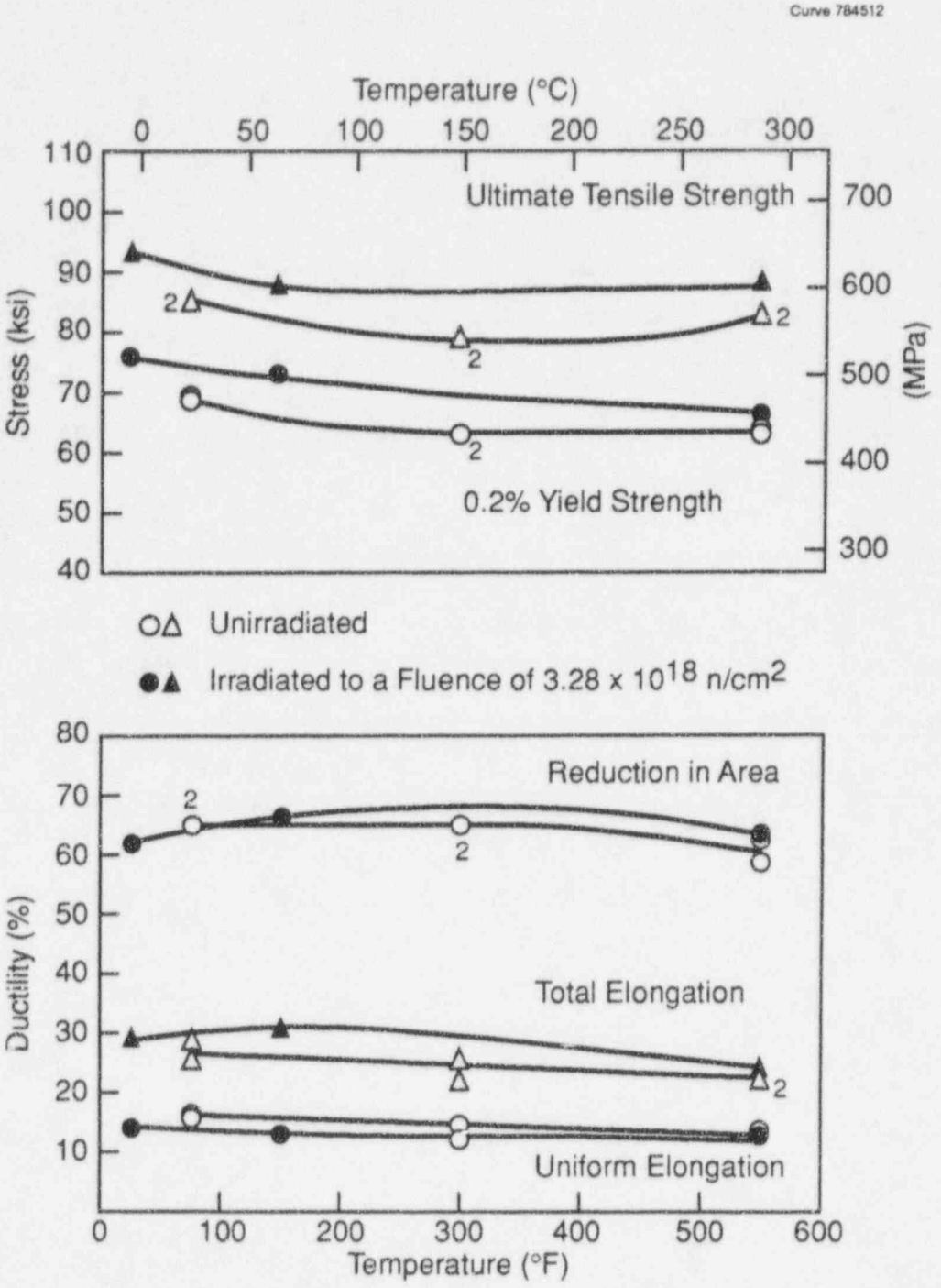

Figure 5-11 Tensile Properties for CPSES Unit No. 2 Reactor Vessel Weld Metal

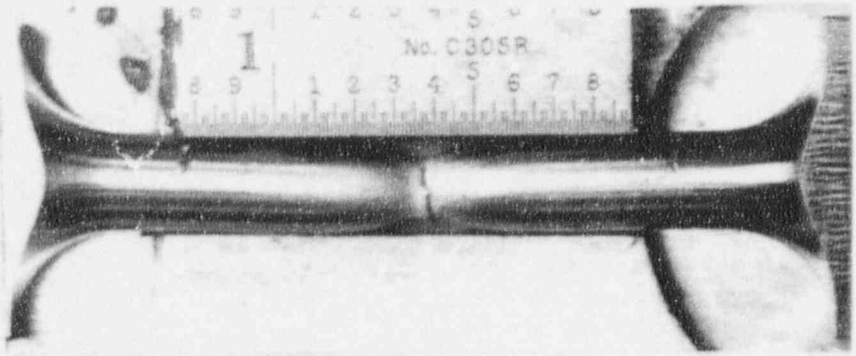

Specimen CL1 tested at 70°F

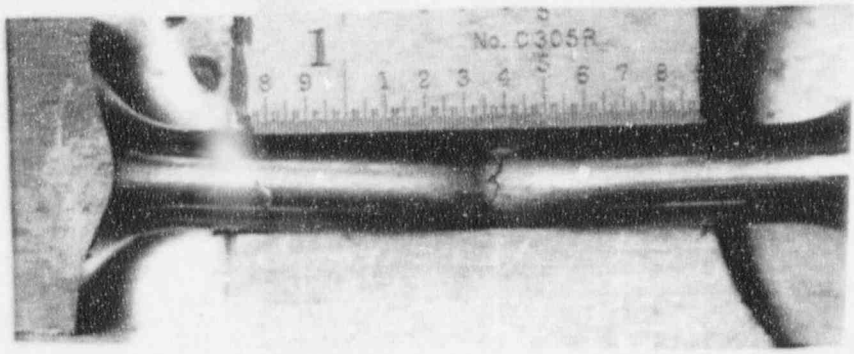

Specimen CL2 tested at 150°F

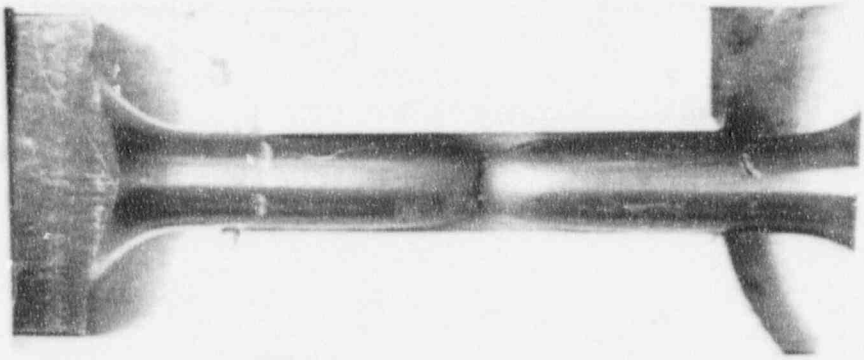

Specimen CL3 tested at 550°F

Figure 5-12 Fractured Tensile Specimens from CPSES Unit No. 2 Reactor Vessel Intermediate Shell Plate R3807-2 (Longitudinal Orientation)

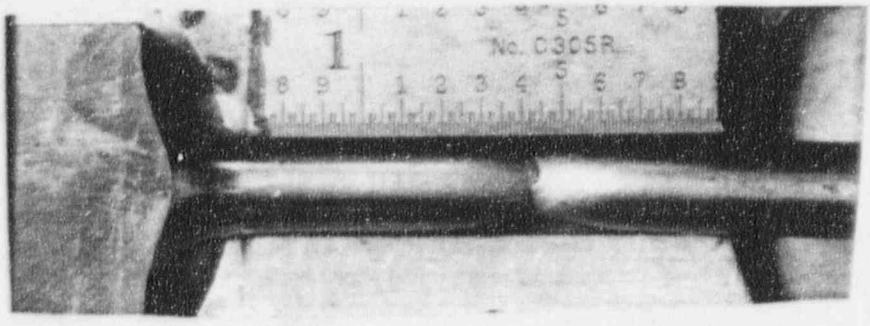

Specimen CT1 tested at 25°F

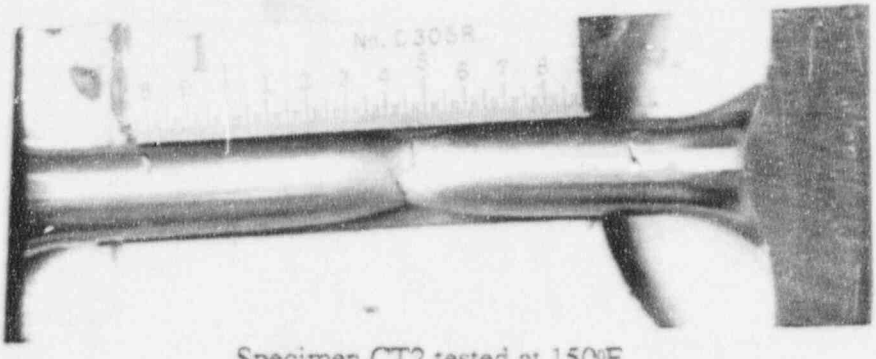

Specimen CT2 tested at 150°F

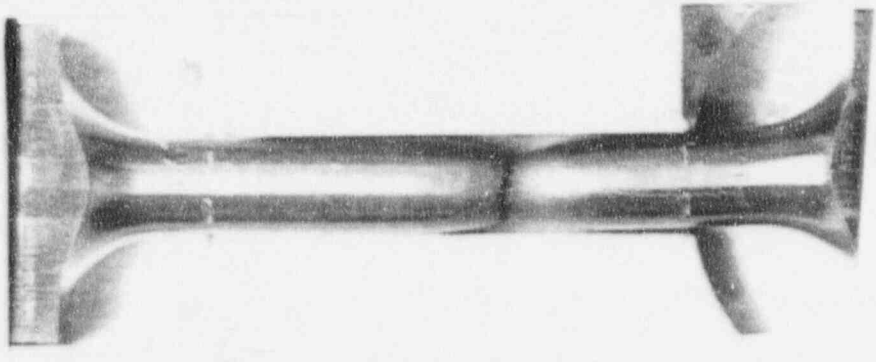

Specimen CT3 tested at 550°F

Figure 5-13 Fractured Tensile Specimens from CPSES Unit No. 2 Reactor Vessel Intermediate Shell Plate R3807-2 (Transverse Orientation)

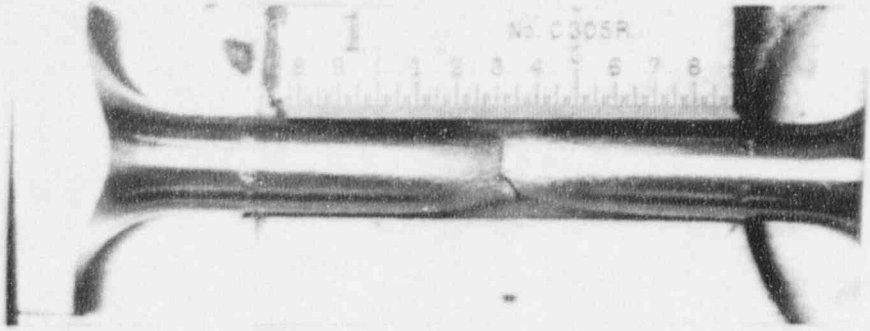

Specimen CW2 tested at 25°F

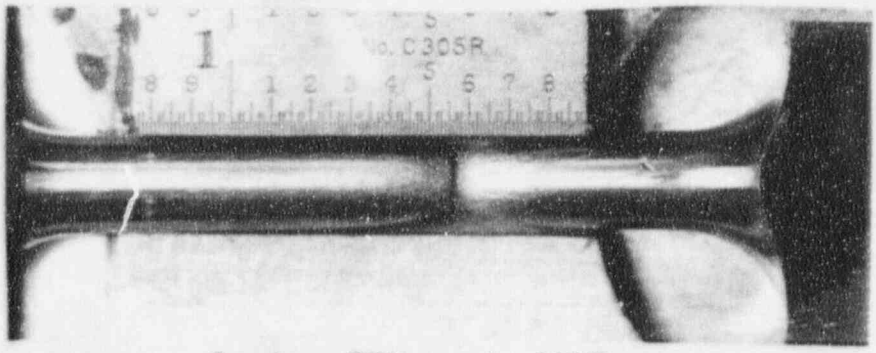

Specimen CW1 tested at 150°F

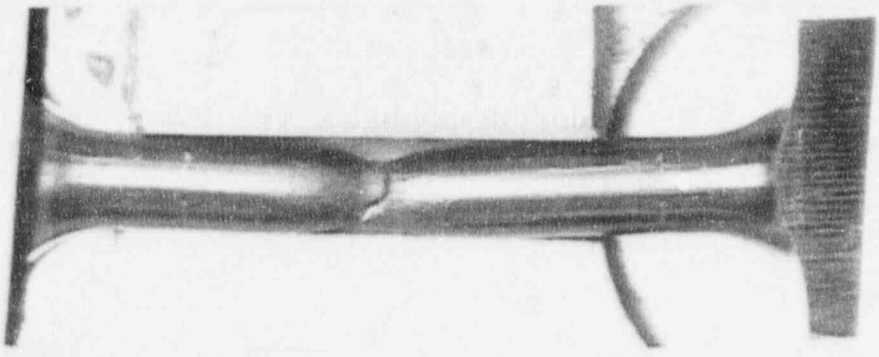

Specimen CW3 tested at 550°F

Figure 5-14 Fractured Tensile Specimens from CPSES Unit No. 2 Reactor Vessel Weld Metal

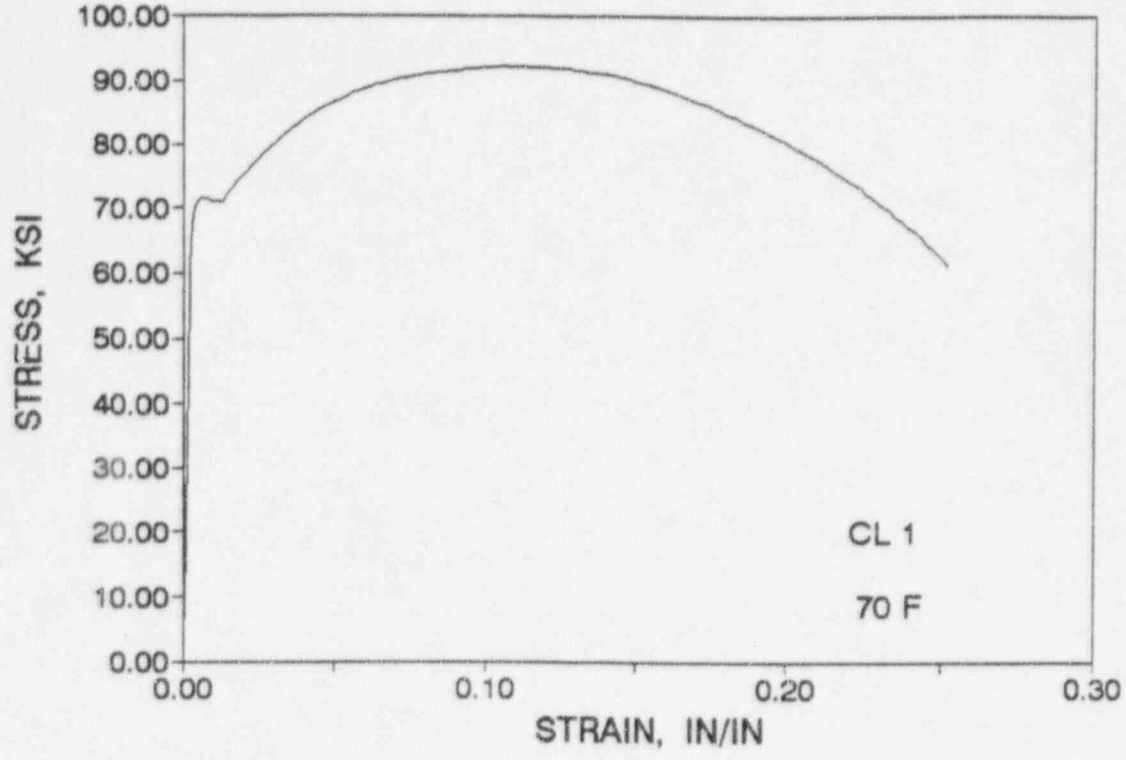

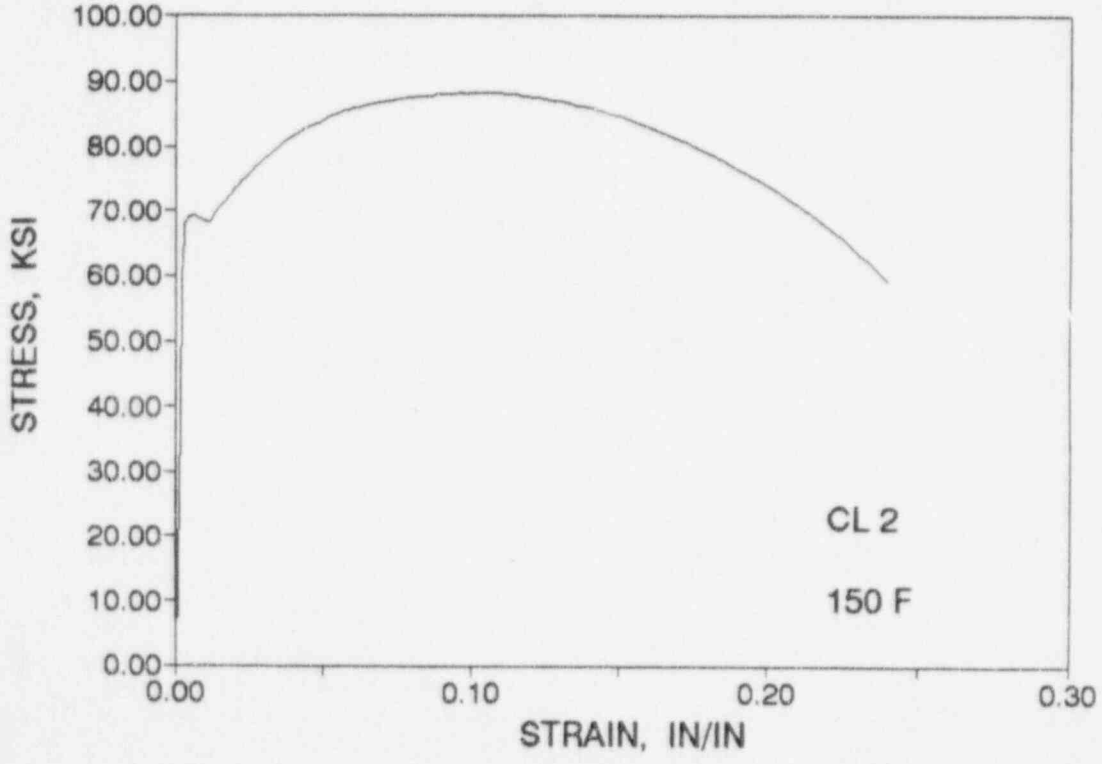

Figure 5-15 Engineering Stress-Strain Curves for Intermediate Shell Plate R3807-2 Tensile Specimens CL1 and CL2 (Longitudinal Orientation)

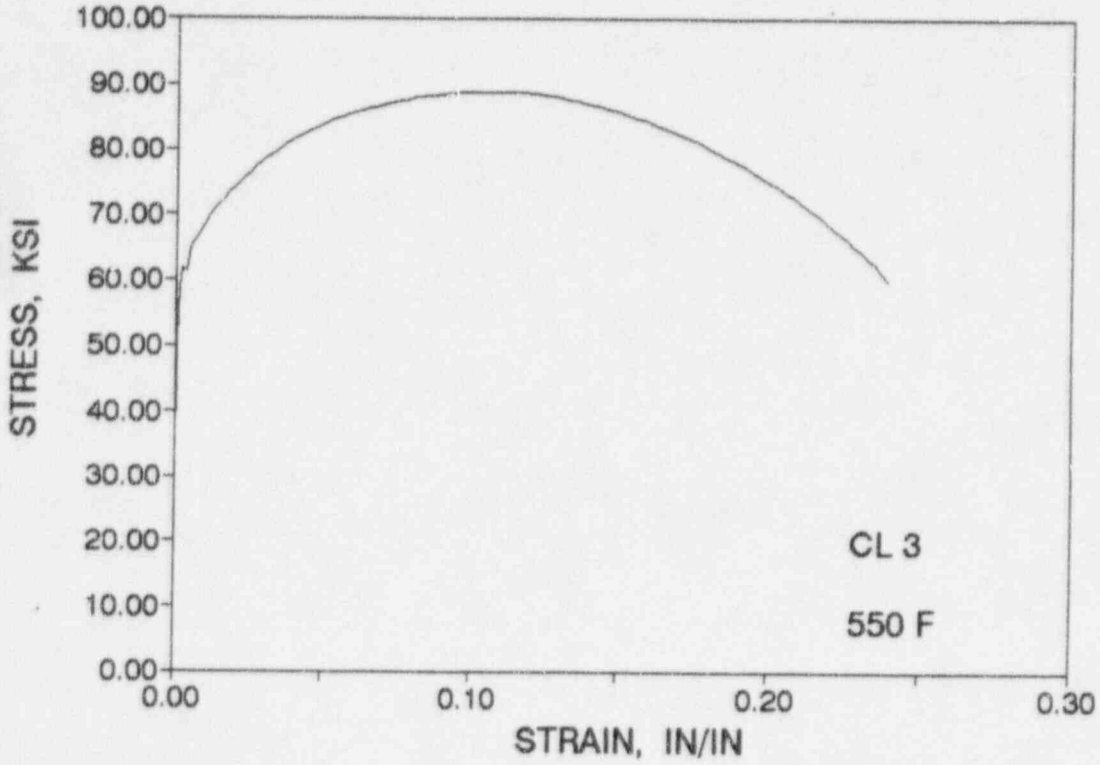

Figure 5-16 Engineering Stress-Strain Curve for Intermediate Shell Plate R3807-2 Tensile Specimen CL3 (Longitudinal Orientation)

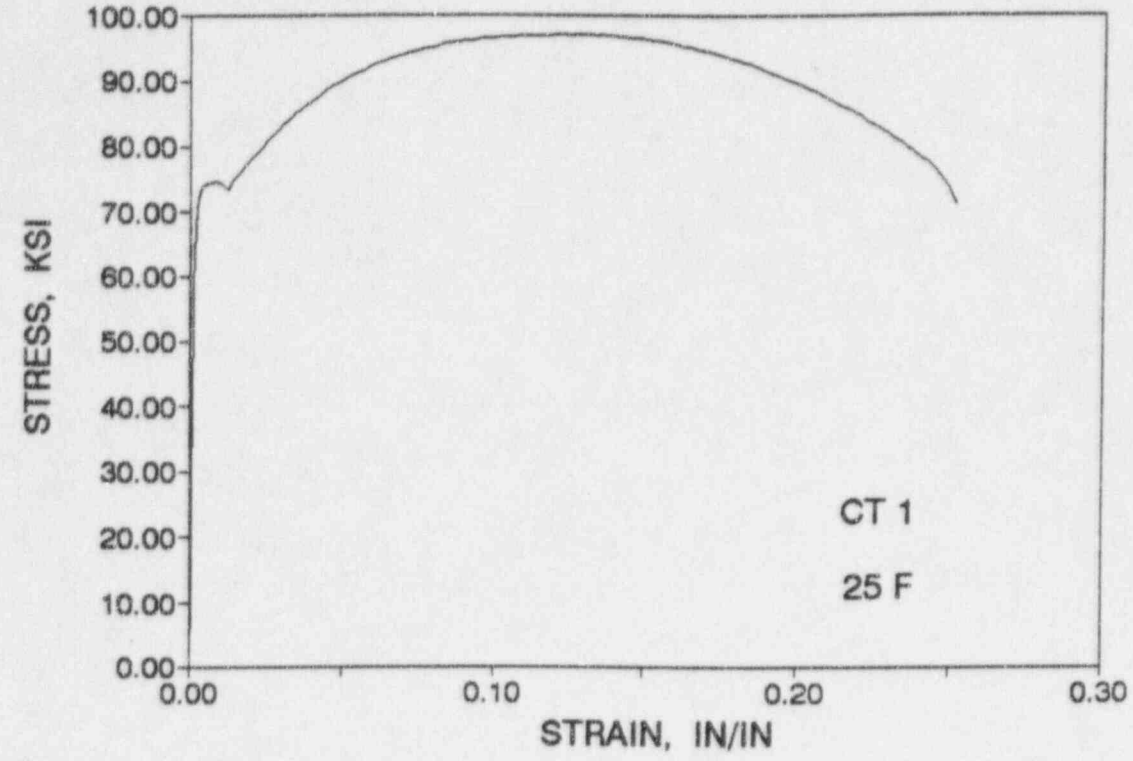

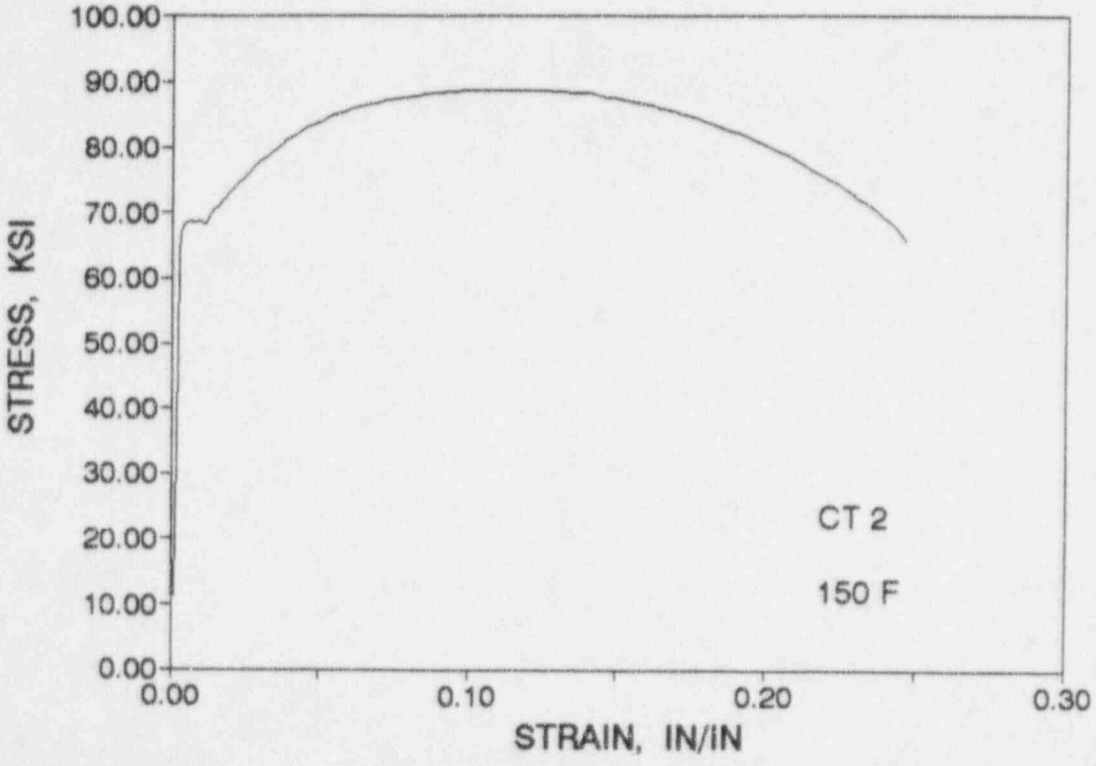

Figure 5-17 Engineering Stress-Strain Curves for Intermediate Shell Plate R3807-2 Tensile Specimens CT1 and CT2 (Transverse Orientation)

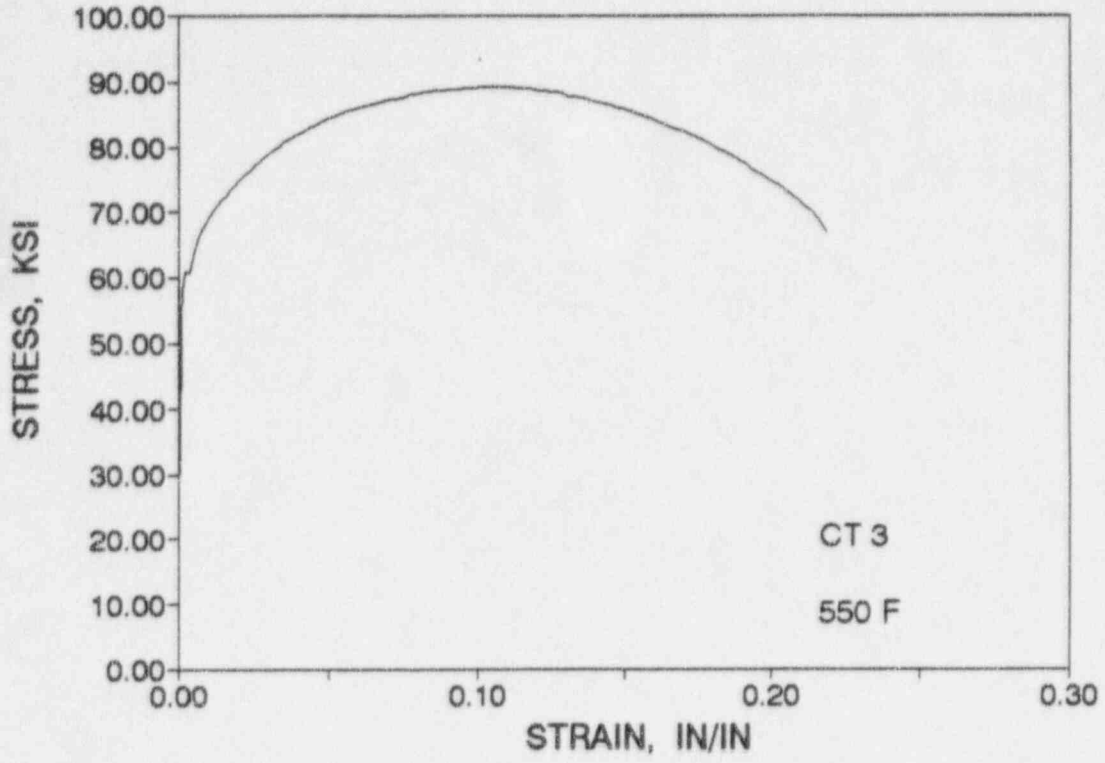

Figure 5-18 Engineering Stress-Strain Curve for Intermediate Shell Plate R3807-2 Tensile Specimen CT3 (Transverse Orientation)

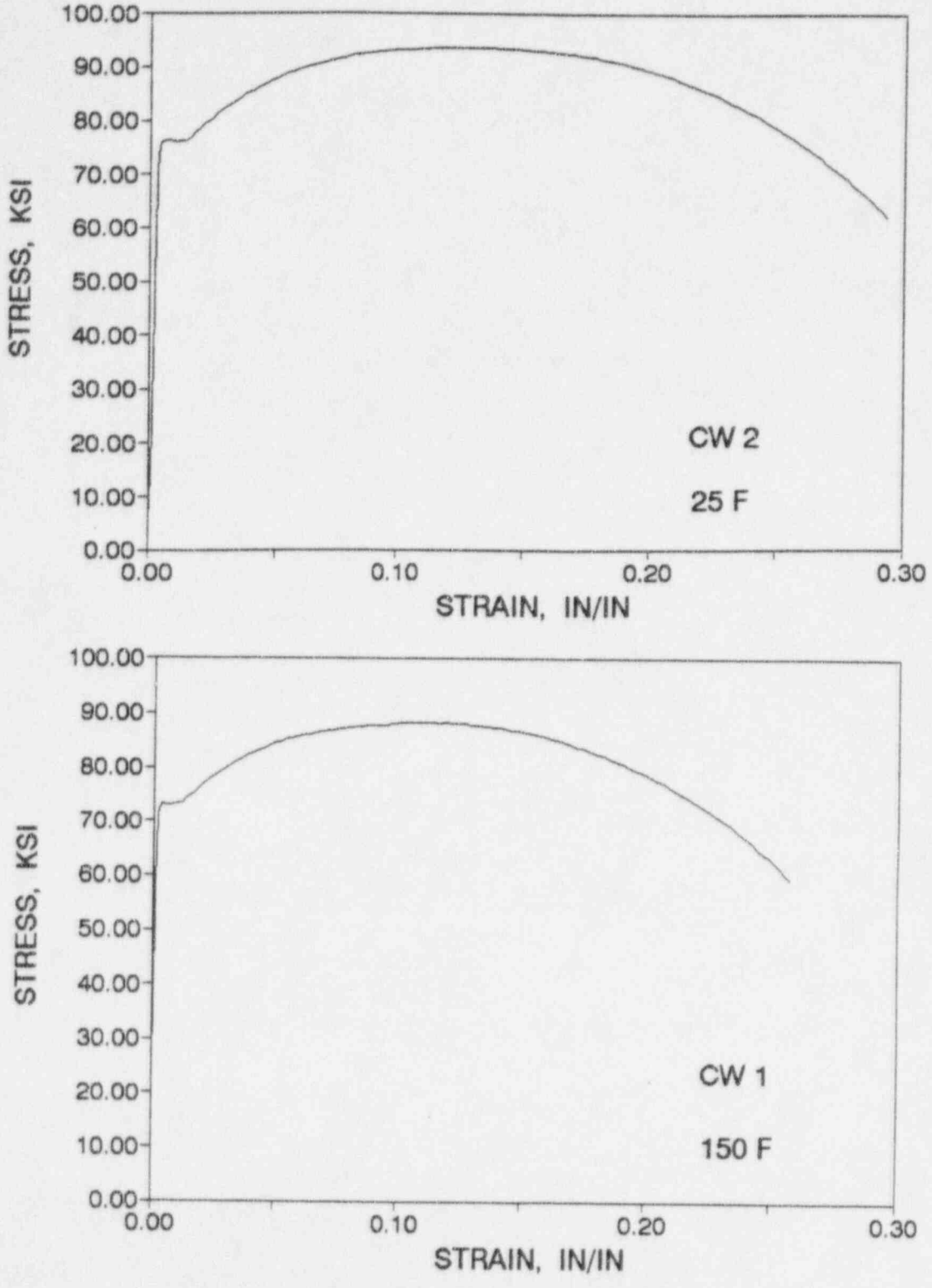

Figure 5-19 Engineering Stress-Strain Curves for Weld Metal Tensile Specimens CW2 and CW1

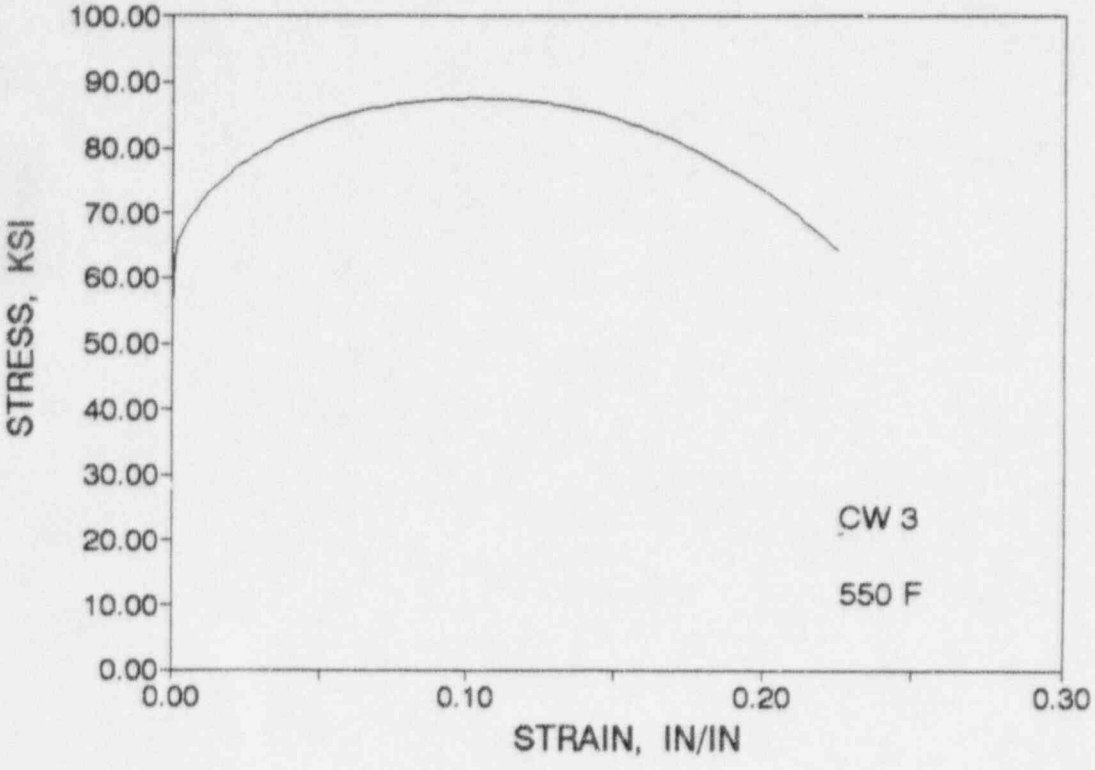

Figure 5-20 Engineering Stress-Strain Curve for Weld Metal Tensile Specimen CW3

SECTION 6.0
RADIATION ANALYSIS AND NEUTRON DOSIMETRY

6.1 Introduction

Knowledge of the neutron environment within the reactor pressure vessel and surveillance capsule geometry is required as an integral part of LWR reactor pressure vessel surveillance programs for two reasons. First, in order to interpret the neutron radiation induced material property changes observed in the test specimens, the neutron environment (energy spectrum, flux, fluence) to which the test specimens were exposed must be known. Second, in order to relate the changes observed in the test specimens to the present and future condition of the reactor vessel, a relationship must be established between the neutron environment at various positions within the pressure vessel and that experienced by the test specimens. The former requirement is normally met by employing a combination of rigorous analytical techniques and measurements obtained with passive neutron flux monitors contained in each of the surveillance capsules. The latter information is generally derived solely from analysis.

The use of fast neutron fluence (E > 1.0 MeV) to correlate measured material property changes to the neutron exposure of the material has traditionally been accepted for development of damage trend curves as well as for the implementation of trend curve data to assess vessel condition. In recent years, however, it has been suggested that an exposure model that accounts for differences in neutron energy spectra between surveillance capsule locations and positions within the vessel wall could lead to an improvement in the uncertainties associated with damage trend curves as well as to a more accurate evaluation of damage gradients through the pressure vessel wall.

Because of this potential shift away from a threshold fluence toward an energy dependent damage function for data correlation, ASTM Standard Practice E853, "Analysis and Interpretation of Light Water Reactor Surveillance Results," recommends reporting displacements per iron atom (dpa) along with fluence (E > 1.0 MeV) to provide a data base for future reference. The energy dependent dpa function to be used for this evaluation is specified in ASTM Standard Practice E693, "Characterizing Neutron Exposures in Ferritic Steels in Terms of Displacements per Atom." The application of the dpa parameter to the assessment of embrittlement gradients through the thickness of the pressure vessel wall has already been promulgated in Revision 2 to Regulatory Guide 1.99, "Radiation Embrittlement of Reactor Vessel Materials."

This section provides the results of the neutron dosimetry evaluations performed in conjunction with the analysis of test specimens contained in surveillance Capsule U, withdrawn at the end of the 1st fuel cycle. This evaluation is based on current state-of-the-art methodology and nuclear data. This report provides a consistent up-to-date database for use in evaluating the material properties of the CPSES Unit 2 reactor vessel.

In each of the dosimetry evaluations, fast neutron exposure parameters in terms of neutron fluence (E > 1.0 MeV), neutron fluence (E > 0.1 MeV), and iron atom displacements (dpa) are established for the capsule irradiation history. The analytical formalism relating the measured capsule exposure to the exposure of the vessel wall is described and used to project the integrated exposure of the vessel wall. Also, uncertainties associated with the derived exposure parameters at the surveillance capsules and with the projected exposure of the pressure vessel are provided.

6.2 Discrete Ordinates Analysis

A plan view of the reactor geometry at the core midplane is shown in Figure 4-1. Six irradiation capsules attached to the thermal shield are included in the reactor design to constitute the reactor vessel surveillance program. The capsules are located at azimuthal angles of 58.5°, 61.0°, 121.5°, 238.5°, 241.0°, and 301.5° relative to the core cardinal axis as shown in Figure 4-1. A plan view of a dual surveillance capsule holder attached to the neutron pad is shown in Figure 6-1. The stainless steel specimen containers are 1.182 by 1-inch and approximately 56 inches in height. The containers are positioned axially such that the test specimens are centered on the core midplane, thus spanning the central 5 feet of the 12 foot high reactor core.

In regard to the geometry depicted in Figure 4-1, it should be noted that, for the neutron pad arrangement in CPSES Unit 2, the azimuthal extent of the pad is not the same for all octants. For octants containing no surveillance capsules the span of the neutron pad is 12.5°; while for octants containing surveillance capsule holders the span extends to 17.5° in order to position the capsules to achieve the desired lead factors. Both of these pad configurations are considered in the fluence evaluations for the capsules and pressure vessel.

From a neutronic standpoint, the surveillance capsules and associated support structures are significant. The presence of these materials has a marked effect on both the spatial distribution of neutron flux and the neutron energy spectrum in the water annulus between the thermal shield and the reactor vessel.

In order to determine the neutron environment at the test specimen location, the capsules themselves must be included in the analytical model.

In performing the fast neutron exposure evaluations for the surveillance capsules and reactor vessel, two distinct sets of transport calculations were carried out. The first, a single computation in the conventional forward mode, was used primarily to obtain relative neutron energy distributions throughout the reactor geometry as well as to establish relative radial distributions of exposure parameters {ϕ(E > 1.0 MeV), ϕ(E > 0.1 MeV), and dpa/sec} through the vessel wall. The neutron spectral information was required for the interpretation of neutron dosimetry withdrawn from the surveillance capsules as well as for the determination of exposure parameter ratios; i.e., [dpa/sec]/[ϕ(E > 1.0 MeV)], within the pressure vessel geometry. The relative radial gradient information was required to permit the projection of measured exposure parameters to locations interior to the pressure vessel wall; i.e., the 1/4T, 1/2T, and 3/4T locations.

The second set of calculations consisted of a series of adjoint analyses relating the fast neutron flux, ϕ(E > 1.0 MeV), at surveillance capsule positions and at several azimuthal locations on the pressure vessel inner radius to neutron source distributions within the reactor core. The source importance functions generated from these adjoint analyses provided the basis for all absolute exposure calculations and comparison with measurement. These importance functions, when combined with fuel cycle specific neutron source distributions, yielded absolute predictions of neutron exposure at the locations of interest for each cycle of irradiation. They also established the means to perform similar predictions and dosimetry evaluations for all subsequent fuel cycles. It is important to note that the cycle specific neutron source distributions utilized in these analyses included not only spatial variations of fission rates within the reactor core but also accounted for the effects of varying neutron yield per fission and fission spectrum introduced by the build-up of plutonium as the burnup of individual fuel assemblies increased.

The absolute cycle specific data from the adjoint evaluations together with the relative neutron energy spectra and radial distribution information from the reference forward calculation provided the means to:

1 - Evaluate neutron dosimetry obtained from surveillance capsules.
2 - Extrapolate dosimetry results to key locations at the inner radius and through the thickness of the pressure vessel wall.
3 - Enable a direct comparison of analytical prediction with measurement.

4 - Establish a mechanism for projection of pressure vessel exposure as the design of each new fuel cycle evolves.

The forward transport calculation for the reactor model summarized in Figures 4-1 and 6-1 was carried out in R,θ geometry using the DORT two-dimensional discrete ordinates code Version 2.8.14[13] and the BUGLE 93 cross-section library[14]. The BUGLE 93 library is a 47 energy group ENDF/B-VI based data set produced specifically for light water reactor applications. In these analyses anisotropic scattering was treated with a P_3 expansion of the scattering cross-sections and the angular discretization was modeled with an S_8 order of angular quadrature.

The core power distribution utilized in the reference forward transport calculation was derived from statistical studies of long-term operation of Westinghouse 4-loop plants. Inherent in the development of this reference core power distribution is the use of an out-in fuel management strategy; i.e., fresh fuel on the core periphery. Furthermore, for the peripheral fuel assemblies, the neutron source was increased by a 2σ margin derived from the statistical evaluation of plant to plant and cycle to cycle variations in peripheral power. Axial leakage effects were taken into account by application of an axial peaking factor of 1.2. Since it is unlikely that any single reactor would exhibit power levels on the core periphery at the nominal $+2\sigma$ value for a large number of fuel cycles; and, since an axial peak to average of 1.2 tends to be bound that observed in fuel assemblies with significant burnup, the use of this reference distribution is expected to yield somewhat conservative results. The degree of conservatism could range from approximately 10% for reactors employing an out/in fuel management strategy to as much as a factor of two for reactors that have transitioned to low-leakage fuel management.

All adjoint calculations were also carried out using an S_8 order of angular quadrature and the P_3 cross-section approximation from the BUGLE 93 library. Adjoint source locations were chosen at several azimuthal locations along the pressure vessel inner radius as well as at the geometric center of each surveillance capsule. Again, these calculations were run in R,θ geometry to provide neutron source distribution importance functions for the exposure parameter of interest, in this case $\phi(E > 1.0\ \text{MeV})$.

Having the importance functions and appropriate core source distributions, the response of interest could be calculated as:

$$R(r,\theta) = \int_r \int_\theta \int_E I(r,\theta,E)\ S(r,\theta,E)\ r\ dr\ d\theta\ dE$$

where: $R(r,\theta)$ = $\phi(E > 1.0\ MeV)$ at radius r and azimuthal angle θ.

$I(r,\theta,E)$= Adjoint source importance function at radius r, azimuthal angle θ, and neutron source energy E.

$S(r,\theta,E)$= Neutron source strength at core location r,θ and energy E.

Although the adjoint importance functions used in this analysis were based on a response function defined by the threshold neutron flux $\phi(E > 1.0\ MeV)$, prior calculations[16] have shown that, while the implementation of low leakage loading patterns significantly impacts both the magnitude and spatial distribution of the neutron field, changes in the relative neutron energy spectrum are of second order. Thus, for a given location the ratio of [dpa/sec]/[$\phi(E > 1.0\ MeV)$] is insensitive to changing core source distributions. In the application of these adjoint importance functions to the CPSES Unit 2 reactor, therefore, the iron atom displacement rates (dpa/sec) and the neutron flux $\phi(E > 0.1\ MeV)$ were computed on a cycle specific basis by using [dpa/sec]/[$\phi(E > 1.0\ MeV)$] and [$\phi(E > 0.1\ MeV)$]/[$\phi(E > 1.0\ MeV)$] ratios from the forward analysis in conjunction with the cycle specific $\phi(E > 1.0\ MeV)$ solutions from the individual adjoint evaluations.

The reactor core power distributions, including the cycle specific axial distribution, used in the plant specific adjoint calculations were taken from the fuel cycle design report for the first operating cycle of CPSES Unit 2[17].

Selected results from the neutron transport analyses are provided in Tables 6-1 through 6-5. The data listed in these tables establish the means for absolute comparisons of analysis and measurement for the capsule irradiation periods and provide the means to correlate dosimetry results with the corresponding exposure of the pressure vessel wall.

In Table 6-1, the calculated exposure parameters [$\phi(E > 1.0\ MeV)$, $\phi(E > 0.1\ MeV)$, and dpa/sec] are given at the geometric center of the two surveillance capsule positions for both the reference and the plant specific core power distributions. The plant specific data, based on the adjoint transport analysis, are meant to establish the absolute comparison of measurement with analysis. The reference data derived from the forward calculation are provided as a conservative exposure evaluation against which plant specific fluence calculations can be compared. Similar data are given in Table 6-2 for the pressure vessel inner radius. Again, the three pertinent exposure parameters are listed for the reference and cycle one plant specific power distributions. It is important to note that the data for the vessel

inner radius were taken at the clad/base metal interface; and, thus, represent the maximum predicted exposure levels of the vessel wall itself.

Radial gradient information applicable to $\phi(E > 1.0\ MeV)$, $\phi(E > 0.1\ MeV)$, and dpa/sec is given in Tables 6-3, 6-4, and 6-5, respectively. The data, obtained from the reference forward neutron transport calculation, are presented on a relative basis for each exposure parameter at several azimuthal locations. Exposure distributions through the vessel wall may be obtained by normalizing the calculated or projected exposure at the vessel inner radius to the gradient data listed in Tables 6-3 through 6-5.

For example, the neutron flux $\phi(E > 1.0\ MeV)$ at the 1/4T depth in the pressure vessel wall along the 45° azimuth is given by:

$$\phi_{1/4T}(45^o) = \phi(220.27,\ 45^o)\ F(225.75,\ 45^o)$$

where: $\phi_{1/4T}(45°)$ = Projected neutron flux at the 1/4T position on the 45° azimuth.

$\phi(220.27,45°)$ = Projected or calculated neutron flux at the vessel inner radius on the 45° azimuth.

$F(225.75,45°)$ = Ratio of the neutron flux at the 1/4T position to the flux at the vessel inner radius for the 45° azimuth. This data is obtained from Table 6-3

Similar expressions apply for exposure parameters expressed in terms of $\phi(E > 0.1\ MeV)$ and dpa/sec where the attenuation function F is obtained from Tables 6-4 and 6-5, respectively.

As noted earlier in this Section, the neutron pad arrangement in CPSES Unit 2 is not the same for all octants of the reactor. For the analysis of the neutron flux to the pressure vessel, the DORT calculations were performed with the neutron pad extending from 32.5° - 45.0°. This configuration produces the maximum flux to the pressure vessel.

6.3 Neutron Dosimetry

The passive neutron sensors included in the CPSES Unit 2 surveillance program are listed in Table 6-6. Also given in Table 6-6 are the primary nuclear reactions and associated nuclear constants that

were used in the evaluation of the neutron energy spectrum within the surveillance capsules and in the subsequent determination of the various exposure parameters of interest [ϕ(E > 1.0 MeV), ϕ(E > 0.1 MeV), dpa/sec]. The relative locations of the neutron sensors within the capsules are shown in Figure 4-2. The iron, nickel, copper, and cobalt-aluminum monitors, in wire form, were placed in holes drilled in spacers at several axial levels within the capsules. The cadmium shielded uranium and neptunium fission monitors were accommodated within the dosimeter block located near the center of the capsule.

The use of passive monitors such as those listed in Table 6-6 does not yield a direct measure of the energy dependent neutron flux at the point of interest. Rather, the activation or fission process is a measure of the integrated effect that the time and energy dependent neutron flux has on the target material over the course of the irradiation period. An accurate assessment of the average neutron flux level incident on the various monitors may be derived from the activation measurements only if the irradiation parameters are well known. In particular, the following variables are of interest:

- The measured specific activity of each monitor.
- The physical characteristics of each monitor.
- The operating history of the reactor.
- The energy response of each monitor.
- The neutron energy spectrum at the monitor location.

The specific activity of each of the neutron monitors was determined using established ASTM procedures[18 through 31]. Following sample preparation and weighing, the activity of each monitor was determined by means of a lithium-drifted germanium, Ge(Li), gamma spectrometer. The irradiation history of the CPSES Unit 2 reactor during cycle one was supplied by NUREG-0020, "Licensed Operating Reactors Status Summary Report," for the applicable period. The irradiation history applicable to capsule U is given in Table 6-7.

Having the measured specific activities, the physical characteristics of the sensors, and the operating history of the reactor, reaction rates referenced to full power operation were determined from the following equation:

$$R = \frac{A}{N_0 F Y \sum \frac{P_j}{P_{ref}} C_j [1-e^{-\lambda t_j}] [e^{-\lambda t_d}]}$$

where:

R = Reaction rate averaged over the irradiation period and referenced to operation at a core power level of P_{ref} (rps/nucleus).

A = Measured specific activity (dps/gm).

N_0 = Number of target element atoms per gram of sensor.

F = Weight fraction of the target isotope in the sensor material.

Y = Number of product atoms produced per reaction.

P_j = Average core power level during irradiation period j (MW).

P_{ref} = Maximum or reference power level of the reactor (MW).

C_j = Calculated ratio of $\phi(E > 1.0\ MeV)$ during irradiation period j to the time weighted average $\phi(E > 1.0\ MeV)$ over the entire irradiation period.

λ = Decay constant of the product isotope (1/sec).

t_j = Length of irradiation period j (sec).

t_d = Decay time following irradiation period j (sec).

and the summation is carried out over the total number of monthly intervals comprising the irradiation period.

In the equation describing the reaction rate calculation, the ratio $[P_j]/[P_{ref}]$ accounts for month by month variation of reactor core power level within any given fuel cycle as well as over multiple fuel cycles. The ratio C_j, which can be calculated for each fuel cycle using the adjoint transport technology discussed in Section 6.2, accounts for the change in sensor reaction rates caused by variations in flux level induced by changes in core spatial power distributions from fuel cycle to fuel cycle. For a single cycle irradiation C_j is normally taken to be 1.0. However, for multiple cycle irradiations, particularly those employing low leakage fuel management, the additional C_j term should be employed. The impact of changing flux levels for constant power operation can be quite significant for sensor sets that have been irradiated for many cycles in a reactor that has transitioned from non-low leakage to low leakage fuel management or for sensor sets contained in surveillance capsules that have been moved from one capsule location to another.

For the irradiation history of Capsule U, the flux level term in the reaction rate calculations was developed from the plant specific analysis provided in Table 6-1. Measured and saturated reaction product specific activities as well as the derived full power reaction rates are listed in Table 6-8.

Values of key fast neutron exposure parameters were derived from the measured reaction rates using the FERRET least squares adjustment code[32]. The FERRET approach used the measured reaction rate data, sensor reaction cross-sections, and a calculated trial spectrum as input and proceeded to adjust the group fluxes from the trial spectrum to produce a best fit (in a least squares sense) to the measured reaction rate data. The "measured" exposure parameters along with the associated uncertainties were then obtained from the adjusted spectrum.

In the FERRET evaluations, a log-normal least squares algorithm weights both the a priori values and the measured data in accordance with the assigned uncertainties and correlations. In general, the measured values f are linearly related to the flux ϕ by some response matrix A:

$$f_i^{(s,\alpha)} = \sum_g A_{ig}^{(s)} \phi_g^{(\alpha)}$$

where i indexes the measured values belonging to a single data set s, g designates the energy group, and α delineates spectra that may be simultaneously adjusted. For example,

$$R_i = \sum_g \sigma_{ig} \phi_g$$

relates a set of measured reaction rates R_i to a single spectrum ϕ_g by the multigroup reaction cross-section σ_{ig}. The log-normal approach automatically accounts for the physical constraint of positive fluxes, even with large assigned uncertainties.

In the least squares adjustment, the continuous quantities (i.e., neutron spectra and cross-sections) were approximated in a multi-group format consisting of 53 energy groups. The trial input spectrum was converted to the FERRET 53 group structure using the SAND-II code[33]. This procedure was carried out by first expanding the 47 group calculated spectrum into the SAND-II 620 group structure using a SPLINE interpolation procedure in regions where group boundaries do not coincide. The 620 point spectrum was then re-collapsed into the group structure used in FERRET.

The sensor set reaction cross-sections, obtained from the ENDF/B-VI dosimetry file[15], were also collapsed into the 53 energy group structure using the SAND-II code. In this instance, the trial spectrum, as expanded to 620 groups, was employed as a weighting function in the cross-section collapsing procedure. Reaction cross-section uncertainties in the form of a 53 x 53 covariance matrix

for each sensor reaction were also constructed from the information contained on the ENDF/B-VI data files. These matrices included energy group to energy group uncertainty correlations for each of the individual reactions. However, correlations between cross-sections for different sensor reactions were not included. The omission of this additional uncertainty information does not significantly impact the results of the adjustment.

Due to the importance of providing a trial spectrum that exhibits a relative energy distribution close to the actual spectrum at the sensor set locations, the neutron spectrum input to the FERRET evaluation was taken from the center of the surveillance capsule modeled in the reference forward transport calculation. While the 53 x 53 group covariance matrices applicable to the sensor reaction cross-sections were developed from the ENDF/B-VI data files, the covariance matrix for the input trial spectrum was constructed from the following relation:

$$M_{gg'} = R_n^2 + R_g R_{g'} P_{gg'}$$

where R_n specifies an overall fractional normalization uncertainty (i.e., complete correlation) for the set of values. The fractional uncertainties R_g specify additional random uncertainties for group g that are correlated with a correlation matrix given by:

$$P_{gg'} = [1-\theta]\ \delta_{gg'} + \theta\ e^{-H}$$

where:

$$H = \frac{(g-g')^2}{2\ \gamma^2}$$

The first term in the correlation matrix equation specifies purely random uncertainties, while the second term describes short range correlations over a group range γ (θ specifies the strength of the latter term). The value of δ is 1 when g = g' and 0 otherwise. For the trial spectrum used in the current evaluations, a short range correlation of γ = 6 groups was used. This choice implies that neighboring groups are strongly correlated when θ is close to 1. Strong long range correlations (or anti-correlations) were justified based on information presented by R. E. Maerker[34]. Maerker's results are closely duplicated when γ = 6.

The uncertainties associated with the measured reaction rates included both statistical (counting) and systematic components. The systematic component of the overall uncertainty accounts for counter efficiency, counter calibrations, irradiation history corrections, and corrections for competing reactions

in the individual sensors. A combination of these sources of uncertainty result in reaction rate uncertainties of ±5% for non-fission reactions and ±10% for the fission reactions.

Results of the FERRET evaluations of the Capsule U dosimetry are given in Table 6-9. The data summarized in this table includes fast neutron exposure evaluations in terms of $\Phi(E > 1.0$ MeV), $\Phi(E > 0.1$ MeV), and dpa. In general good results were achieved in the fits of the adjusted spectra to the individual measured reaction rates. The measured and FERRET adjusted reaction rates for each reaction are given in Table 6-10. Table 6-10 also depicts the level of precision associated with each reaction via a ratio of calculated rate to measured rate. The adjusted spectra from the least squares evaluation is given in Table 6-11 in the FERRET 53 energy group structure. Table 6-12, titled "Comparison of Calculated and Measured Neutron Exposure Levels for CPSES Unit 2 Surveillance Capsule U", compares the measured and calculated fluence at the capsule. The results for capsule U are consistent with results obtained from similar evaluations of dosimetry from other Westinghouse reactors.

6.4 Projections of Pressure Vessel Exposure

Neutron exposure projections at key locations on the pressure vessel inner radius are given in Table 6-13. Along with the current (0.904 EFPY) exposure, projections are also provided for exposure periods of 15 EFPY, 32 EFPY and 48 EFPY. In computing these vessel exposures, the calculated values from Table 6-13 were scaled by the average measurement/calculation ratios (M/C) observed from the evaluations of dosimetry from Capsule U for each fast neutron exposure parameter. This procedure resulted in bias factors of 1.091, 1.225, and 1.148 being applied to the calculated values of $\Phi(E > 1.0$ MeV), $\Phi(E > 0.1$ MeV), and dpa, respectively. Projections for future operation were based on the assumption that the best estimate exposure rates characteristic of the first cycle irradiation would continue to be applicable throughout plant life.

The overall uncertainty in the best estimate exposure projections within the pressure vessel wall stem primarily from two sources;

1) the uncertainty in the M/C ratios derived from the plant specific measurement data base; and
2) the analytical uncertainty associated with relating the results at the measurement locations to the desired results within the pressure vessel wall.

Uncertainty in the M/C ratios derives directly from the individual uncertainties in the measurement process, in the least squares adjustment procedure, and in the location of the surveillance capsule and cavity dosimetry sensor sets. The analytical uncertainty in the relationship between the exposure of the pressure vessel and the exposure at the measurement locations is and on downcomer water density variations and vessel inner radius tolerance relative to the surveillance capsule data.

The 1σ uncertainties associated with the M/C ratios applicable to $\Phi(E > 1.0$ MeV), $\Phi(E > 0.1$ MeV), and dpa are given in Table 6-9 of this report. The additional information pertinent to the required analytical uncertainty for vessel locations has been obtained from benchmarking studies using the Westinghouse neutron transport methodology and from several comparisons of power reactor internal surveillance capsule dosimetry and reactor cavity dosimetry for which the irradiation history of all sensors was the same.

Based on these benchmarking evaluations the additional uncertainty associated with the tolerances in dosimetry positioning, vessel thickness, vessel inner radius and downcomer temperature was estimated to be approximately 6% for all exposure parameters. These uncertainty components were then combined as follows:

	1σ UNCERTAINTY		
	$\Phi(E > 1.0$ MeV)	$\Phi(E > 0.1$ MeV)	dpa
M/C Ratio	8%	16%	11%
Analytical	6%	6%	6%
Combined	10.0%	17%	13%

Thus, the total uncertainty associated with the neutron exposure projections at the pressure vessel clad/base metal interface for CPSES Unit 2 was estimated to be:

	1σ Uncertainty
$\Phi(E > 1.0$ MeV)	10%
$\Phi(E > 0.1$ MeV)	17%
dpa	13%

These uncertainty values are well within the 20% 1σ uncertainty in vessel fluence projections required by the PTS rule.

In the calculation of exposure gradients for the CPSES Unit 2 reactor vessel, exposure projections to 15, 32, and 48 EFPY were also employed. Data based on both a $\Phi(E > 1.0\ MeV)$ slope and a plant specific dpa slope through the vessel wall are provided in Table 6-14.

In order to access RT_{NDT} vs fluence curves, dpa equivalent fast neutron fluence levels for the 1/4T and 3/4T positions were defined by the relations:

$$\phi(1/4T) = \phi(0T)\ \frac{dpa(1/4T)}{dpa(0T)}$$

and

$$\phi(3/4T) = \phi(0T)\ \frac{dpa(3/4T)}{dpa(0T)}$$

Using this approach results in the dpa equivalent fluence values listed in Table 6-14. In Table 6-15 updated lead factors are listed for each of the CPSES Unit 2 surveillance capsules. Lead factor data based on the accumulated fluence for cycle one are provided for each remaining capsule.

FIGURE 6-1

PLAN VIEW OF A DUAL REACTOR VESSEL SURVEILLANCE CAPSULE

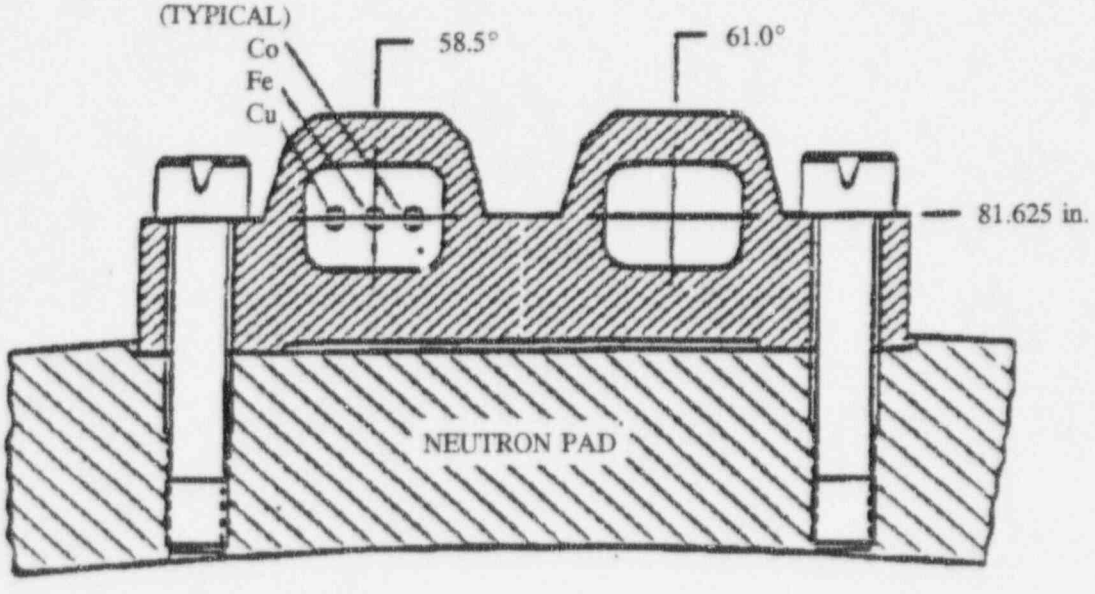

TABLE 6-1

CALCULATED FAST NEUTRON EXPOSURE RATES AT

THE SURVEILLANCE CAPSULE CENTER

ϕ (E >1.0 MeV) [n/cm2-sec]

LOCATION	29.0°	31.5°
CYCLE 1	9.64E+10	1.06E+11
CRSD Data	1.20E+11	1.28E+11

ϕ (E > 0.1 MeV) [n/cm2-sec]

LOCATION	29.0°	31.5°
CYCLE 1	4.05E+11	4.49E+11
CRSD Data	5.02E+11	5.43E+11

Iron Displacement Rate [dpa/sec]

LOCATION	29.0°	31.5°
CYCLE 1	1.84E-10	2.02E-10
CRSD Data	2.28E-10	2.44E-10

TABLE 6-2

CALCULATED AZIMUTHAL VARIATION OF FAST NEUTRON EXPOSURE RATES AT THE PRESSURE VESSEL CLAD/BASE METAL INTERFACE

$\phi(E > 1.0MeV)$ [n/cm^2-sec]

	0.0°	15.0°	25.0°	30.0°	35.0°	45.0°
CYCLE 1	1.26E+10	1.93E+10	2.33E+10	2.31E+10	2.12E+10	2.58E+10
CRSD Data	1.61E+10	2.51E+10	2.97E+10	2.86E+10	2.53E+10	2.99E+10

$\phi(E > 0.1MeV)$ [n/cm^2-sec]

	0.0°	15.0°	25.0°	30.0°	35.0°	45.0°
CYCLE 1	2.53E+10	3.93E+10	4.80E+10	4.81E+10	4.92E+10	6.15E+10
CRSD Data	3.23E+10	5.11E+10	6.11E+10	5.94E+10	5.88E+10	7.15E+10

Iron Atom Displacement Rate [dpa/sec]

	0.0°	15.0°	25.0°	30.0°	35.0°	45.0°
CYCLE 1	1.94E-11	2.95E-11	3.55E-11	3.53E-11	3.30E-11	4.02E-11
CRSD Data	2.48E-11	3.83E-11	4.52E-11	4.36E-11	3.95E-11	4.68E-11

TABLE 6-3

RELATIVE RADIAL DISTRIBUTION OF ϕ(E > 1.0 MeV)

WITHIN THE PRESSURE VESSEL WALL

Radius (cm)	0.0°	15.0°	25.0°	35.0°	45.0°
220.35[1]	1.00	1.00	1.00	1.00	1.00
221.00	0.959	0.958	0.958	0.954	0.957
222.30	0.852	0.850	0.850	0.841	0.846
223.60	0.739	0.736	0.738	0.728	0.730
224.89	0.634	0.630	0.630	0.623	0.623
225.87	0.562	0.557	0.556	0.551	0.548
227.01	0.487	0.482	0.481	0.474	0.473
228.63	0.395	0.390	0.390	0.385	0.381
230.90	0.326	0.321	0.320	0.318	0.312
231.39	0.274	0.269	0.268	0.266	0.260
232.68	0.229	0.225	0.224	0.222	0.217
234.14	0.188	0.184	0.183	0.181	0.176
235.76	0.150	0.146	0.146	0.144	0.140
236.90	0.127	0.124	0.124	0.124	0.118
237.88	0.110	0.107	0.107	0.106	0.102
239.18	0.091	0.089	0.088	0.087	0.083
240.47	0.075	0.073	0.072	0.072	0.068
241.77	0.061	0.058	0.058	0.058	0.054
242.42[2]	0.058	0.055	0.055	0.055	0.051

NOTES: 1) Base Metal Inner Radius
2) Base Metal Outer Radius

TABLE 6-4

RELATIVE RADIAL DISTRIBUTION OF $\phi(E > 0.1$ MeV)

WITHIN THE PRESSURE VESSEL WALL

Radius (cm)	0.0°	15.0°	25.0°	35.0°	45.0°
220.35[1]	1.00	1.00	1.00	1.00	1.00
221.00	1.00	1.00	1.00	1.00	1.00
222.30	1.00	0.997	0.997	0.990	0.989
223.60	0.967	0.958	0.958	0.951	0.945
224.89	0.922	0.909	0.909	0.902	0.893
225.87	0.884	0.869	0.869	0.863	0.850
227.01	0.837	0.821	0.821	0.814	0.800
228.63	0.770	0.753	0.753	0.748	0.729
230.09	0.710	0.692	0.693	0.689	0.667
231.39	0.657	0.639	0.639	0.635	0.612
232.68	0.604	0.587	0.586	0.583	0.558
234.14	0.546	0.529	0.529	0.526	0.500
235.76	0.484	0.469	0.468	0.467	0.438
236.90	0.441	0.427	0.427	0.426	0.396
237.88	0.403	0.391	0.390	0.389	0.360
239.18	0.356	0.345	0.344	0.343	0.313
240.47	0.310	0.300	0.298	0.298	0.267
241.77	0.265	0.252	0.251	0.251	0.220
242.42[2]	0.256	0.242	0.240	0.240	0.210

NOTES: 1) Base Metal Inner Radius
2) Base Metal Outer Radius

TABLE 6-5

RELATIVE RADIAL DISTRIBUTION OF dpa/sec

WITHIN THE PRESSURE VESSEL WALL

Radius (cm)	0.0°	15.0°	25.0°	35.0°	45.0°
220.35[1]	1.00	1.00	1.00	1.00	1.00
221.00	0.965	0.964	0.965	0.963	0.965
222.30	0.877	0.876	0.877	0.873	0.878
223.60	0.785	0.782	0.784	0.784	0.788
224.89	0.699	0.695	0.697	0.699	0.703
225.87	0.638	0.634	0.636	0.641	0.642
227.01	0.575	0.571	0.573	0.578	0.579
228.63	0.495	0.491	0.493	0.499	0.500
230.09	0.432	0.427	0.430	0.438	0.437
231.39	0.383	0.378	0.380	0.389	0.387
232.68	0.339	0.334	0.336	0.345	0.342
234.14	0.295	0.291	0.292	0.300	0.297
235.76	0.252	0.248	0.250	0.258	0.253
236.90	0.224	0.221	0.222	0.231	0.224
237.88	0.202	0.199	0.200	0.208	0.201
239.18	0.175	0.173	0.174	0.180	0.172
240.47	0.150	0.148	0.149	0.155	0.145
241.77	0.128	0.124	0.124	0.130	0.120
242.42[2]	0.124	0.119	0.119	0.125	0.115

NOTES: 1) Base Metal Inner Radius
2) Base Metal Outer Radius

TABLE 6-6

NUCLEAR PARAMETERS USED IN THE EVALUATION OF NEUTRON SENSORS

Monitor Material	Reaction of Interest	Target Weight Fraction	Response Range	Product Half-Life	Fission Yield (%)
Copper	$Cu^{63}(n,\alpha)Co^{60}$	0.6917	E > 4.7 MeV	5.271 yrs	
Iron	$Fe^{54}(n,p)Mn^{54}$	0.0580	E > 1.0 MeV	312.5 days	
Nickel	$Ni^{58}(n,p)Co^{58}$	0.6827	E > 1.0 MeV	70.78 days	
Uranium-238*	$U^{238}(n,f)Cs^{137}$	1.0	E > 0.4 MeV	30.17 yrs	6.00
Neptunium-237*	$Np^{237}(n,f)Cs^{137}$	1.0	E > 0.08 MeV	30.17 yrs	6.27
Cobalt-Aluminum*	$Co^{59}(n,\gamma)Co^{60}$	0.0015	0.4ev>E>0.015 MeV	5.271 yrs	
Cobalt-Aluminum	$Co^{59}(n,\gamma)Co^{60}$	0.0015	E > 0.015 MeV	5.271 yrs	

Notes: 1) * Denotes that sensor is cadmium shielded.
2) Nuclear data for sensor materials were taken from the following ASTM Standards:
ASTM-E1005-84 (91)
ASTM-E704-90
ASTM-E705-90

TABLE 6-7

MONTHLY THERMAL GENERATION DURING THE FIRST FUEL CYCLE

OF THE CPSES UNIT 2 REACTOR

Year	Month	Thermal Generation (MW-hr)
1993	Mar	13,098
	Apr	665,234
	May	499,370
	Jun	0
	Jul	1,398,238
	Aug	2,327,446
	Sep	1,317,156
	Oct	2,397,394
	Nov	2,063,460
	Dec	2,512,502
1994	Jan	2,471,383
	Feb	1,545,139
	Mar	1,165,937
	Apr	1,225,908
	May	0
	Jun	608,844
	Jul	2,417,832
	Aug	1,728,622
	Sep	2,323,594
	Oct	342,494

TABLE 6-8

MEASURED SENSOR ACTIVITIES AND REACTION RATES

SURVEILLANCE CAPSULE U

SATURATED ACTIVITIES AND REACTION RATES

Reaction	Measured Activity (DPS/GM)	Saturated Activity (DPS/GM)	Reaction Rate (DPS/ATOM)
Cu-63 (n,α) Co-60			
95-218 Top	4.78E+04	4.59E+05	7.01E-17
95-223 Mid	4.28E+04	4.11E+05	6.27E-17
95-228 Bottom	4.29E+04	4.12E+05	6.29E-17
** AVERAGES **	4.45E+04	4.27E+05	6.52E-17
Fe-54 (n,p) Mn-54			
95-220 Top	1.39E+06	4.11E+06	6.57E-15
95-225 Mid	1.27E+06	3.75E+06	6.00E-15
95-230 Bottom	1.27E+06	3.75E+06	6.00E-15
** AVERAGES **	1.31E+06	3.87E+06	6.19E-15
Ni-58 (n,p) Co-58			
95-219 Top	1.30E+07	6.07E+07	8.67E-15
95-224 Middle	1.21E+07	5.65E+07	8.07E-15
95-229 Bottom	1.21E+07	5.65E+07	8.07E-15
** AVERAGES **	1.24E+07	5.79E+07	8.27E-15
Co-59 (n,γ) Co-60			
95-216 Top	9.83E+06	9.44E+07	6.16E-12
95-221 Middle	1.03E+07	9.89E+07	6.46E-12
95-226 Bottom	1.03E+07	9.89E+07	6.46E-12
** AVERAGES **	1.01E+07	9.74E+07	6.36E-12

TABLE 6-8

MEASURED SENSOR ACTIVITIES AND REACTION RATES

SURVEILLANCE CAPSULE U

SATURATED ACTIVITIES AND REACTION RATES

Reaction	Measured Activity (DPS/GM)	Saturated Activity (DPS/GM)	Reaction Rate (DPS/ATOM)
Co-59 (n,γ) Co-60*			
95-217 Top	5.29E+06	5.08E+07	3.32E-12
95-222 Middle	5.65E+06	5.43E+07	3.54E-12
95-227 Bottom	5.55E+06	5.33E+07	3.48E-12
** AVERAGES **	5.50E+06	5.28E+07	3.45E-12
U-238 (n,f) Cs-137*			
95-214 Middle	1.37E+05	6.75E+06	3.88E-14**
Np-237 (n,f) Cs-137*			
95-215 Middle	1.21E+06	5.97E+07	3.75E-13

*Denotes that monitor is cadmium shielded.
**Corrected for Pu-239 build-in at .87

TABLE 6-9

SUMMARY OF NEUTRON DOSIMETRY RESULTS

SURVEILLANCE CAPSULE U

Quantity	Flux (n/cm^2-sec)	Fluence (n/cm^2)	Uncertainty
FLUX, E< 0.414 EV	1.19E+11	3.41E+18	±22 %
FLUX, E> 0.1 MEV	5.50E+11	1.57E+19	±16 %
FLUX, E> 1.0 MEV	1.15E+11	3.28E+18	± 8 %
DPA/SECOND	2.32E-10	6.61E-03	±11 %

TABLE 6-10

COMPARISON OF MEASURED AND FERRET CALCULATED

REACTION RATES AT THE SURVEILLANCE CAPSULE CENTER

SURVEILLANCE CAPSULE U

	REACTION RATE (DPS/NUCLEUS)		RATIO CALC/MEAS
Reaction	Meas	Adj Calc	Adj Calc
Cu63(n,α) Co60	6.52E-17	6.35E-17	0.97
Np237(n,f) Cs137*	3.74E-13	3.66E-13	0.98
Fe54(n,p) Mn54	6.19E-15	6.33E-15	1.02
Ni58(n,p) Co58	8.27E-15	8.57E-15	1.04
U238(n,f) Cs137*	3.88E-14	3.50E-14	0.90
Co59(n,γ) Co60	6.36E-12	6.28E-12	0.99
Co59(n,γ) Co60*	3.44E-12	3.47E-12	1.01

*Denotes that monitor is cadmium shielded.

TABLE 6-11

ADJUSTED NEUTRON ENERGY SPECTRUM AT THE

CENTER OF SURVEILLANCE CAPSULE U

Group #	Energy (MeV)	Flux (n/cm^2-sec)	Group #	Energy (MeV)	Flux (n/cm^2-sec)
1	1.73E+01	8.63E+06	28	9.12E-03	2.48E+10
2	1.49E+01	1.83E+07	29	5.53E-03	3.19E+10
3	1.35E+01	6.64E+07	30	3.36E-03	9.93E+09
4	1.16E+01	1.79E+08	31	2.84E-03	9.51E+09
5	1.00E+01	3.99E+08	32	2.40E-03	9.24E+09
6	8.61E+00	6.85E+08	33	2.04E-03	2.71E+10
7	7.41E+00	1.64E+09	34	1.23E-03	2.63E+10
8	6.07E+00	2.46E+09	35	7.49E-04	2.42E+10
9	4.97E+00	5.05E+09	36	4.54E-04	2.18E+10
10	3.68E+00	5.92E+09	37	2.75E-04	2.40E+10
11	2.87E+00	1.08E+10	38	1.67E-04	2.50E+10
12	2.23E+00	1.73E+10	39	1.01E-04	2.53E+10
13	1.74E+00	2.45E+10	40	6.14E-05	2.51E+10
14	1.35E+00	2.87E+10	41	3.73E-05	2.47E+10
15	1.11E-00	5.10E+10	42	2.26E-05	2.40E+10
16	8.21E-01	6.05E+10	43	1.37E-05	2.32E+10
17	6.39E-01	6.68E+10	44	8.32E-06	2.24E+10
18	4.98E-01	4.60E+10	45	5.04E-06	2.15E+10
19	3.88E-01	6.99E+10	46	3.06E-06	2.13E+10
20	3.02E-01	7.36E+10	47	1.86E-06	2.12E+10
21	1.83E-01	7.29E+10	48	1.13E-06	1.59E+10
22	1.11E-01	5.33E+10	49	6.83E-07	2.00E+10
23	6.74E-02	4.14E+10	50	4.14E-07	2.20E+10
24	4.09E-02	2.23E+10	51	2.51E-07	2.12E+10
25	2.55E-02	2.58E+10	52	1.52E-07	1.89E+10
26	1.99E-02	1.24E+10	53	9.24E-08	5.74E+10
27	1.50E-02	2.16E+10			

Note: Tabulated energy levels represent the upper energy in each group.

TABLE 6-12

COMPARISON OF CALCULATED AND MEASURED NEUTRON EXPOSURE LEVELS FOR CPSES UNIT 2 SURVEILLANCE CAPSULE U

	Calculated	Measured	M/C
Fluence (E > 1.0 MeV) [n/cm^2-sec]	3.01E+18	3.28E+18	1.09
Fluence (E > 0.1 MeV) [n/cm^2-sec]	1.28E+19	1.57E+19	1.23
dpa	5.76E-03	6.61E-03	1.15

TABLE 6-13

NEUTRON EXPOSURE PROJECTIONS AT KEY LOCATIONS

ON THE PRESSURE VESSEL CLAD/BASE METAL INTERFACE

BEST ESTIMATE EXPOSURE (0.904 EFPY) AT THE PRESSURE VESSEL INNER RADIUS

	0.0°	15.0°	25.0°	30.0°	35°	45°
E > 1.0	3.92E+17	6.02E+17	7.26E+17	7.20E+17	6.59E+17	8.02E+17
E > 0.1	8.84E+17	1.38E+18	1.68E+18	1.68E+18	1.72E+18	2.15E+18
dpa	6.35E-04	9.66E-04	1.16E-03	1.16E-03	1.08E-03	1.32E-03

BEST ESTIMATE EXPOSURE (15 EFPY) AT THE PRESSURE VESSEL INNER RADIUS

	0.0°	15.0°	25.0°	30.0°	35°	45°
E > 1.0	6.51E+18	9.98E+18	1.20E+19	1.19E+19	1.09E+19	1.33E+19
E > 0.1	1.47E+19	2.28E+19	2.78E+19	2.79E+19	2.85E+19	3.56E+19
dpa	1.05E-02	1.60E-02	1.93E-02	1.92E-02	1.79E-02	2.19E-02

BEST ESTIMATE EXPOSURE (32 EFPY) AT THE PRESSURE VESSEL INNER RADIUS

	0.0°	15.0°	25.0°	30.0°	35°	45°
E > 1.0	1.39E+19	2.13E+19	2.57E+19	2.55E+19	2.33E+19	2.84E+19
E > 0.1	3.13E+19	4.87E+19	5.93E+19	5.95E+19	6.08E+19	7.61E+19
dpa	2.25E-02	3.42E-02	4.12E-02	4.09E-02	3.83E-02	4.66E-02

BEST ESTIMATE EXPOSURE (48 EFPY) AT THE PRESSURE VESSEL INNER RADIUS

	0.0°	15.0°	25.0°	30.0°	35°	45°
E > 1.0	2.08E+19	3.19E+19	3.86E+19	3.82E+19	3.50E+19	4.26E+19
E > 0.1	4.69E+19	7.30E+19	8.90E+19	8.92E+19	9.12E+19	1.14E+20
dpa	3.37E-02	5.13E-02	6.17E-02	6.14E-02	5.74E-02	6.99E-02

TABLE 6-14

NEUTRON EXPOSURE VALUES FOR THE

CPSES UNIT 2 REACTOR VESSEL

FLUENCE BASED ON E > 1.0 MeV SLOPE

	0 DEG	15 DEG	25 DEG	30 DEG	35 DEG	45 DEG
			15 EFPY FLUENCE			
SURFACE	6.51E+18	9.98E+18	1.20E+19	1.19E+19	1.09E+19	1.33E+19
1/4T	3.66E+18	5.56E+18	6.70E+18	6.62E+18	6.03E+18	7.29E+18
3/4T	8.26E+17	1.24E+18	1.49E+18	1.47E+18	1.36E+18	1.57E+18
			32 EFPY FLUENCE			
SURFACE	1.39E+19	2.13E+19	2.57E+19	2.55E+19	2.33E+19	2.84E+19
1/4T	7.80E+18	1.19E+19	1.43E+19	1.41E+19	1.29E+19	1.55E+19
3/4T	1.76E+18	2.64E+18	3.19E+18	3.13E+18	2.89E+18	3.35E+18
			48 EFPY FLUENCE			
SURFACE	2.08E+19	3.19E+19	3.86E+19	3.82E+19	3.50E+19	4.26E+19
1/4T	1.17E+19	1.78E+19	2.14E+19	2.12E+19	1.93E+19	2.33E+19
3/4T	2.64E+18	3.96E+18	4.78E+18	4.70E+18	4.34E+18	5.02E+18

FLUENCE BASED ON dpa SLOPE

	0 DEG	15 DEG	25 DEG	30 DEG	35 DEG	45 DEG
			15 EFPY FLUENCE			
SURFACE	6.51E+18	9.98E+18	1.20E+19	1.19E+19	1.09E+19	1.33E+19
1/4T	4.15E+18	6.33E+18	7.66E+18	7.59E+18	7.01E+18	8.54E+18
3/4T	1.46E+18	2.21E+18	2.67E+18	2.66E+18	2.53E+18	2.67E+18
			32 EFPY FLUENCE			
SURFACE	1.39E+19	2.13E+19	2.57E+19	2.55E+19	2.33E+19	2.84E+19
1/4T	8.86E+18	1.35E+19	1.63E+19	1.62E+19	1.50E+19	1.82E+19
3/4T	3.11E+18	4.71E+18	5.71E+18	5.68E+18	5.39E+18	5.70E+18
			48 EFPY FLUENCE			
SURFACE	2.08E+19	3.19E+19	3.86E+19	3.82E+19	3.50E+19	4.26E+19
1/4T	1.33E+19	2.03E+19	2.45E+19	2.43E+19	2.24E+19	2.73E+19
3/4T	4.66E+18	7.06E+18	8.56E+18	8.52E+18	8.09E+18	8.55E+18

TABLE 6-15

UPDATED LEAD FACTORS FOR CPSES UNIT 2

SURVEILLANCE CAPSULES

CAPSULE	LEAD FACTOR
V	3.74
U	4.10*
X	4.10
W	4.10
Y	3.74
Z	4.10

*WITHDRAWN EOC 1

SECTION 7.0

RECOMMENDED SURVEILLANCE CAPSULE REMOVAL SCHEDULE

The following surveillance capsule removal schedule meets the requirements of ASTM E185-82 and is recommended for future capsules to be removed from the CPSES Unit No. 2 reactor vessel:

TABLE 7-1

Recommended Surveillance Capsule Removal Schedule for the CPSES Unit No. 2 Reactor Vessel

Capsule	Capsule Location (degree)	Lead Factor	Withdrawal EFPY[a]	Fluence (n/cm^2, $E > 1.0$ MeV)
U[b]	58.5	4.098	0.904	3.28×10^{18}
X	238.5	4.098	7.805	2.836×10^{19}
W	121.5	4.098	11.701	4.255×10^{19} [c]
Z	301.5	4.098	Standby	-----
V	61.0	3.744	Standby	-----
Y	241.0	3.744	Standby	------

NOTES:

(a) Effective Full Power Years (EFPY) from plant startup.

(b) Actual measured neutron fluence

(c) Approximately equal to the projected vessel fluence at 48 EFPY.

SECTION 8.0
REFERENCES

1. Regulatory Guide 1.99, Revision 2, "Radiation Embrittlement of Reactor Vessel Materials", U.S. Nuclear Regulatory Commission, May, 1988.

2. Code of Federal Regulations, 10 CFR Part 50, Appendix G, "Fracture Toughness Requirements", U.S. Nuclear Regulatory Commission, Washington, D.C.

3. WCAP-10684, "Texas Utilities Generating Company Comanche Peak Unit No. 2 Reactor Vessel Radiation Surveillance Program", L. R. Singer, October 1984.

4. Section III of the ASME Boiler and Pressure Vessel Code, Appendix G, "Protection Against Nonductile Failure".

5. ASTM E208, "Standard Test Method for Conducting Drop-Weight Test to Determine Nil-Ductility Transition Temperature of Ferritic Steels", in ASTM Standards, Section 3, American Society for Testing and Materials, Philadelphia, PA.

6. Code of Federal Regulations, 10 CFR Part 50, Appendix H, "Reactor Vessel Material Surveillance Program Requirements", U.S. Nuclear Regulatory Commission, Washington, D.C.

7. ASTM E185-82, "Standard Practice for Conducting Surveillance Tests for Light-Water Cooled Nuclear Power Reactor Vessels", E706 (IF), in ASTM Standards, Section 3, American Society for Testing and Materials, Philadelphia, PA, 1993.

8. ASTM E23-93a, "Standard Test Methods for Notched Bar Impact Testing of Metallic Materials", in ASTM Standards, Section 3, American Society for Testing and Materials, Philadelphia, PA, 1993.

9. ASTM A370-92, "Standard Test Methods and Definitions for Mechanical Testing of Steel Products", in ASTM Standards, Section 3, American Society for Testing and Materials, Philadelphia, PA, 1993.

10. ASTM E8-93, "Standard Test Methods for Tension Testing of Metallic Materials", in ASTM Standards, Section 3, American Society for Testing and Materials, Philadelphia, PA, 1993.

11. ASTM E21-92, "Standard Test Methods for Elevated Temperature Tension Tests of Metallic Materials", in ASTM Standards, Section 3, American Society for Testing and Materials, Philadelphia, PA, 1993.

12. ASTM E83-93, "Standard Practice for Verification and Classification of Extensometers", in ASTM Standards, Section 3, American Society for Testing and Materials, Philadelphia, PA, 1993.

13. RSIC Computer Code Collection CCC-543, "TORT-DORT Two- and Three-Dimensional Discrete Ordinates Transport", Version 2.8.14", January 1994.

14. RSIC Data Library Collection DLC-175, "BUGLE-93, Production and Testing of the VITAMIN-B6 Fine Group and the BUGLE-93 Broad Group Neutron/Photon Cross-Section Libraries Derived from ENDF/B-VI Nuclear Data", April 1994.

15. RSIC Data Library Collection DLC-178, "SNLRML Recommended Dosimetry Cross-Section Compendium", July 1994.

16. Nuclear Science and Engineering, Volume 94, "Accounting for Changing Source Distributions in Light Water Reactor Surveillance Dosimetry Analysis", R. E. Maerker, et al, Pages 291-308, 1986.

17. WCAP-10804-R1, "The Nuclear Design and Core Physics Characteristics of the Comanche Peak Unit 2 Nuclear Power Plant Cycle 1", P. J. Sipush, March 1993.

18. ASTM Designation E482-89, "Standard Guide for Application of Neutron Transport Methods for Reactor Vessel Surveillance", in ASTM Standards, Section 12, American Society for Testing and Materials, Philadelphia, PA, 1993.

19. ASTM Designation E560-84, "Standard Recommended Practice for Extrapolating Reactor Vessel Surveillance Dosimetry Results", in ASTM Standards, Section 12, American Society for Testing and Materials, Philadelphia, PA, 1993.

20. ASTM Designation E693-79," Standard Practice for Characterizing Neutron Exposures in Ferritic Steels in Terms of Displacements per Atom (dpa)", in ASTM Standards, Section 12, American Society for Testing and Materials, Philadelphia, PA, 1993.

21. ASTM Designation E706-87, "Standard Master Matrix for Light-Water Reactor Pressure Vessel Surveillance Standards", in ASTM Standards, Section 12, American Society for Testing and Materials, Philadelphia, PA, 1993.

22. ASTM Designation E853-87, "Standard Practice for Analysis and Interpretation of Light-Water Reactor Surveillance Results", in ASTM Standards, Section 12, American Society for Testing and Materials, Philadelphia, PA, 1993.

23. ASTM Designation E261-90, "Standard Practice for Determining Neutron Fluence Rate, Fluence, and Spectra by Radioactivation Techniques", in ASTM Standards, Section 12, American Society for Testing and Materials, Philadelphia, PA, 1993.

24. ASTM Designation E262-86, "Standard Method for Determining Thermal Neutron Reaction and Fluence Rates by Radioactivation Techniques", in ASTM Standards, Section 12, American Society for Testing and Materials, Philadelphia, PA, 1993.

25. ASTM Designation E263-88, "Standard Method for Measuring Fast-Neutron Reaction Rates by Radioactivation of Iron", in ASTM Standards, Section 12, American Society for Testing and Materials, Philadelphia, PA, 1993.

26. ASTM Designation E264-92, "Standard Method for Measuring Fast-Neutron Reaction Rates by Radioactivation of Nickel", in ASTM Standards, Section 12, American Society for Testing and Materials, Philadelphia, PA, 1993.

27. ASTM Designation E481-92, "Standard Method for Measuring Neutron-Fluence Rate by Radioactivation of Cobalt and Silver", in ASTM Standards, Section 12, American Society for Testing and Materials, Philadelphia, PA, 1993.

28. ASTM Designation E523-87, "Standard Test Method for Measuring Fast-Neutron Reaction Rates by Radioactivation of Copper", in ASTM Standards, Section 12, American Society for Testing and Materials, Philadelphia, PA, 1993.

29. ASTM Designation E704-90, "Standard Test Method for Measuring Reaction Rates by Radioactivation of Uranium-238", in ASTM Standards, Section 12, American Society for Testing and Materials, Philadelphia, PA, 1993.

30. ASTM Designation E705-90, "Standard Test Method for Measuring Reaction Rates by Radioactivation of Neptunium-237", in ASTM Standards, Section 12, American Society for Testing and Materials, Philadelphia, PA, 1993.

31. ASTM Designation E1005-84, "Standard Test Method for Application and Analysis of Radiometric Monitors for Reactor Vessel Surveillance", in ASTM Standards, Section 12, American Society for Testing and Materials, Philadelphia, PA, 1993.

32. HEDL-TME 79-40, "FERRET Data Analysis Core", F. A. Schmittroth, Hanford Engineering Development Laboratory, Richland, WA, September 1979.

33. AFWL-TR-7-41, Vol. I-IV, "A Computer-Automated Iterative Method of Neutron Flux Spectra Determined by Foil Activation", W. N. McElroy, S. Berg and T. Crocket, Air Force Weapons Laboratory, Kirkland AFB, NM, July 1967.

34. EPRI-NP-2188, "Development and Demonstration of an Advanced Methodology for LWR Dosimetry Applications", R. E. Maerker, et al., 1981.

APPENDIX A

Load-Time Records for Charpy Specimen Tests

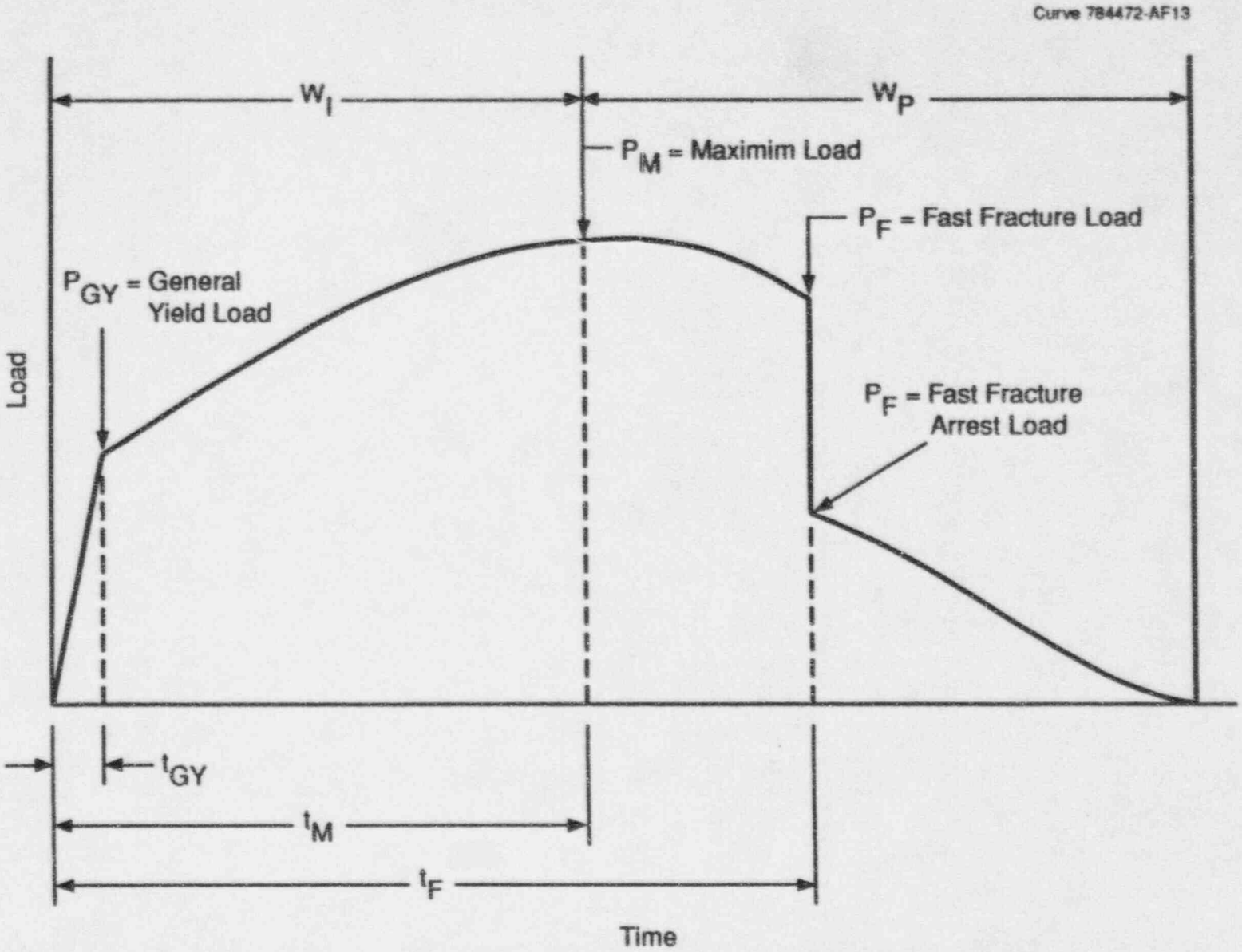

W_I = Fracture Initiation Region
W_P = Fracture Propagation Region

t_{GY} = Time to General Yielding
t_M = Time to Maximum Load
t_F = Time to Fast (Brittle) Fracture Start

Fig. A-1-Idealized load-time record

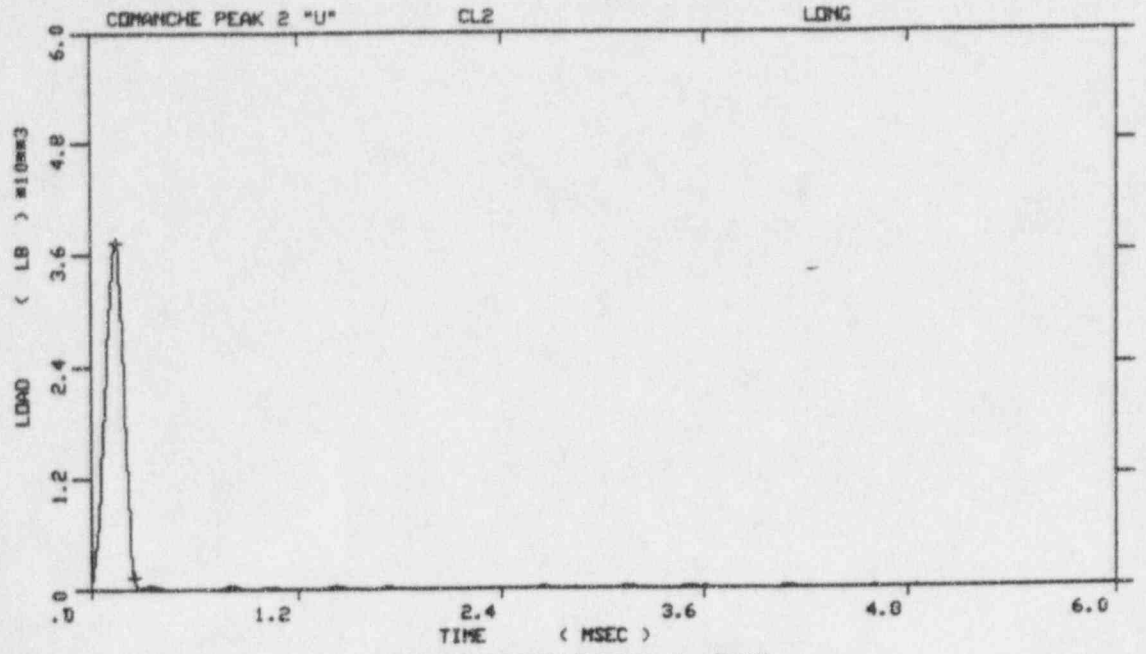

COMANCHE PEAK 2 "U"
SPECIMEN NUMBER :CL2
MATERIAL :LONG
CAPSULE :COMANCHE PEAK 2
:"U" CAPSULE

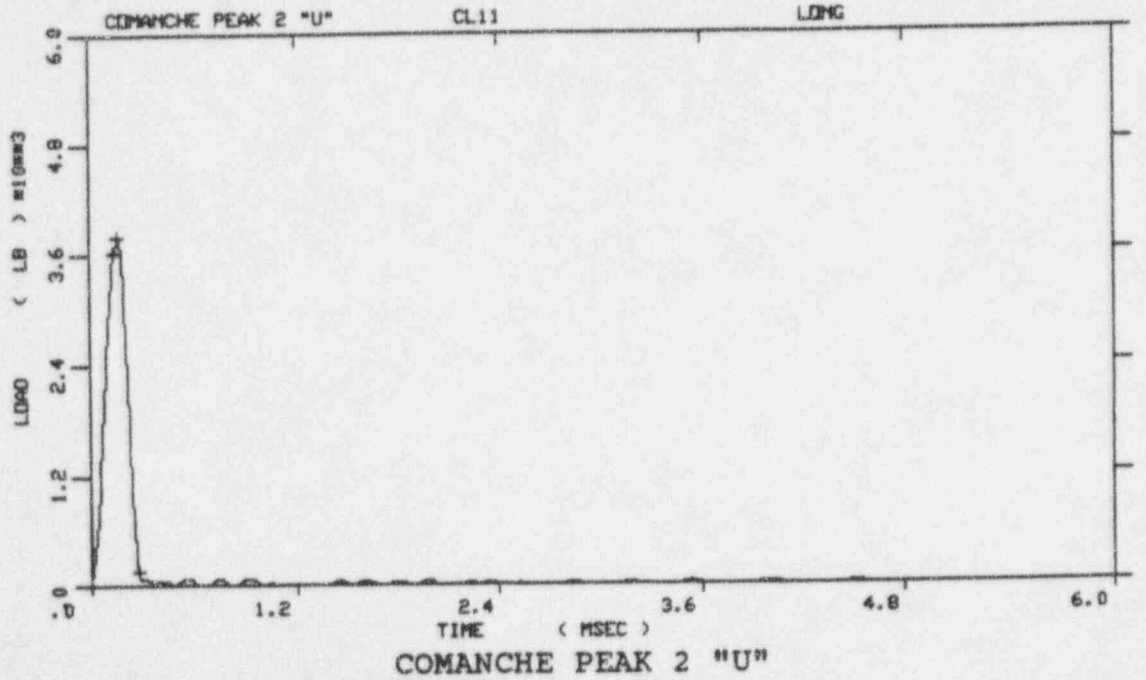

COMANCHE PEAK 2 "U"
SPECIMEN NUMBER :CL11
MATERIAL :LONG
CAPSULE :COMANCHE PEAK 2
:"U" CAPSULE

Figure A-2. Load-time records for Specimens CL2 (-75°F) and CL11 (-50°F).

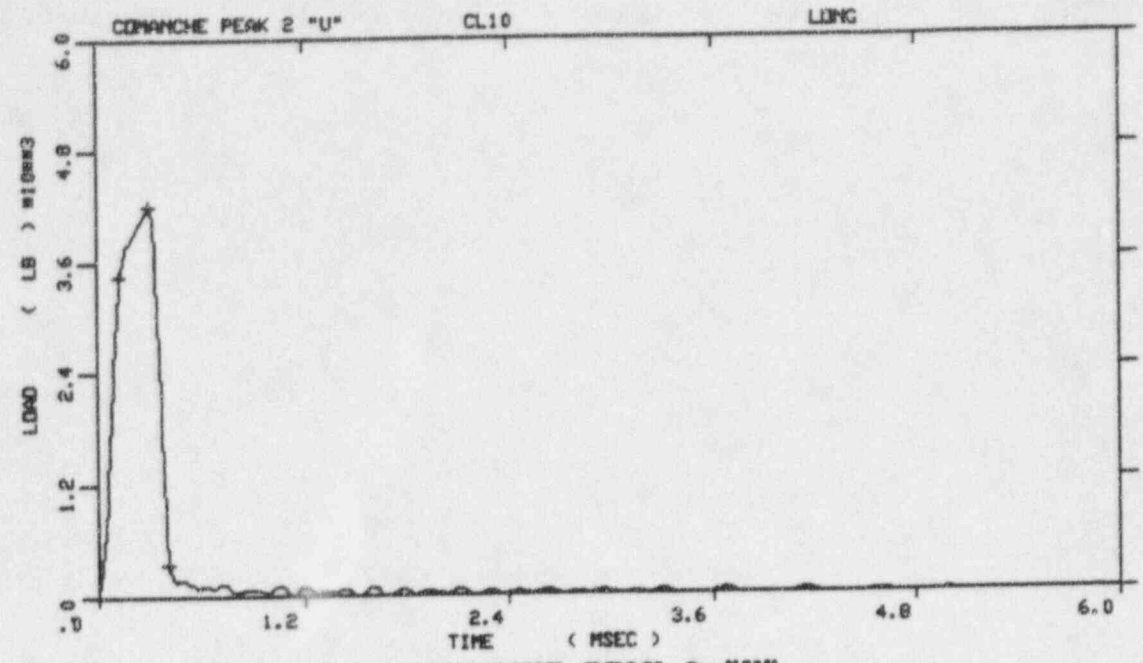

COMANCHE PEAK 2 "U"

SPECIMEN NUMBER :CL10
MATERIAL :LONG
CAPSULE :COMANCHE PEAK 2
:"U" CAPSULE

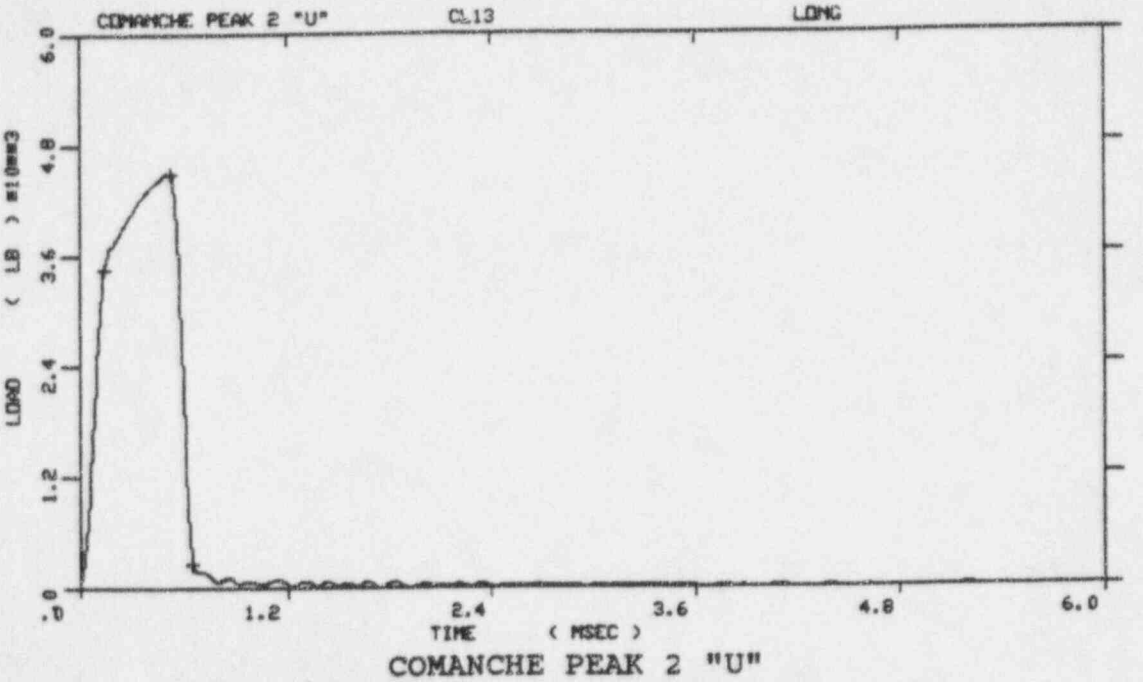

COMANCHE PEAK 2 "U"

SPECIMEN NUMBER :CL13
MATERIAL :LONG
CAPSULE :COMANCHE PEAK 2
:"U" CAPSULE

Figure A-3. Load-time records for Specimens CL10 (-25°F) and CL13 (-10°F).

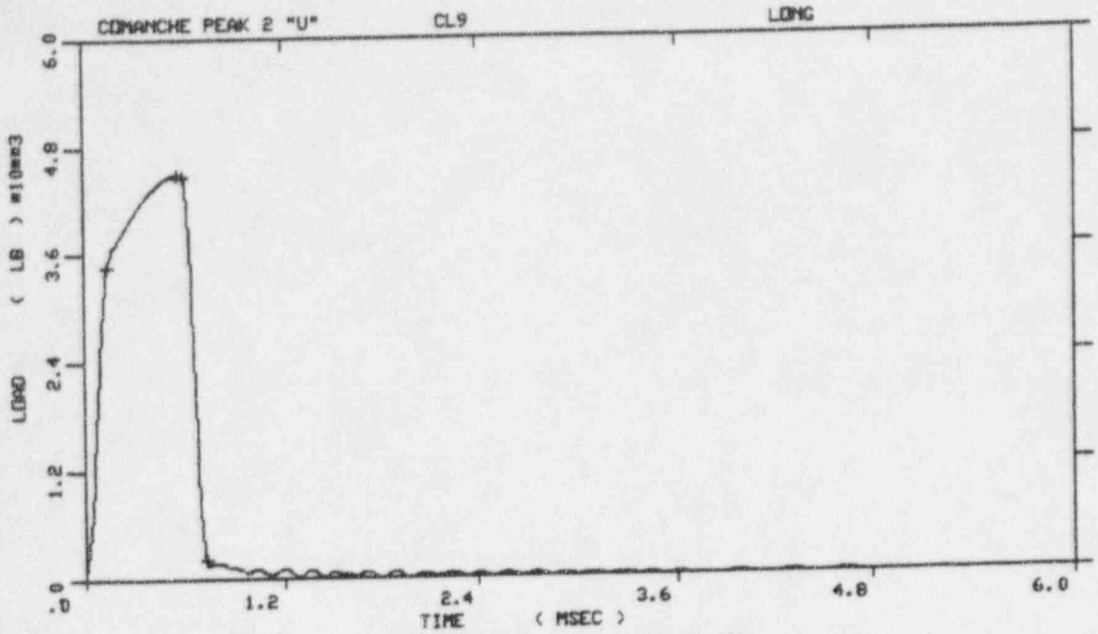

COMANCHE PEAK 2 "U"
SPECIMEN NUMBER :CL9
MATERIAL :LONG
CAPSULE :COMANCHE PEAK 2
:"U" CAPSULE

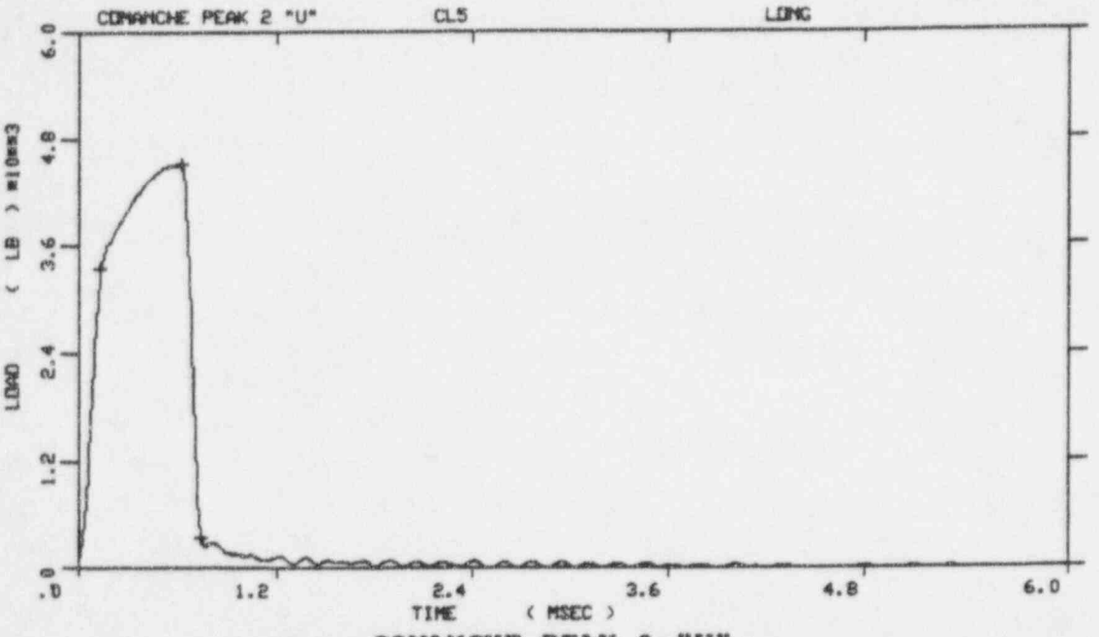

COMANCHE PEAK 2 "U"
SPECIMEN NUMBER :CL5
MATERIAL :LONG
CAPSULE :COMANCHE PEAK 2
:"U" CAPSULE

Figure A-4. Load-time records for Specimens CL9 (-0°F) and CL5 (10°F).

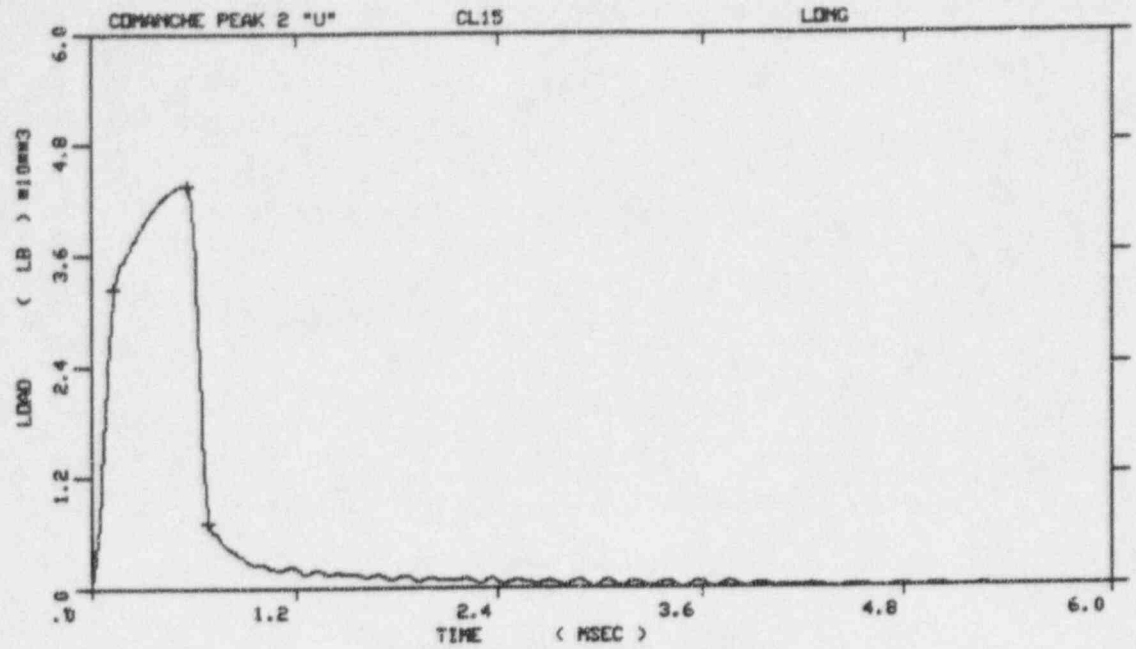

COMANCHE PEAK 2 "U"
SPECIMEN NUMBER :CL15
MATERIAL :LONG
CAPSULE :COMANCHE PEAK 2
:"U" CAPSULE

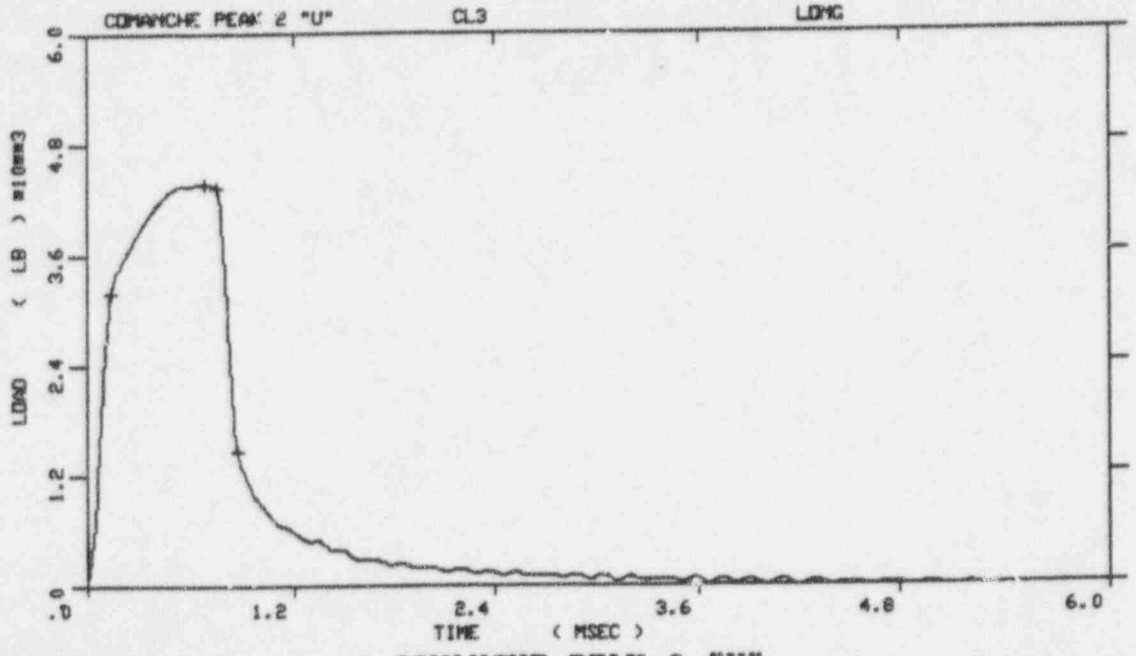

COMANCHE PEAK 2 "U"
SPECIMEN NUMBER :CL3
MATERIAL :LONG
CAPSULE :COMANCHE PEAK 2
:"U" CAPSULE

Figure A-5. Load-time records for Specimens CL15 (25°F) and CL3 (50°F).

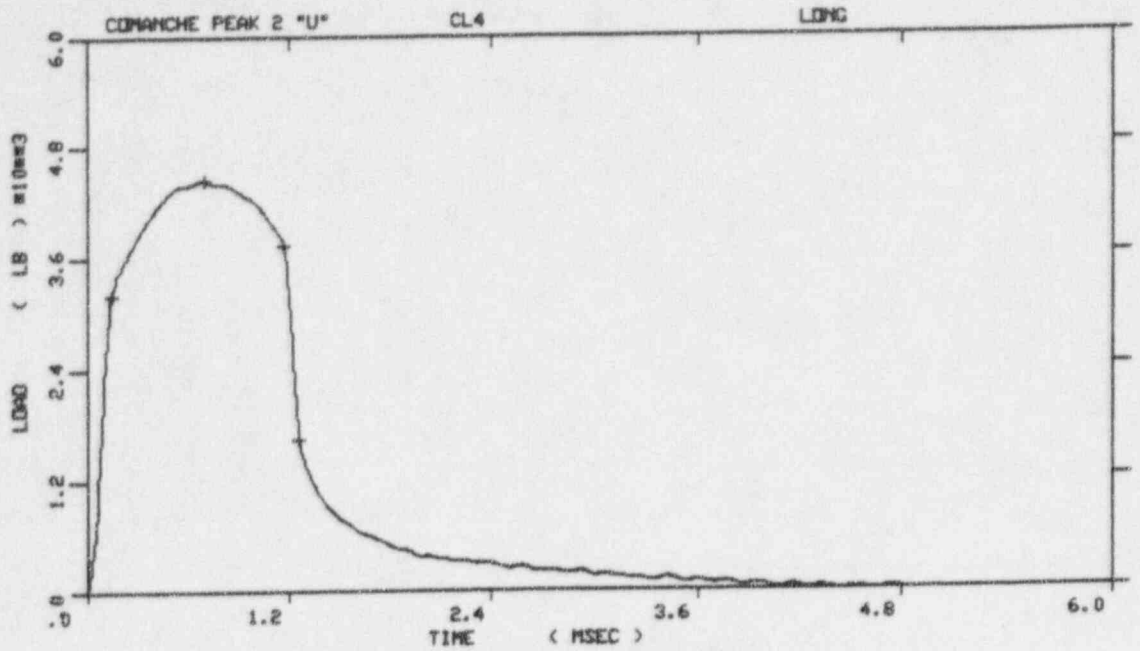

COMANCHE PEAK 2 "U"

SPECIMEN NUMBER :CL4
MATERIAL :LONG
CAPSULE :COMANCHE PEAK 2
:"U" CAPSULE

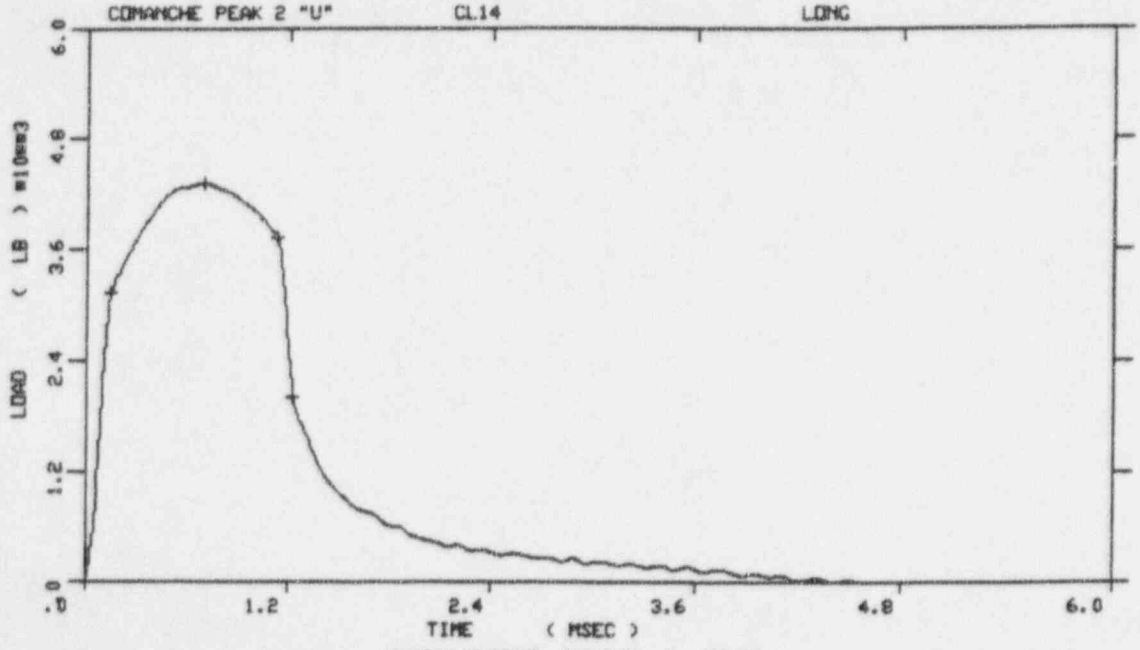

COMANCHE PEAK 2 "U"

SPECIMEN NUMBER :CL14
MATERIAL :LONG
CAPSULE :COMANCHE PEAK 2
:"U" CAPSULE

Figure A-6. Load-time records for Specimens CL4 (72°F) and CL14 (100°F).

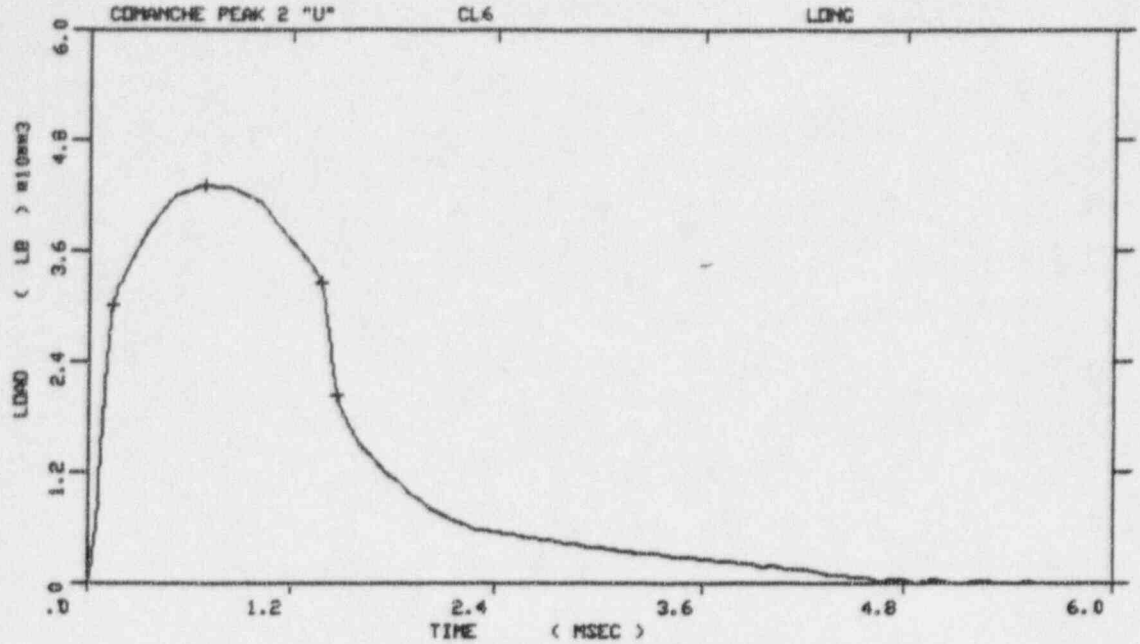

COMANCHE PEAK 2 "U"
SPECIMEN NUMBER :CL6
MATERIAL :LONG
CAPSULE :COMANCHE PEAK 2
:"U" CAPSULE

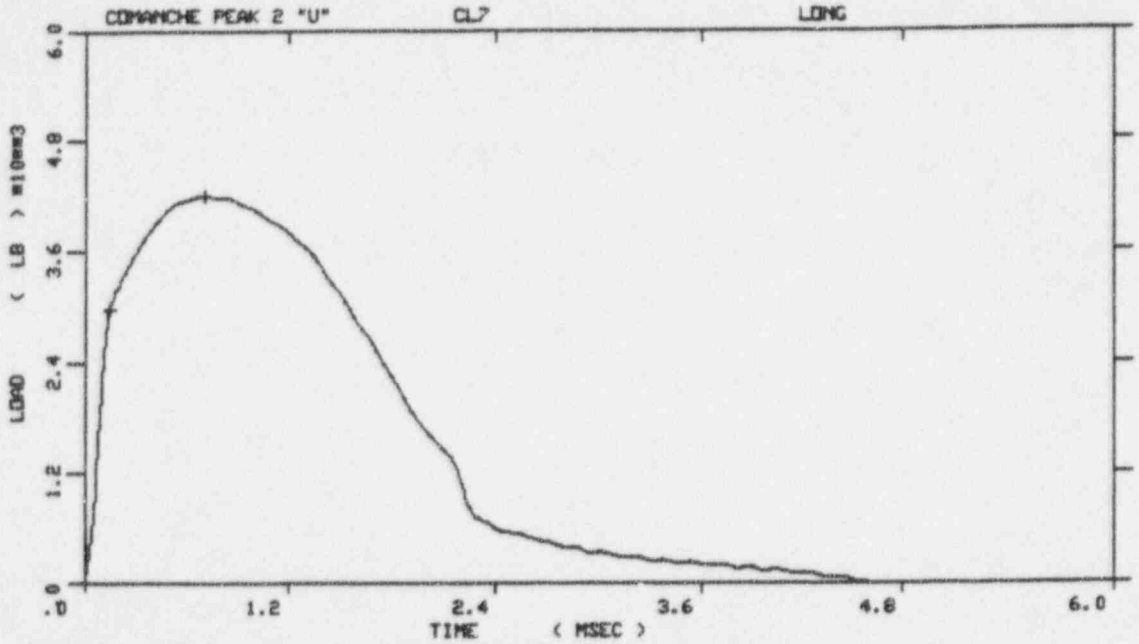

COMANCHE PEAK 2 "U"
SPECIMEN NUMBER :CL7
MATERIAL :LONG
CAPSULE :COMANCHE PEAK 2
:"U" CAPSULE

Figure A-7. Load-time records for Specimens CL6 (125°F) and CL7 (150°F).

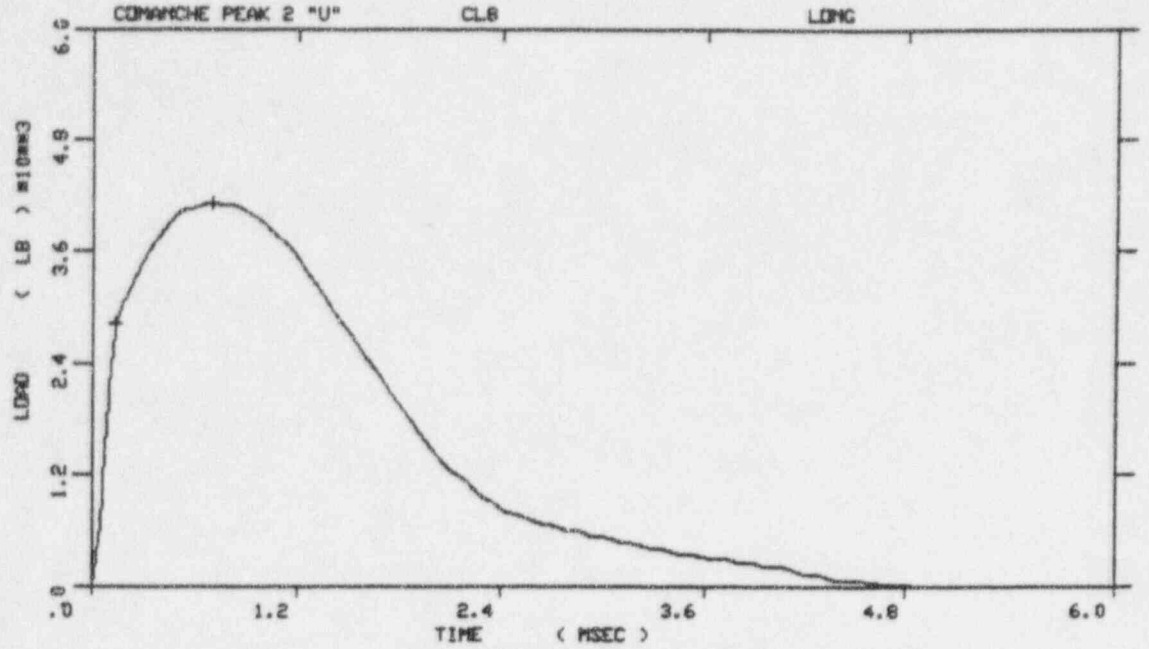

COMANCHE PEAK 2 "U"
SPECIMEN NUMBER :CL8
MATERIAL :LONG
CAPSULE :COMANCHE PEAK 2
:"U" CAPSULE

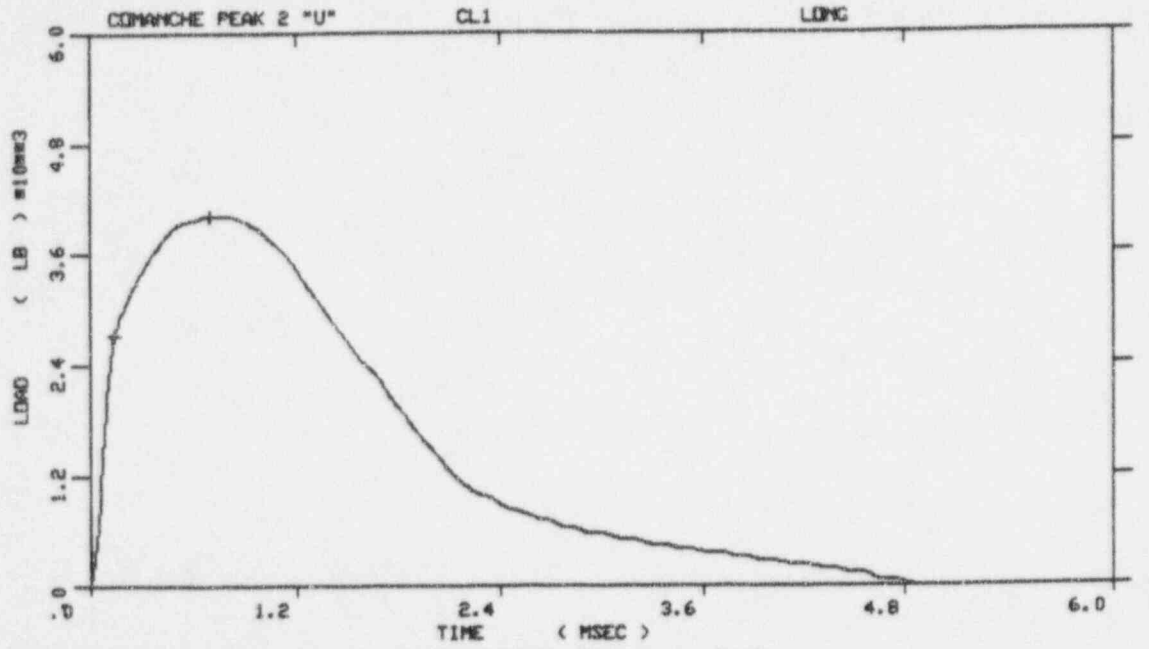

COMANCHE PEAK 2 "U"
SPECIMEN NUMBER :CL1
MATERIAL :LONG
CAPSULE :COMANCHE PEAK 2
:"U" CAPSULE

Figure A-8. Load-time records for Specimens CL8 (200°F) and CL1 (250°F).

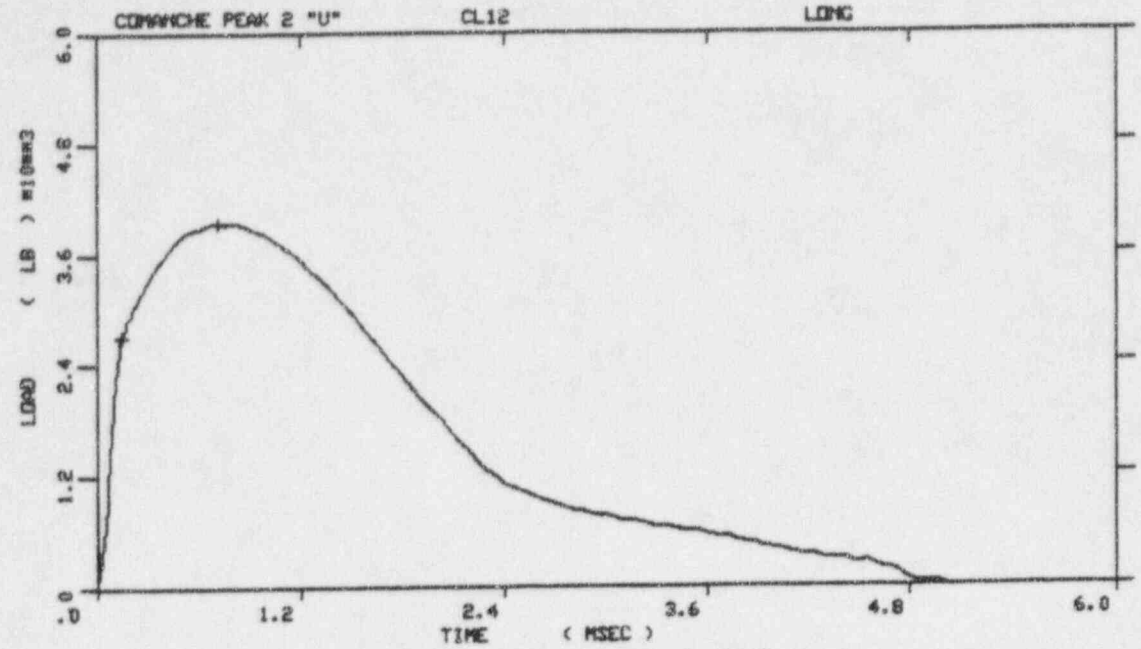

COMANCHE PEAK 2 "U"
SPECIMEN NUMBER :CL12
MATERIAL :LONG
CAPSULE :COMANCHE PEAK 2
:"U" CAPSULE

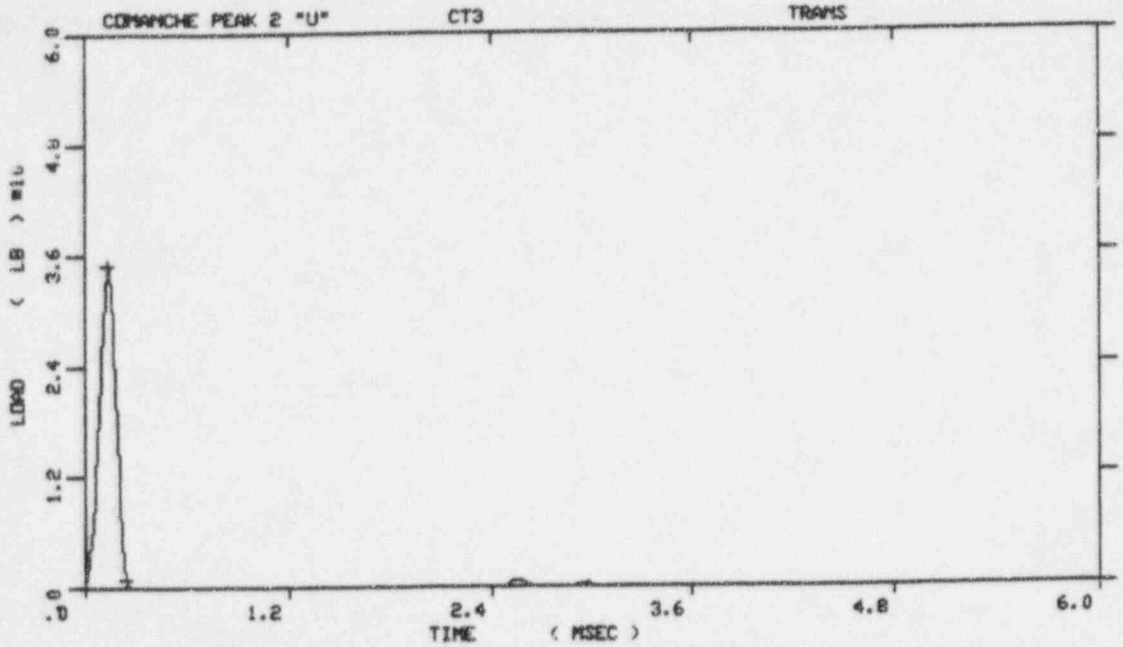

COMANCHE PEAK 2 "U"
SPECIMEN NUMBER :CT3
MATERIAL :TRANS
CAPSULE :COMANCHE PEAK 2
:"U" CAPSULE

Figure A-9. Load-time records for Specimens CL12 (300°F) and CT3 (-125°F).

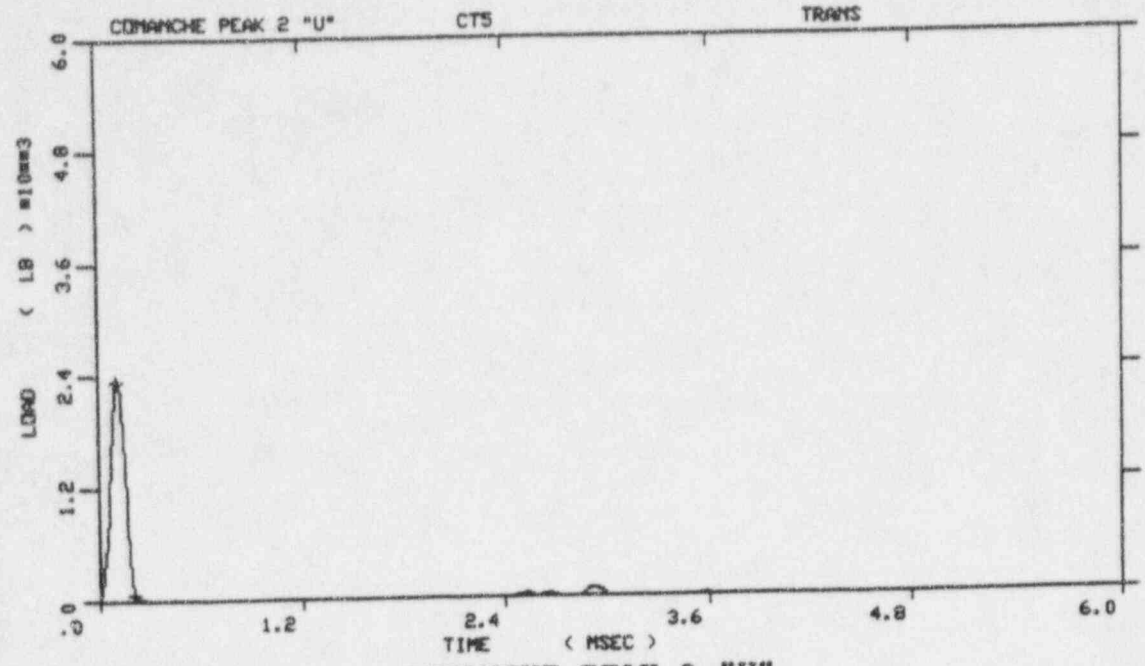

COMANCHE PEAK 2 "U"

SPECIMEN NUMBER :CT5
MATERIAL :TRANS
CAPSULE :COMANCHE PEAK 2
:"U" CAPSULE

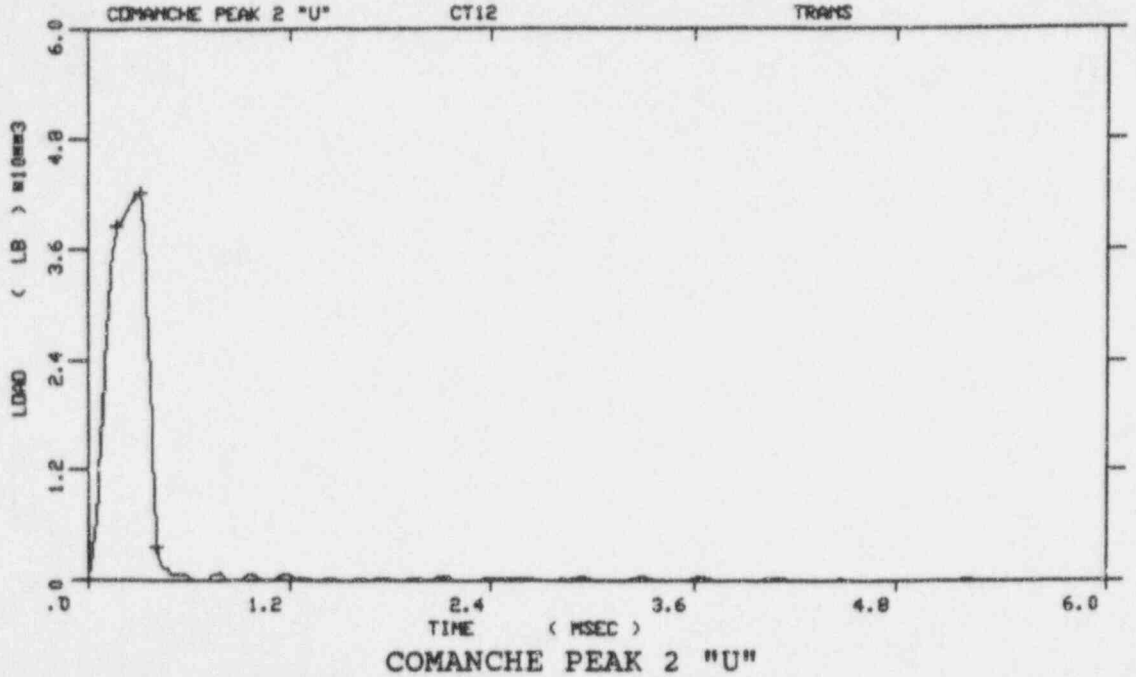

COMANCHE PEAK 2 "U"

SPECIMEN NUMBER :CT12
MATERIAL :TRANS
CAPSULE :COMANCHE PEAK 2
:"U" CAPSULE

Figure A-10. Load-time records for Specimens CT5 (-95°F) and CT12 (-50°F).

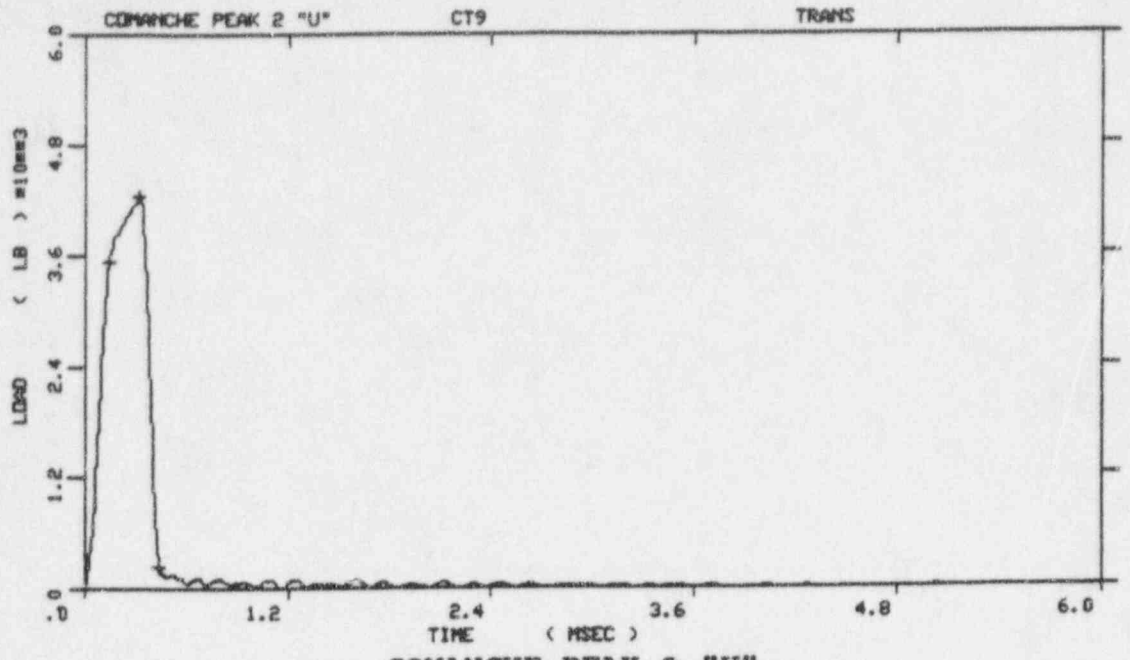

COMANCHE PEAK 2 "U"
SPECIMEN NUMBER :CT9
MATERIAL :TRANS
CAPSULE :COMANCHE PEAK 2
:"U" CAPSULE

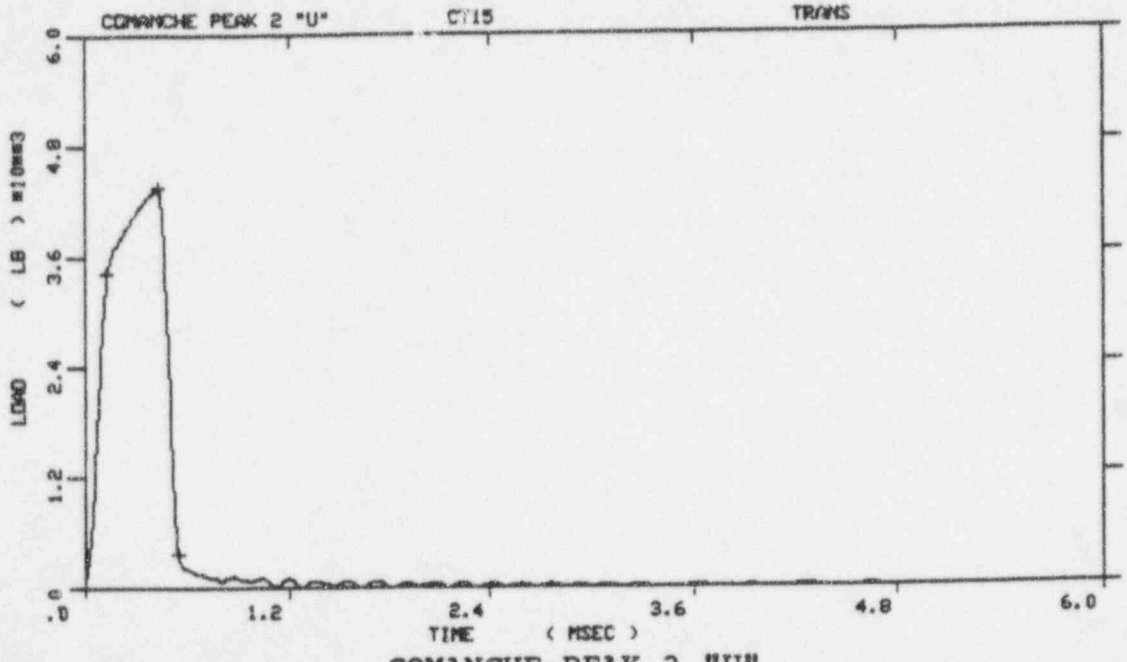

COMANCHE PEAK 2 "U"
SPECIMEN NUMBER : CT15
MATERIAL :TRANS
CAPSULE :COMANCHE PEAK 2
:"U" CAPSULE

Figure A-11. Load-time records for Specimens CT9 (-25°F) and CT15 (-10°F).

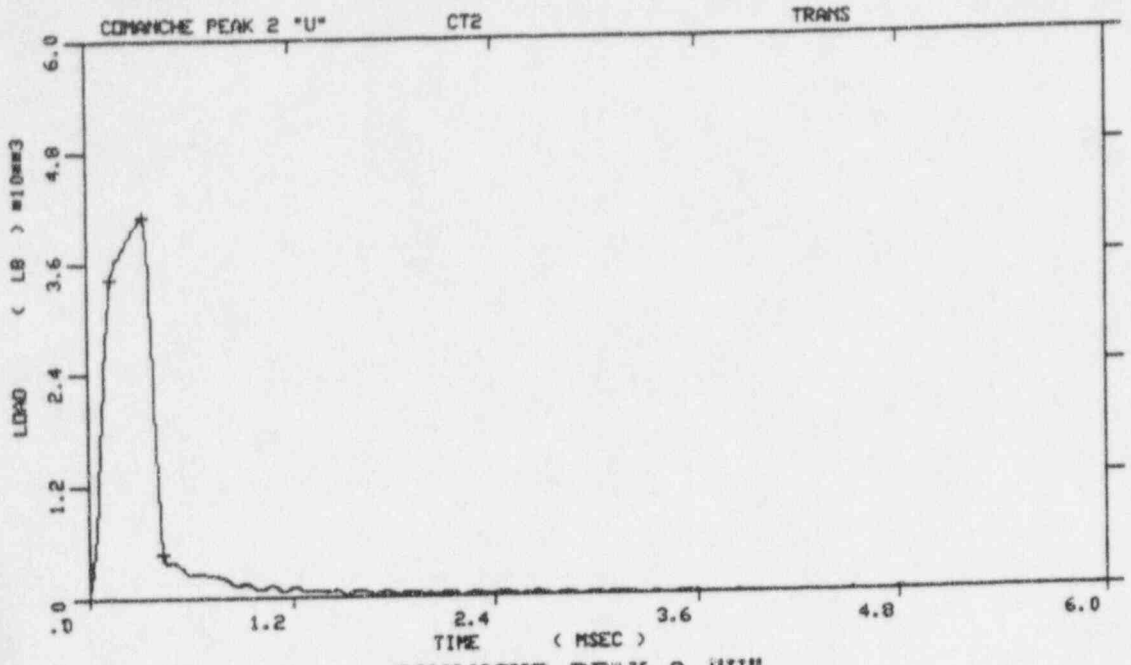

COMANCHE PEAK 2 "U"

SPECIMEN NUMBER :CT2
MATERIAL :TRANS
CAPSULE :COMANCHE PEAK 2
:"U" CAPSULE

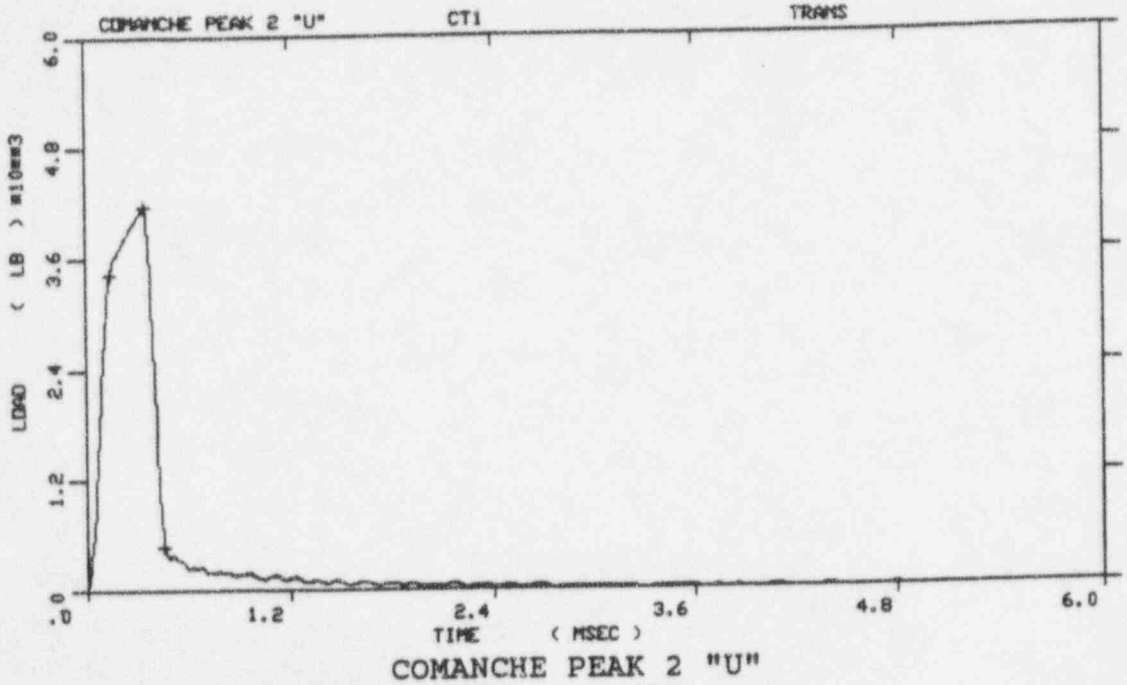

COMANCHE PEAK 2 "U"

SPECIMEN NUMBER :CT1
MATERIAL :TRANS
CAPSULE :COMANCHE PEAK 2
:"U" CAPSULE

Figure A-12. Load-time records for Specimens CT2 (0°F) and CT1 (10°F).

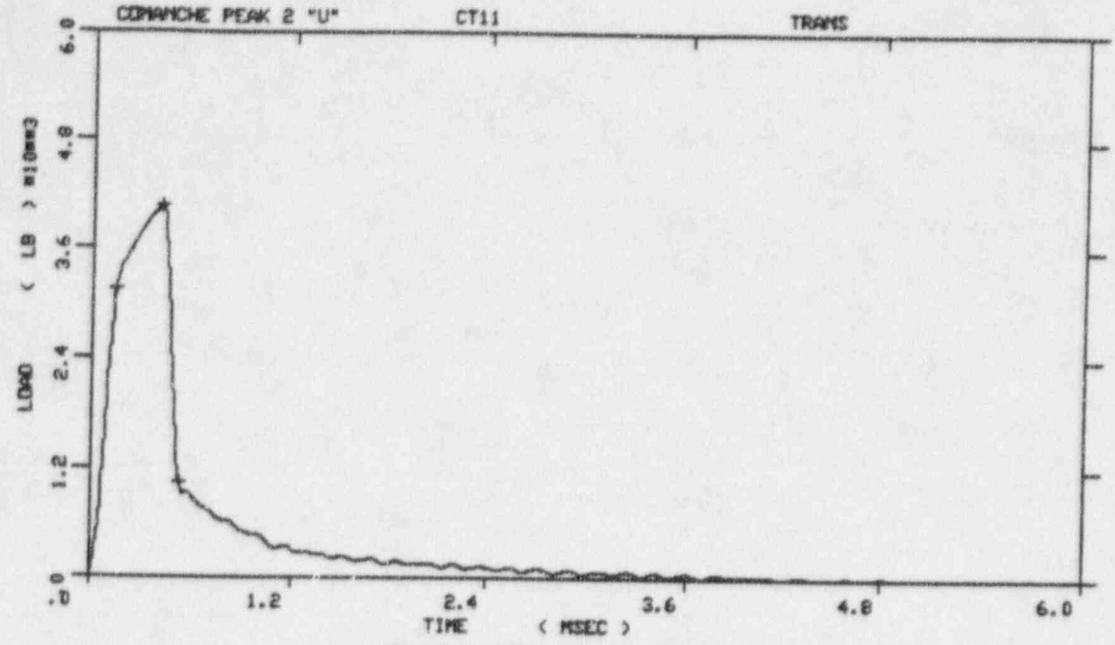

COMANCHE PEAK 2 "U"
SPECIMEN NUMBER :CT11
MATERIAL :TRANS
CAPSULE :COMANCHE PEAK 2
:"U" CAPSULE

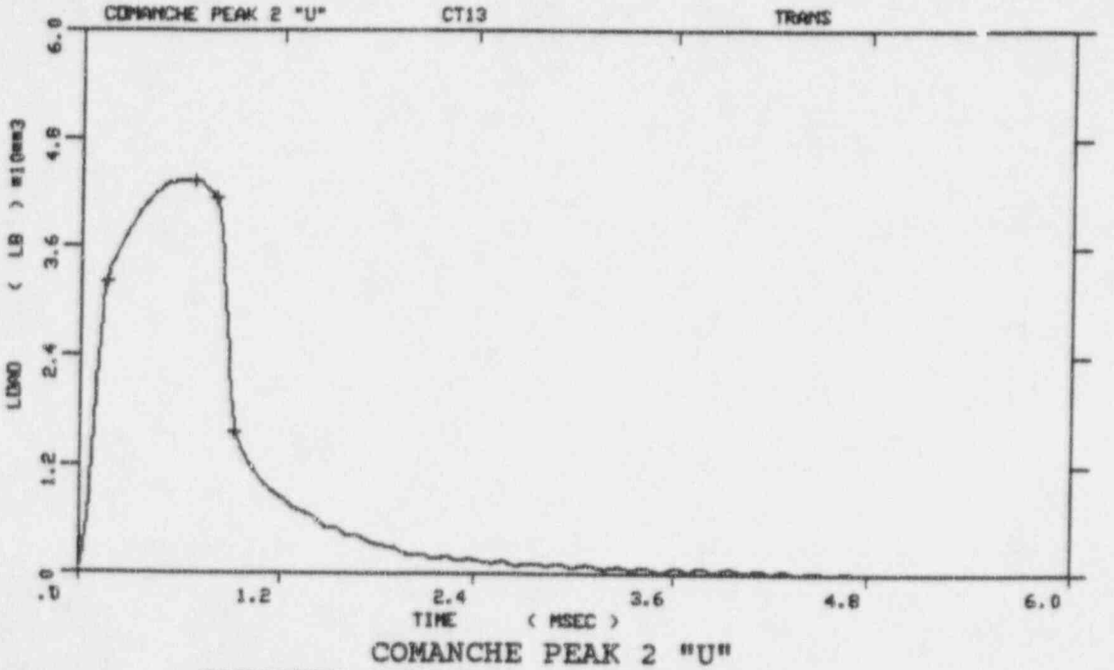

COMANCHE PEAK 2 "U"
SPECIMEN NUMBER :CT13
MATERIAL :TRANS
CAPSULE :COMANCHE PEAK 2
:"U" CAPSULE

Figure A-13. Load-time records for Specimens CT11 (50°F) and CT13 (72°F).

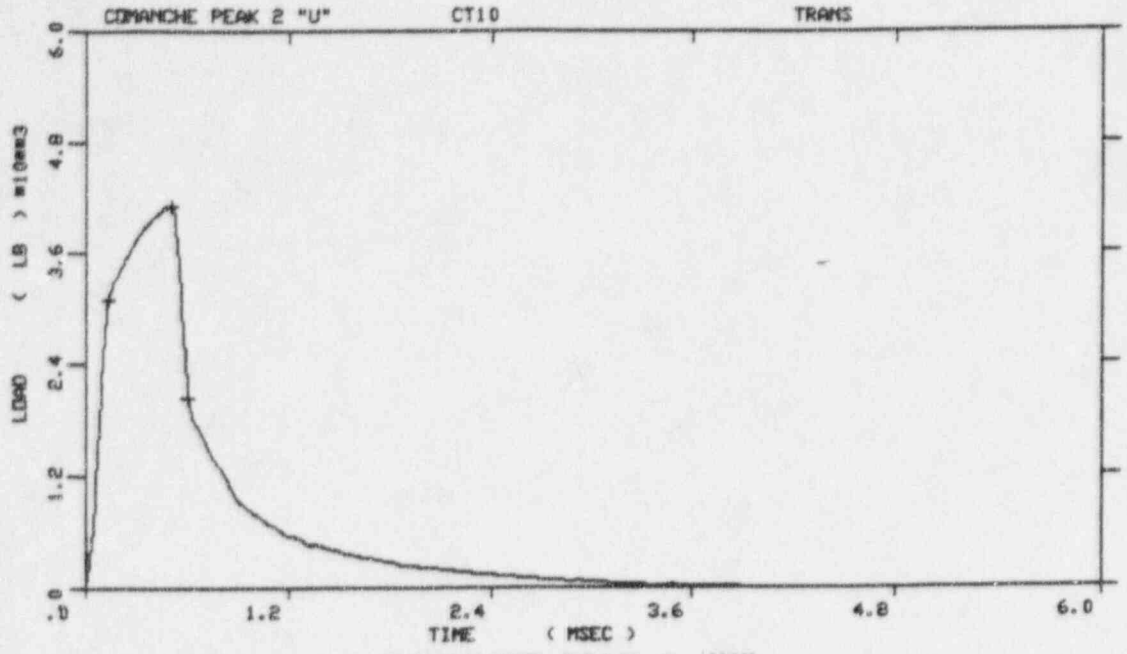

COMANCHE PEAK 2 "U"
SPECIMEN NUMBER :CT10
MATERIAL :TRANS
CAPSULE :COMANCHE PEAK 2
:"U" CAPSULE

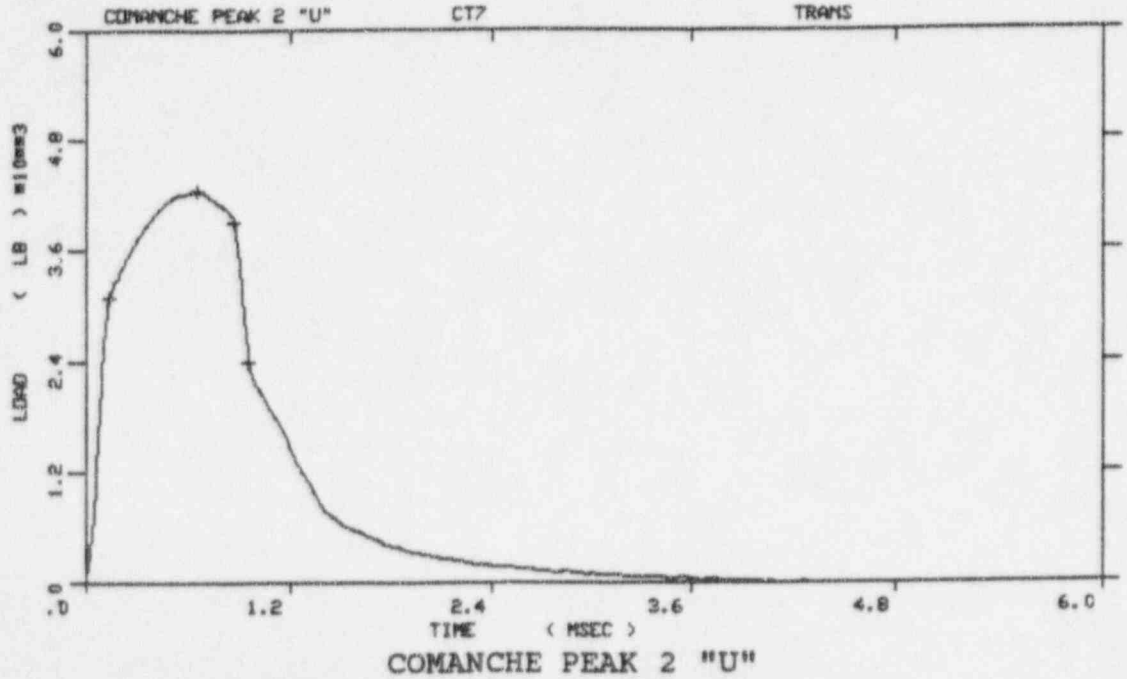

COMANCHE PEAK 2 "U"
SPECIMEN NUMBER :CT7
MATERIAL :TRANS
CAPSULE :COMANCHE PEAK 2
:"U" CAPSULE

Figure A-14. Load-time records for Specimens CT10 (100°F) and CT7 (125°F).

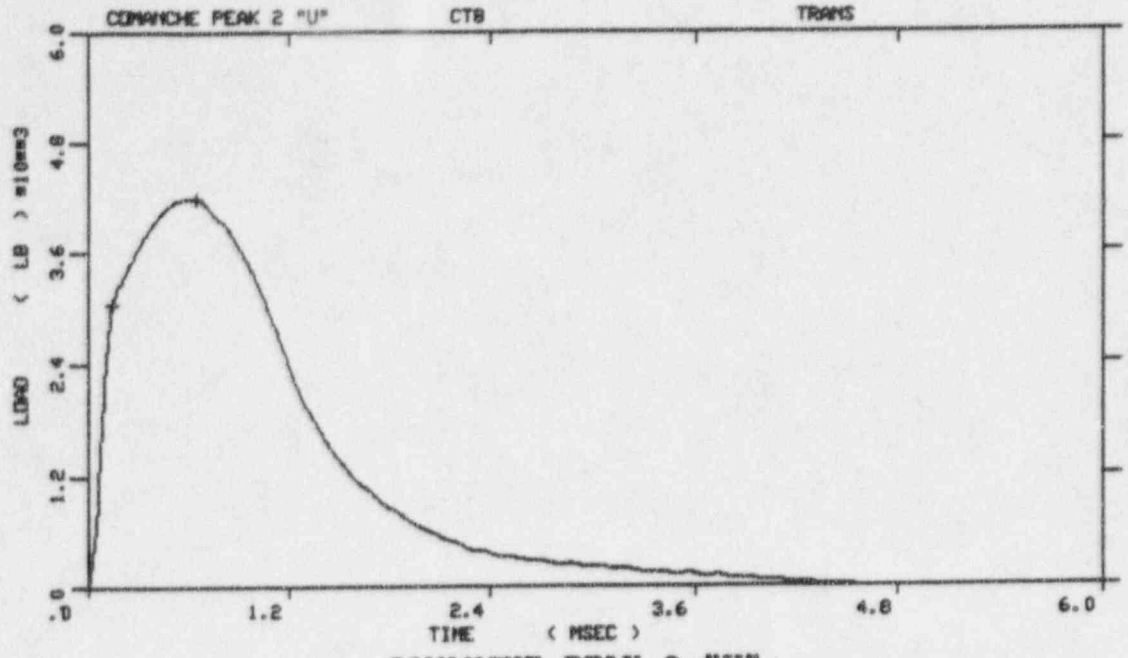

COMANCHE PEAK 2 "U"
SPECIMEN NUMBER :CT8
MATERIAL :TRANS
CAPSULE :COMANCHE PEAK 2
:"U" CAPSULE

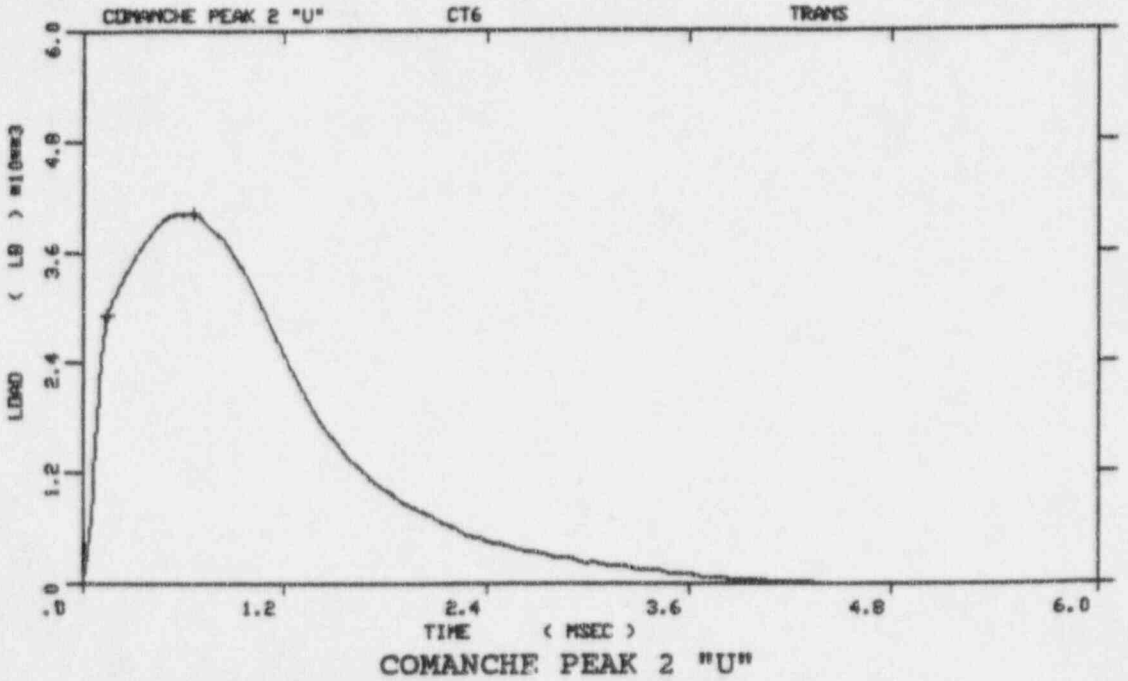

COMANCHE PEAK 2 "U"
SPECIMEN NUMBER :CT6
MATERIAL :TRANS
CAPSULE :COMANCHE PEAK 2
:"U" CAPSULE

Figure A-15. Load-time records for Specimens CT8 (150°F) and CT6 (200°F).

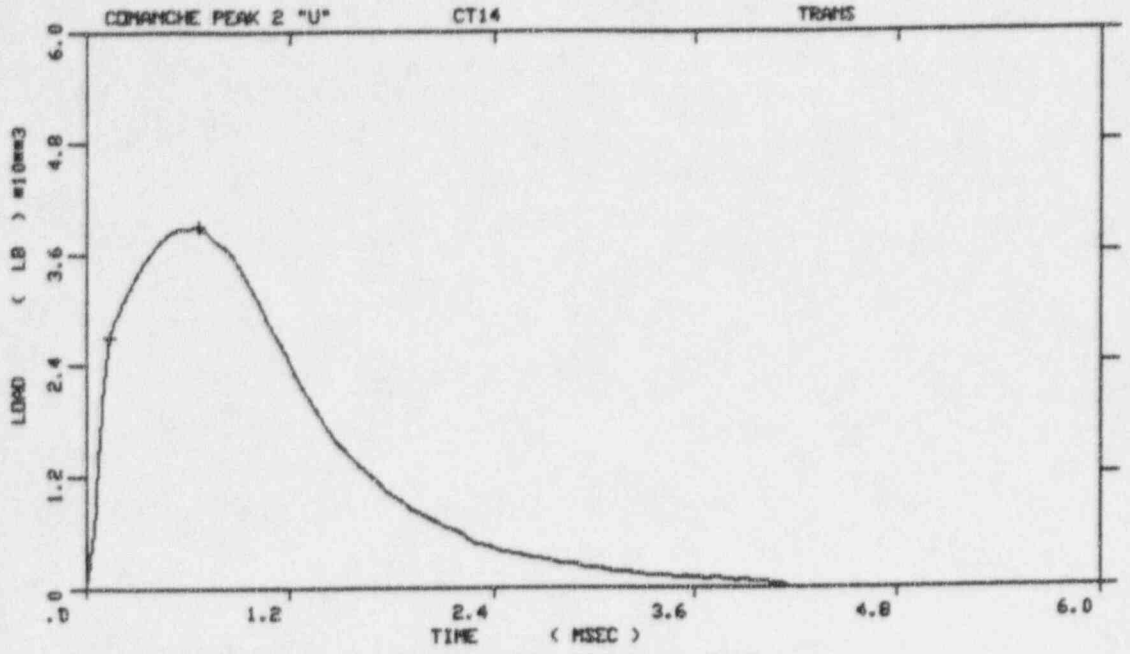

COMANCHE PEAK 2 "U"

SPECIMEN NUMBER :CT14
MATERIAL :TRANS
CAPSULE :COMANCHE PEAK 2
:"U" CAPSULE

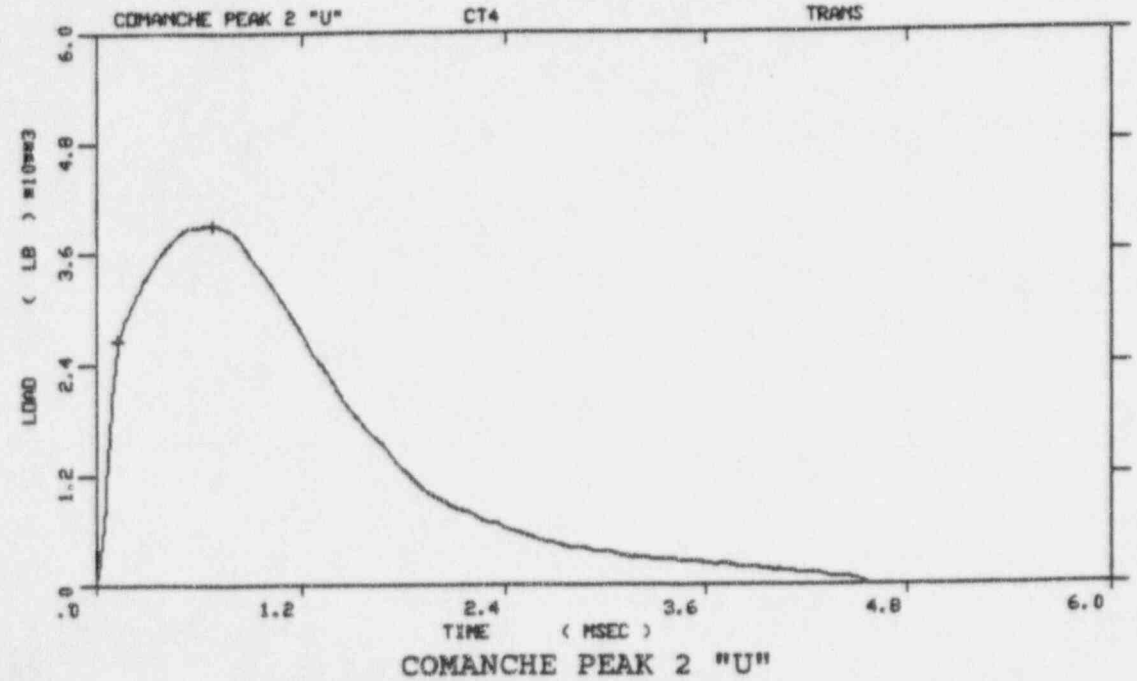

COMANCHE PEAK 2 "U"

SPECIMEN NUMBER :CT4
MATERIAL :TRANS
CAPSULE :COMANCHE PEAK 2
:"U" CAPSULE

Figure A-16. Load-time records for Specimens CT14 (250°F) and CT4 (300°F).

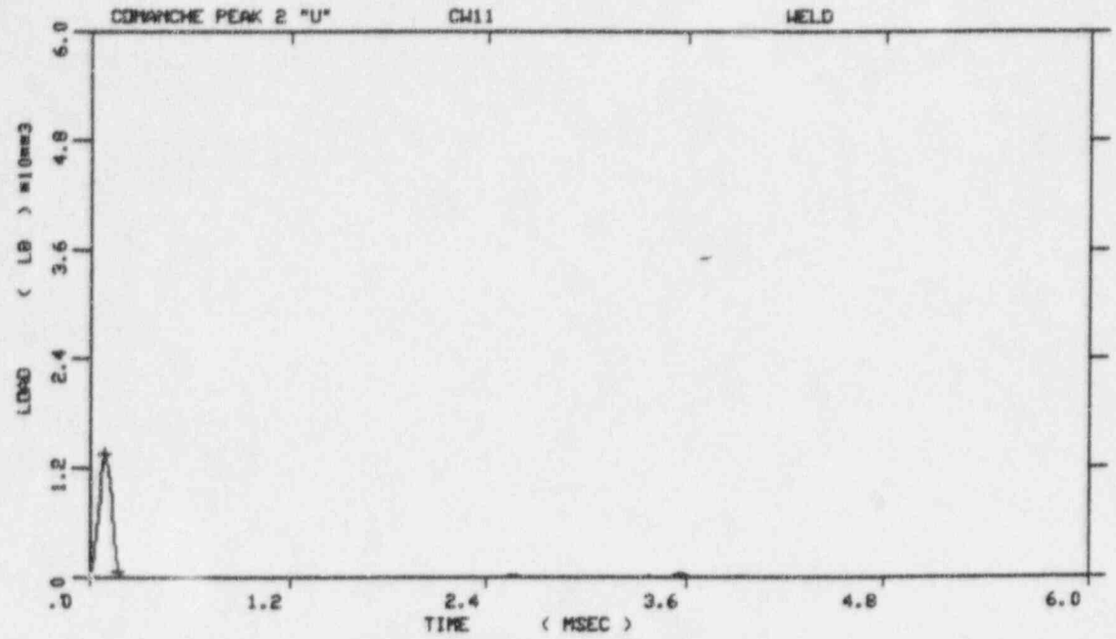

COMANCHE PEAK 2 "U"
SPECIMEN NUMBER :CW11
MATERIAL :WELD
CAPSULE :COMANCHE PEAK 2
:"U" CAPSULE

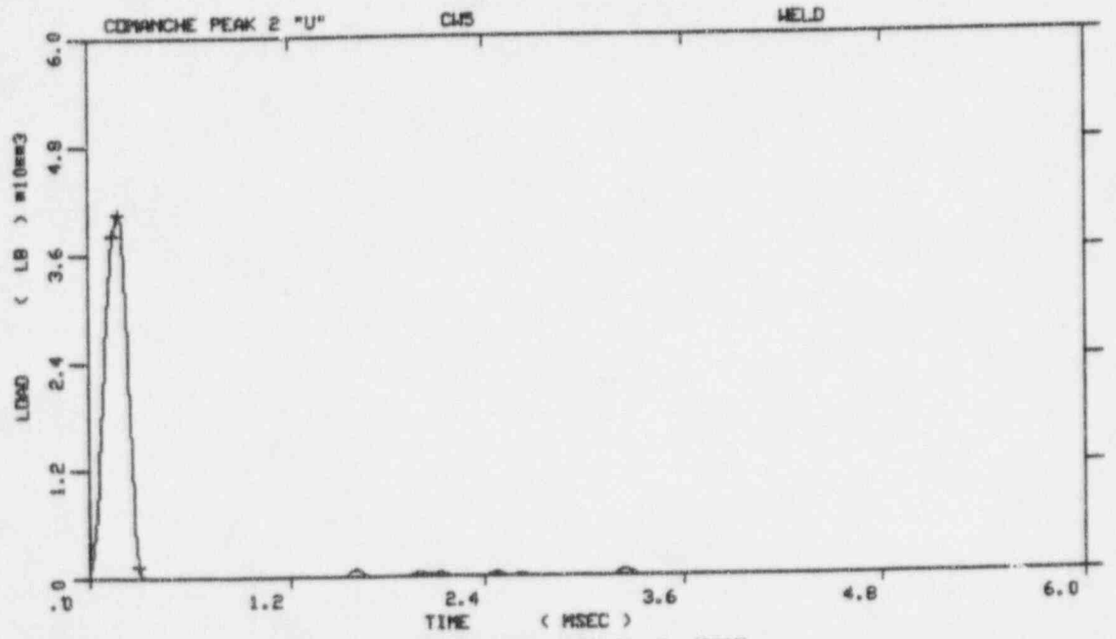

COMANCHE PEAK 2 "U"
SPECIMEN NUMBER :CW5
MATERIAL :WELD
CAPSULE :COMANCHE PEAK 2
:"U" CAPSULE

Figure A-17. Load-time records for Specimens CW11 (-125°F) and CW5 (-95°F).

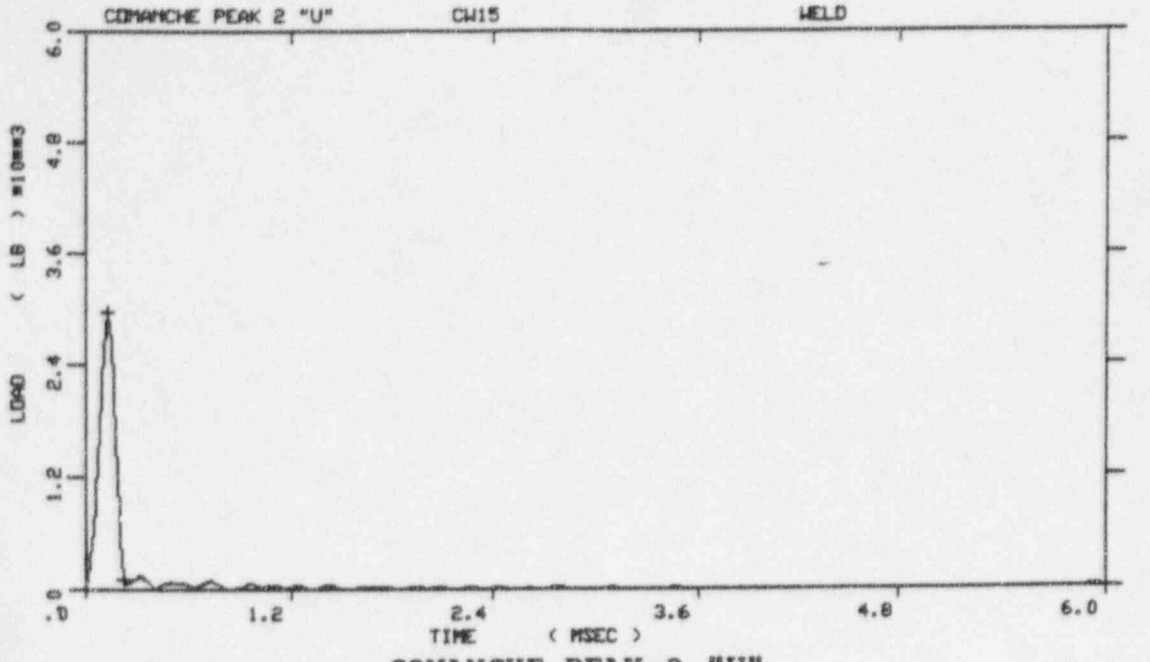

COMANCHE PEAK 2 "U"
SPECIMEN NUMBER :CW15
MATERIAL :WELD
CAPSULE :COMANCHE PEAK 2
:"U" CAPSULE

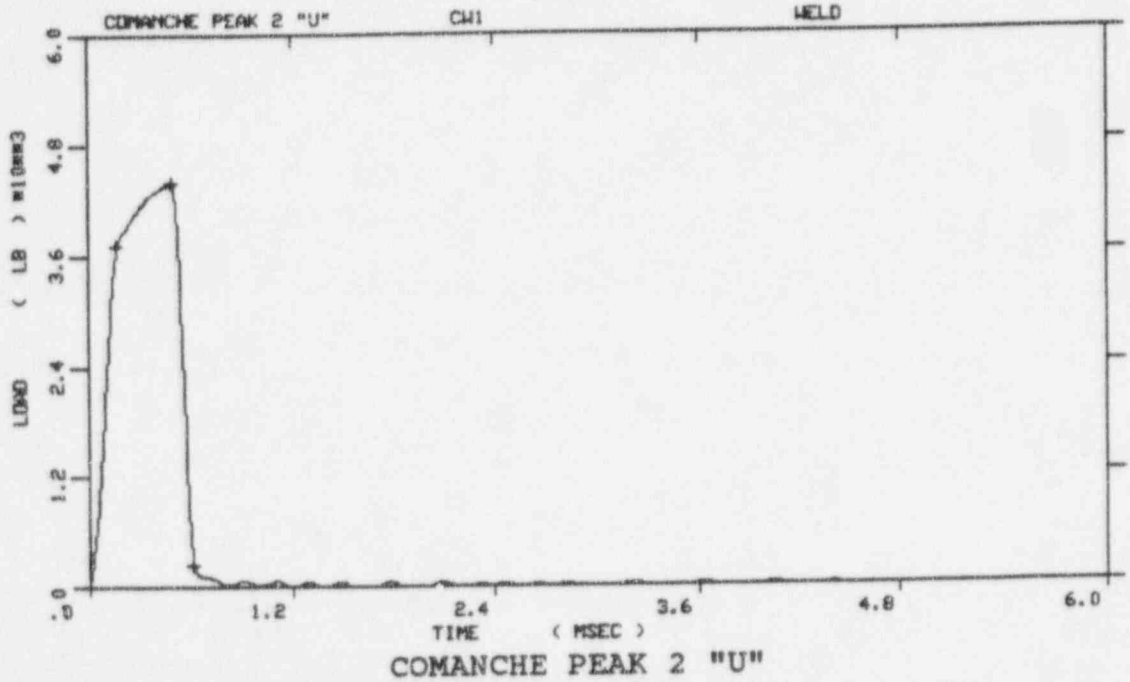

COMANCHE PEAK 2 "U"
SPECIMEN NUMBER :CW1
MATERIAL :WELD
CAPSULE :COMANCHE PEAK 2
:"U" CAPSULE

Figure A-18. Load-time records for Specimens CW15 (-75°F) and CW1 (-60°F).

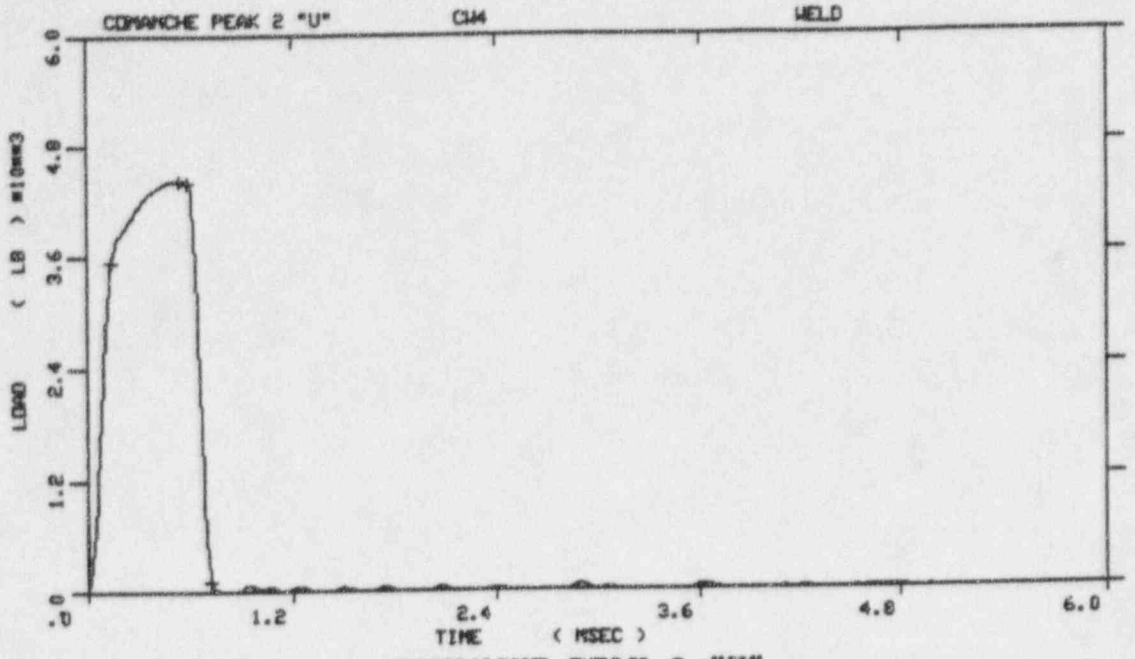

COMANCHE PEAK 2 "U"

SPECIMEN NUMBER :CW4
MATERIAL :WELD
CAPSULE :COMANCHE PEAK 2
:"U" CAPSULE

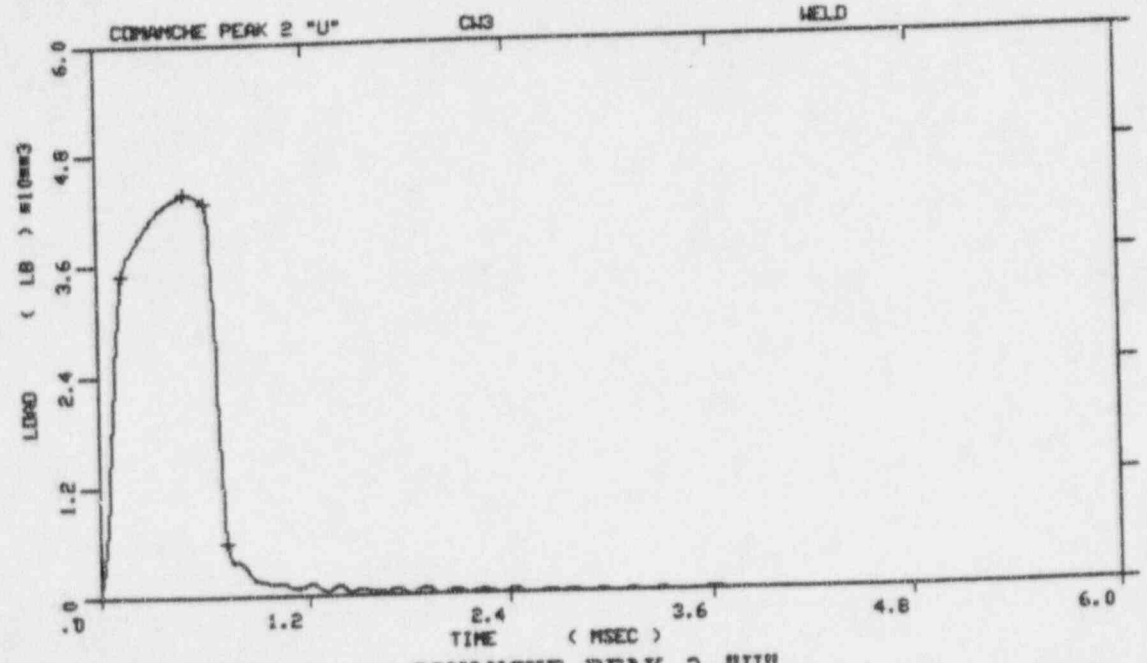

COMANCHE PEAK 2 "U"

SPECIMEN NUMBER :CW3
MATERIAL :WELD
CAPSULE :COMANCHE PEAK 2
:"U" CAPSULE

Figure A-19. Load-time records for Specimens CW4 (-50°F) and CW3 (-25°F).

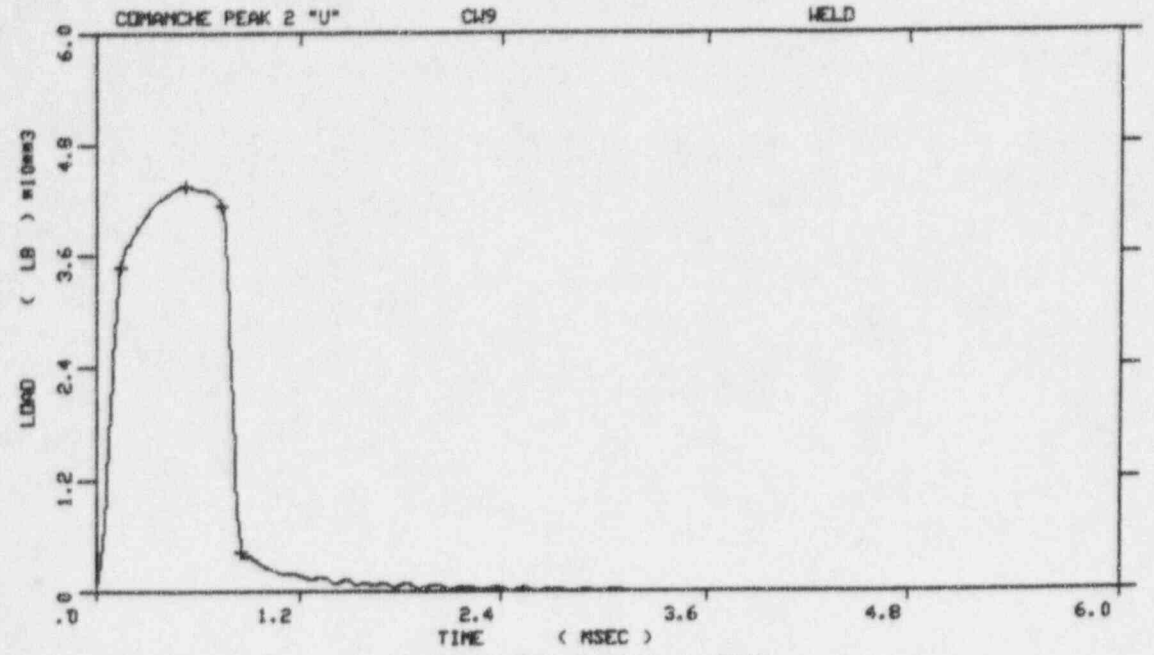

COMANCHE PEAK 2 "U"

SPECIMEN NUMBER :CW9
MATERIAL :WELD
CAPSULE :COMANCHE PEAK 2
:"U" CAPSULE

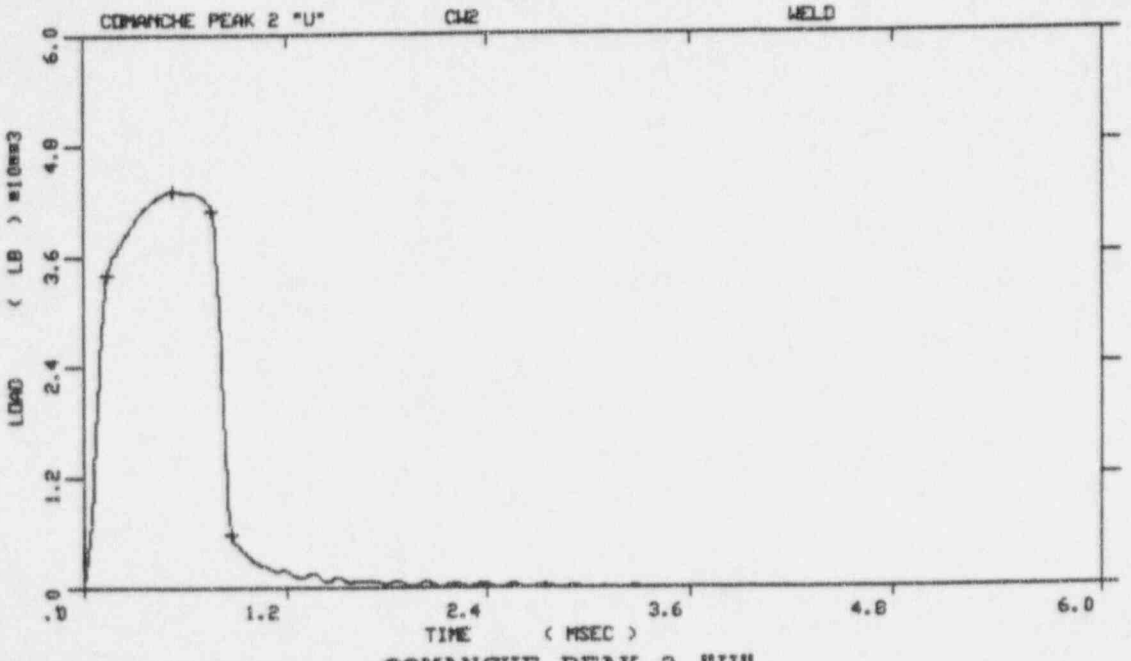

COMANCHE PEAK 2 "U"

SPECIMEN NUMBER :CW2
MATERIAL :WELD
CAPSULE :COMANCHE PEAK 2
:"U" CAPSULE

Figure A-20. Load-time records for Specimens CW9 (-10°F) and CW2 (0°F).

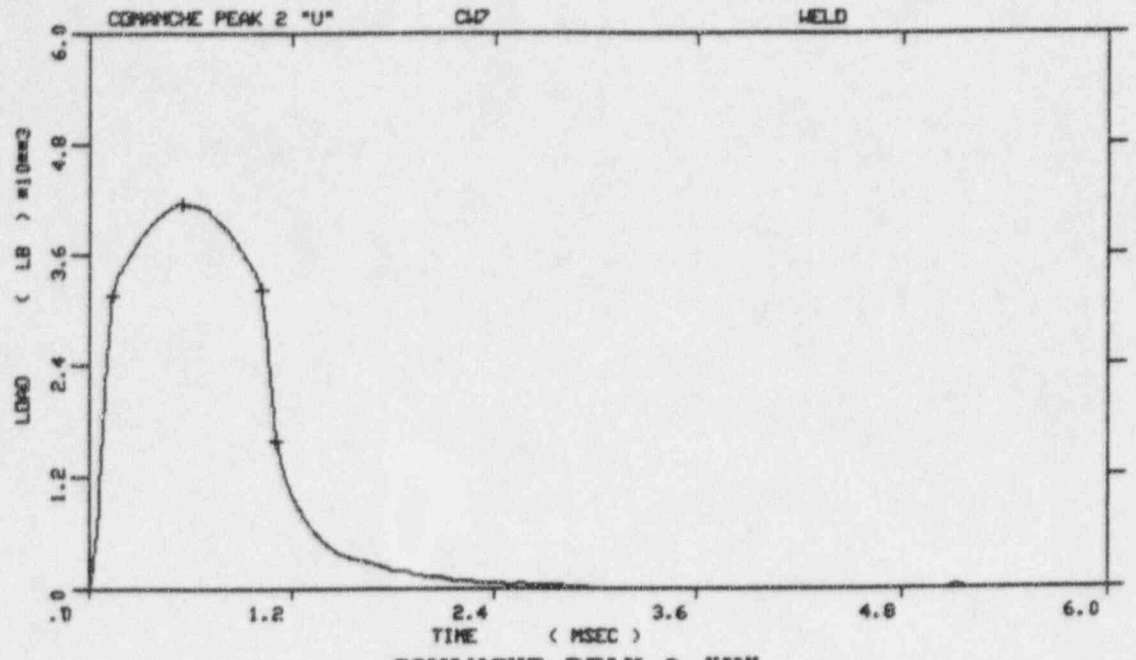

COMANCHE PEAK 2 "U"
SPECIMEN NUMBER :CW7
MATERIAL :WELD
CAPSULE :COMANCHE PEAK 2
:"U" CAPSULE

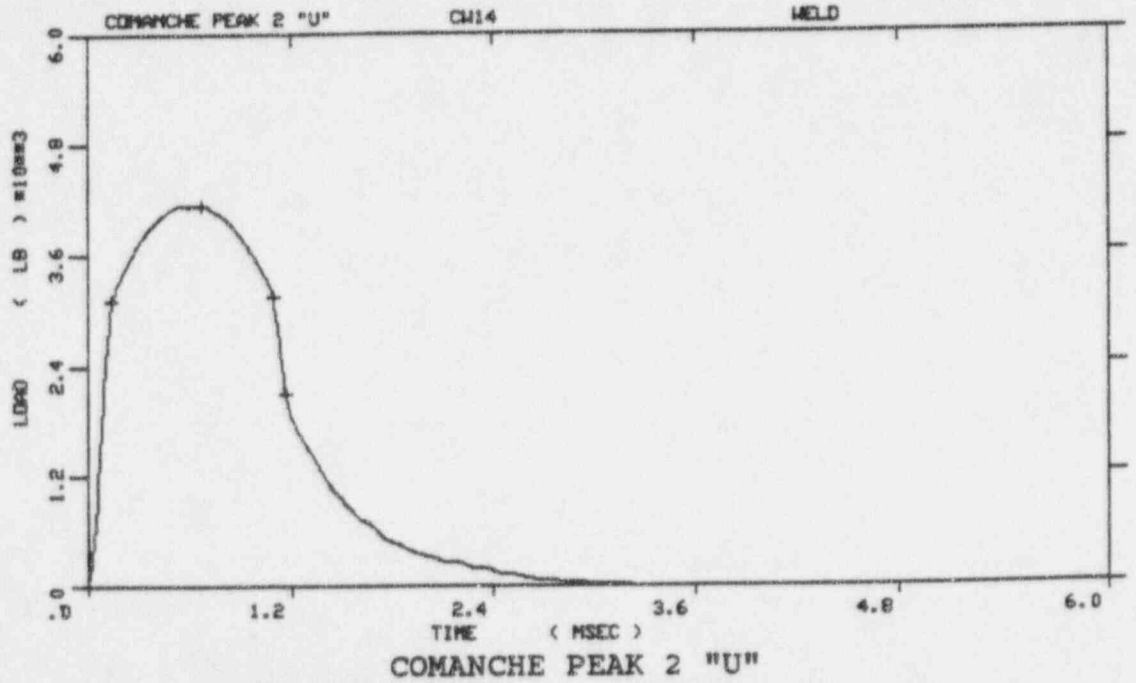

COMANCHE PEAK 2 "U"
SPECIMEN NUMBER :CW14
MATERIAL :WELD
CAPSULE :COMANCHE PEAK 2
:"U" CAPSULE

Figure A-21. Load-time records for Specimens CW7 (50°F) and CW14 (72°F).

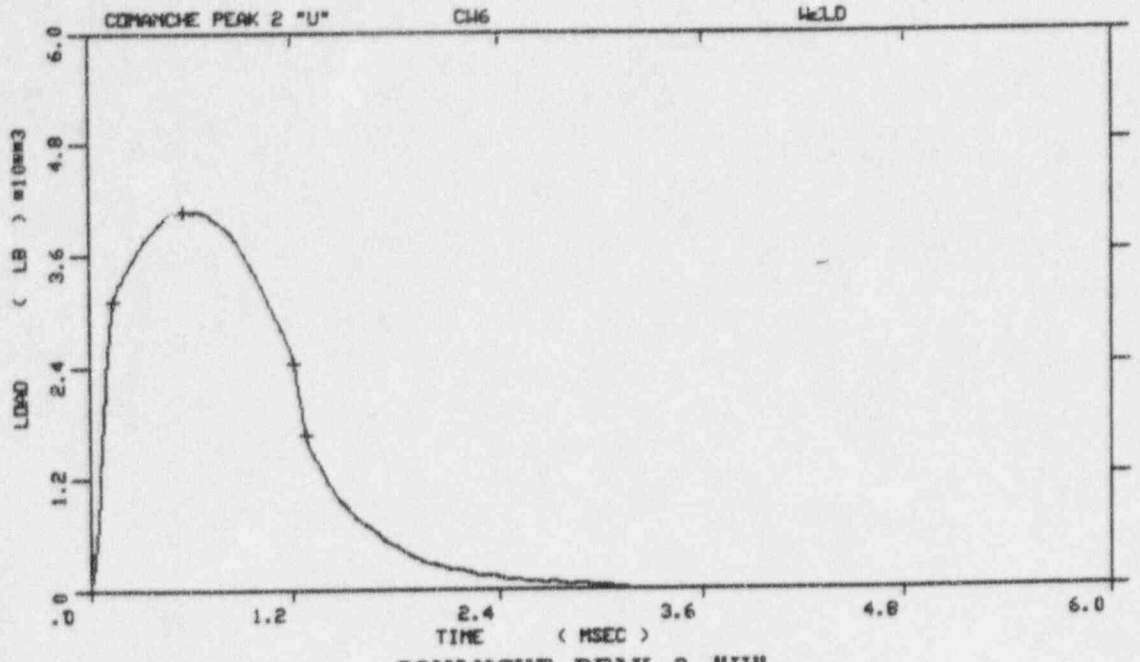

COMANCHE PEAK 2 "U"

SPECIMEN NUMBER :CW6
MATERIAL :WELD
CAPSULE :COMANCHE PEAK 2
:"U" CAPSULE

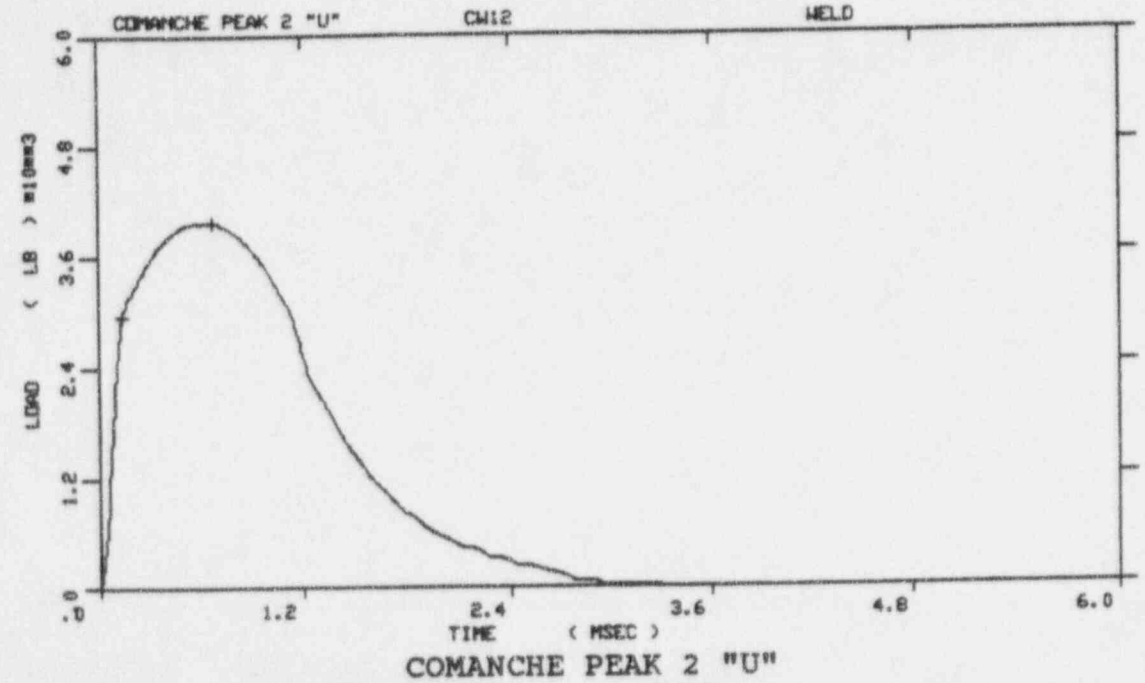

COMANCHE PEAK 2 "U"

SPECIMEN NUMBER :CW12
MATERIAL :WELD
CAPSULE :COMANCHE PEAK 2
:"U" CAPSULE

Figure A-22. Load-time records for Specimens CW6 (100°F) and CW12 (150°F).

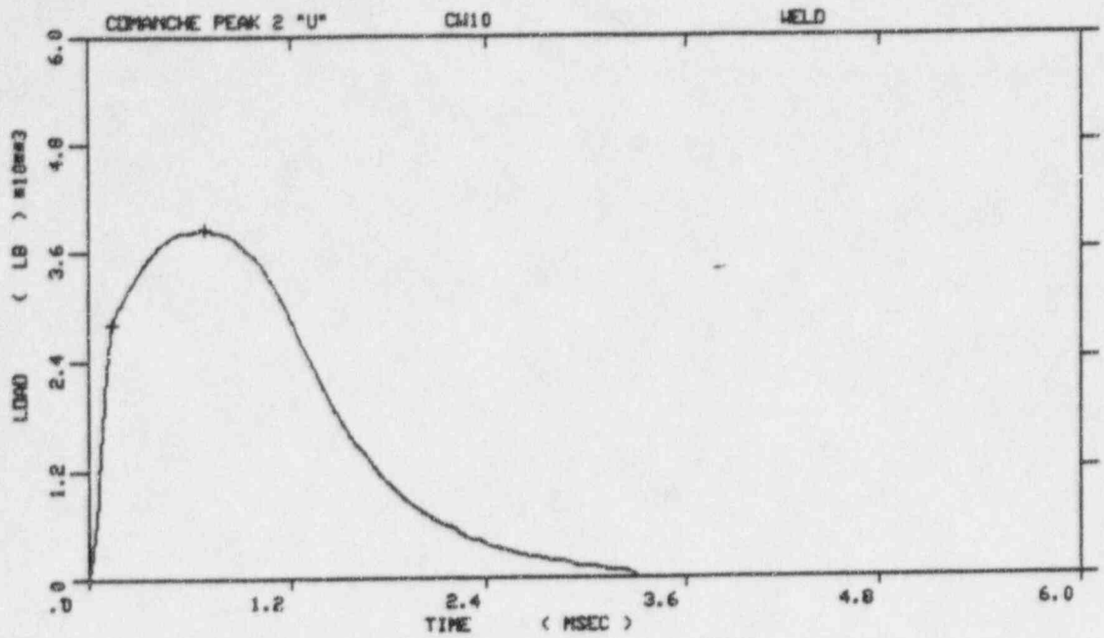

COMANCHE PEAK 2 "U"
SPECIMEN NUMBER :CW10
MATERIAL :WELD
CAPSULE :COMANCHE PEAK 2
:"U" CAPSULE

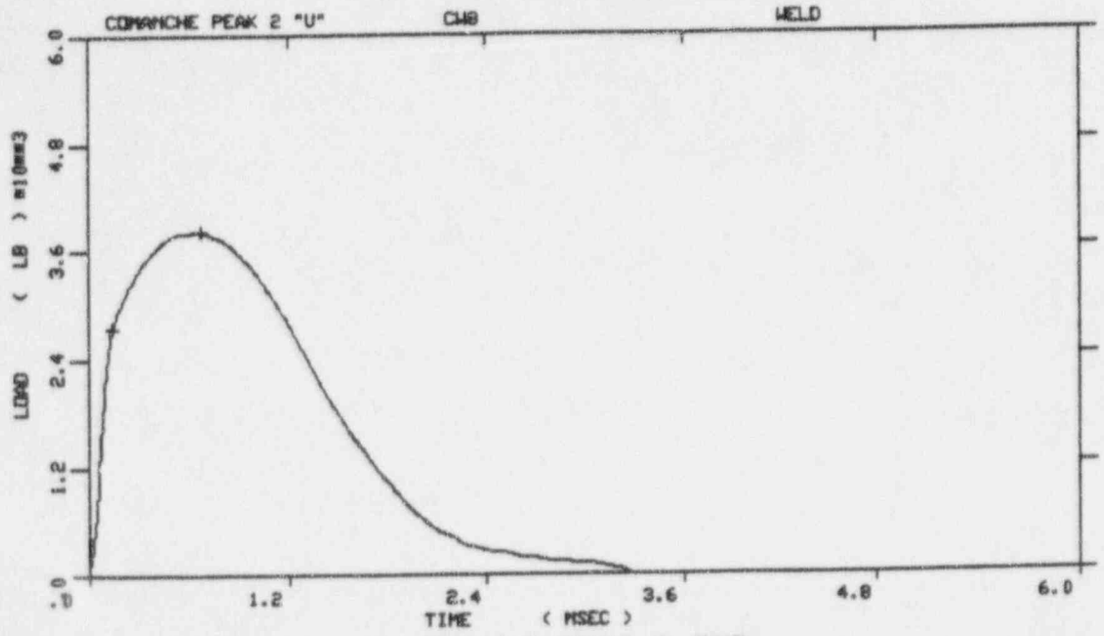

COMANCHE PEAK 2 "U"
SPECIMEN NUMBER :CW8
MATERIAL :WELD
CAPSULE :COMANCHE PEAK 2
:"U" CAPSULE

Figure A-23. Load-time records for Specimens CW10 (200°F) and CW8 (250°F).

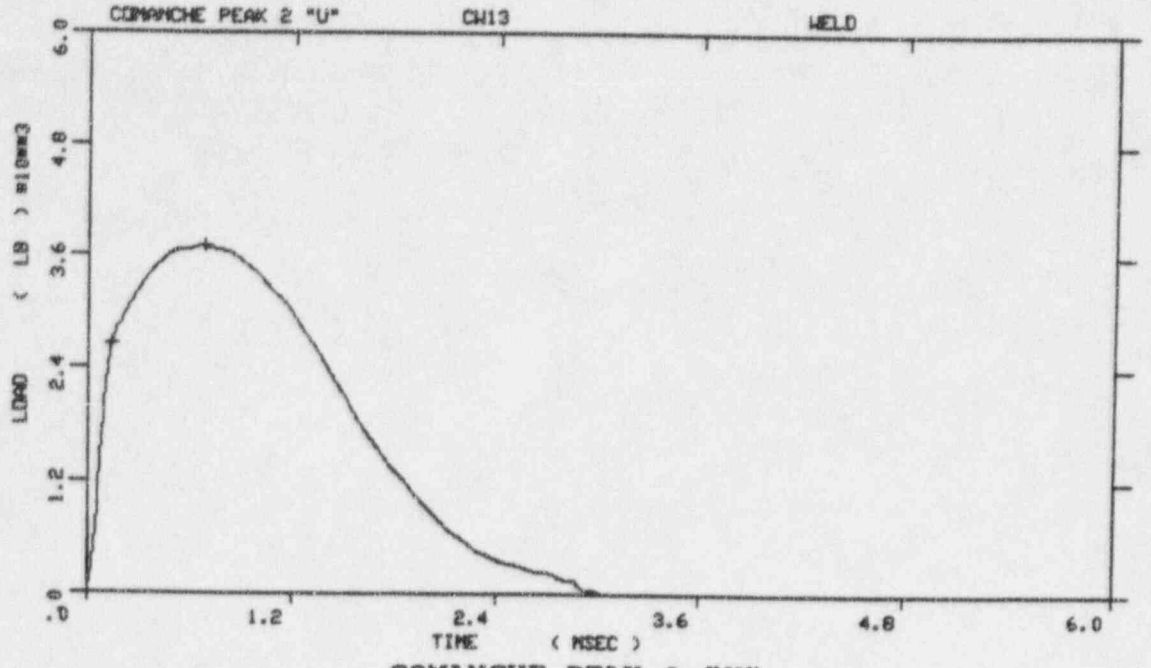

COMANCHE PEAK 2 "U"
SPECIMEN NUMBER :CW13
MATERIAL :WELD
CAPSULE :COMANCHE PEAK 2
:"U" CAPSULE

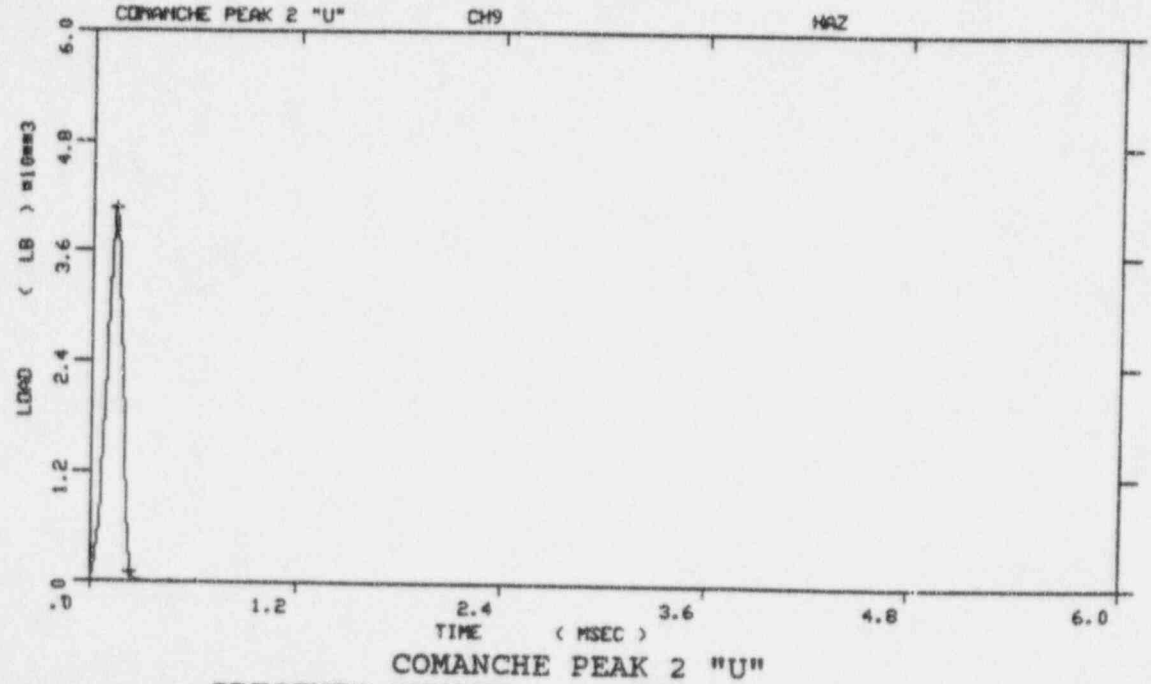

COMANCHE PEAK 2 "U"
SPECIMEN NUMBER :CH9
MATERIAL :HAZ
CAPSULE :COMANCHE PEAK 2
:"U" CAPSULE

Figure A-24. Load-time records for Specimens CW13 (300°F) and CH9 (-225°F).

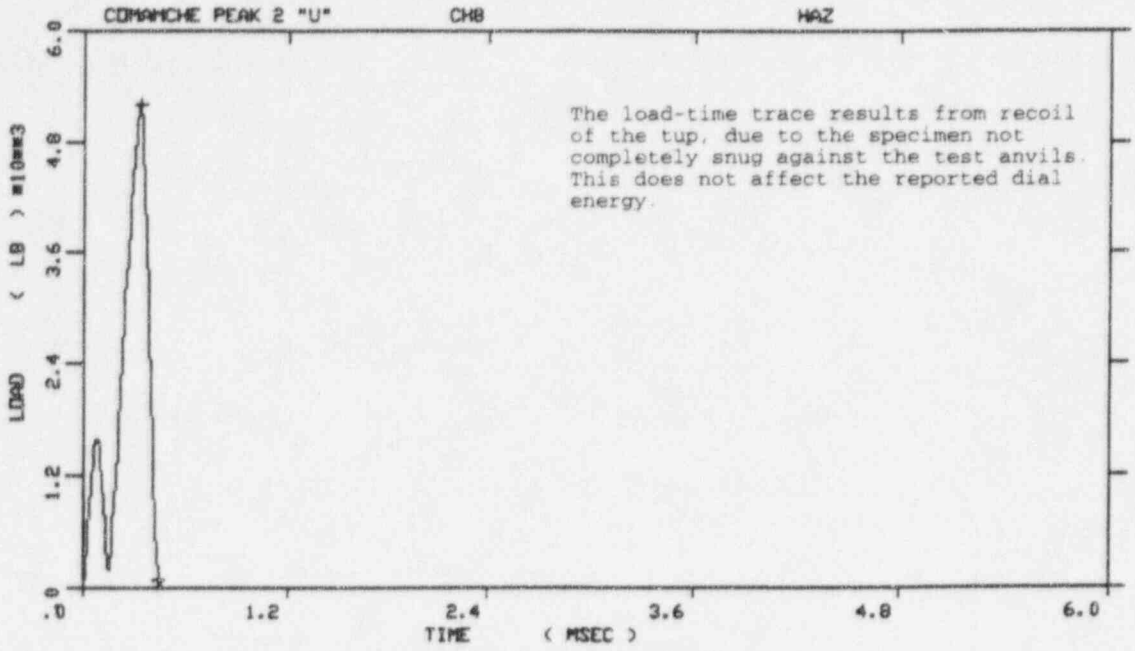

COMANCHE PEAK 2 "U"
SPECIMEN NUMBER :CH8
MATERIAL :HAZ
CAPSULE :COMANCHE PEAK 2
:"U" CAPSULE

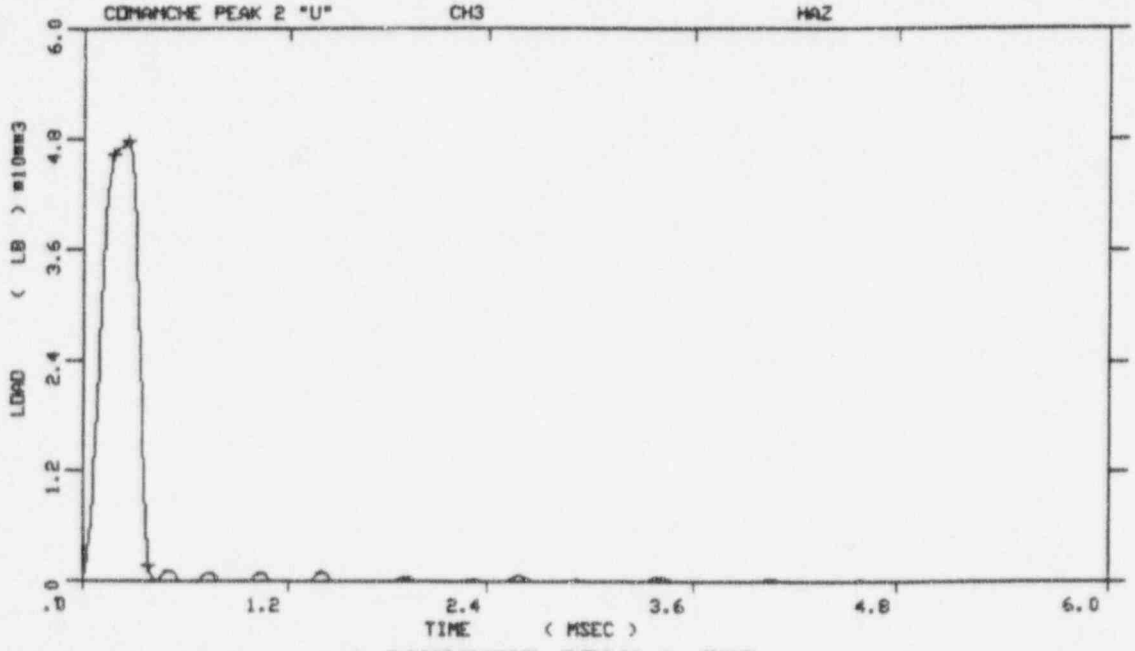

COMANCHE PEAK 2 "U"
SPECIMEN NUMBER :CH3
MATERIAL :HAZ
CAPSULE :COMANCHE PEAK 2
:"U" CAPSULE

Figure A-25. Load-time records for Specimens CH8 (-175°F) and CH3 (-150°F).

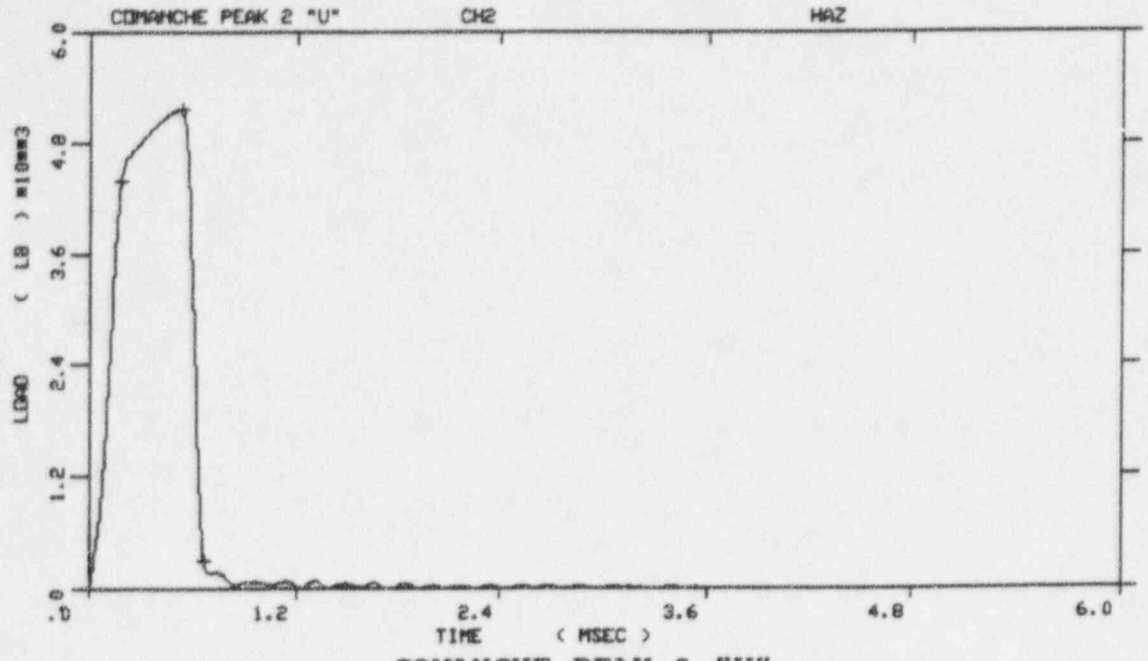

COMANCHE PEAK 2 "U"
SPECIMEN NUMBER :CH2
MATERIAL :HAZ
CAPSULE :COMANCHE PEAK 2
:"U" CAPSULE

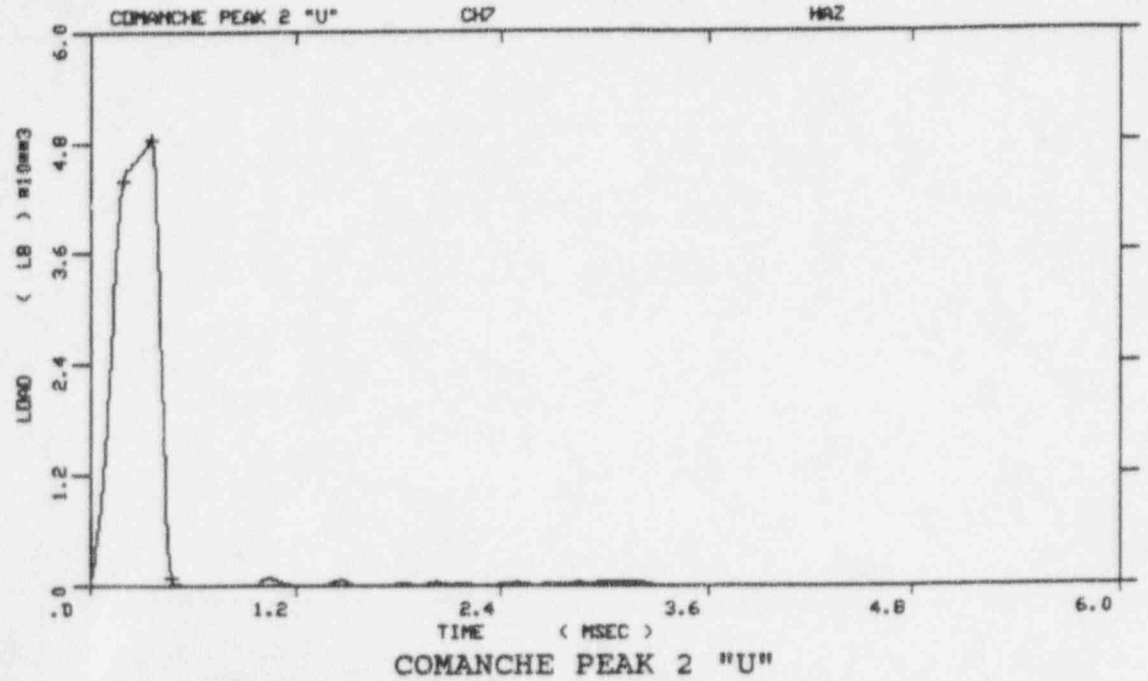

COMANCHE PEAK 2 "U"
SPECIMEN NUMBER :CH7
MATERIAL :HAZ
CAPSULE :COMANCHE PEAK 2
:"U" CAPSULE

Figure A-26. Load-time records for Specimens CH2 (-125°F) and CH7 (-100°F).

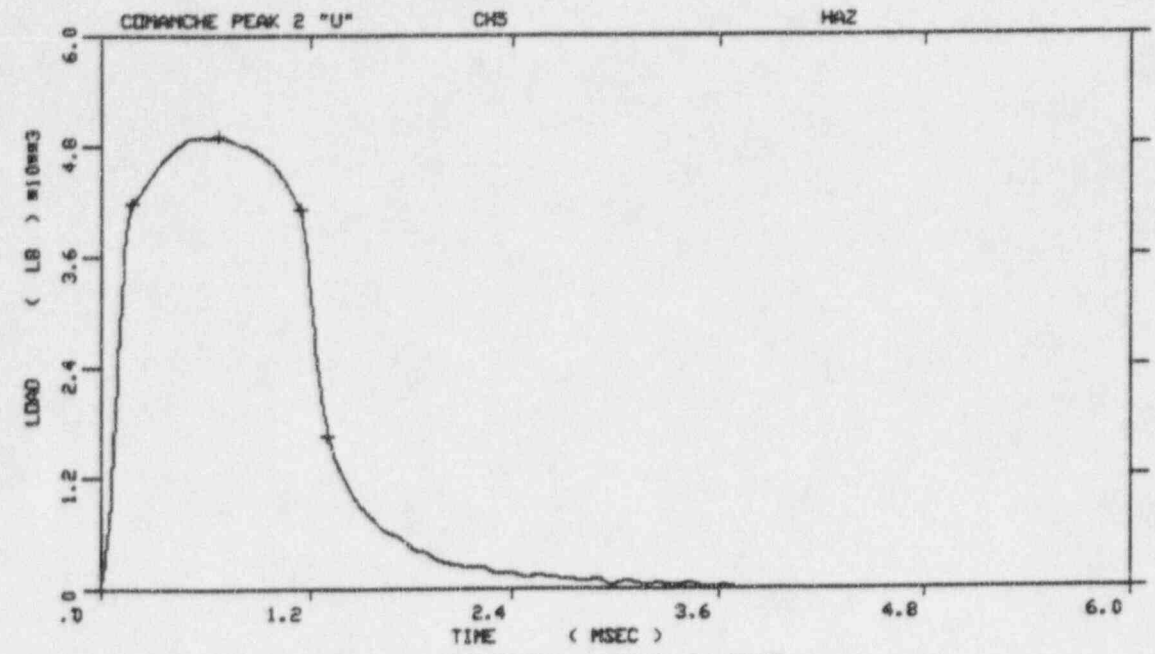

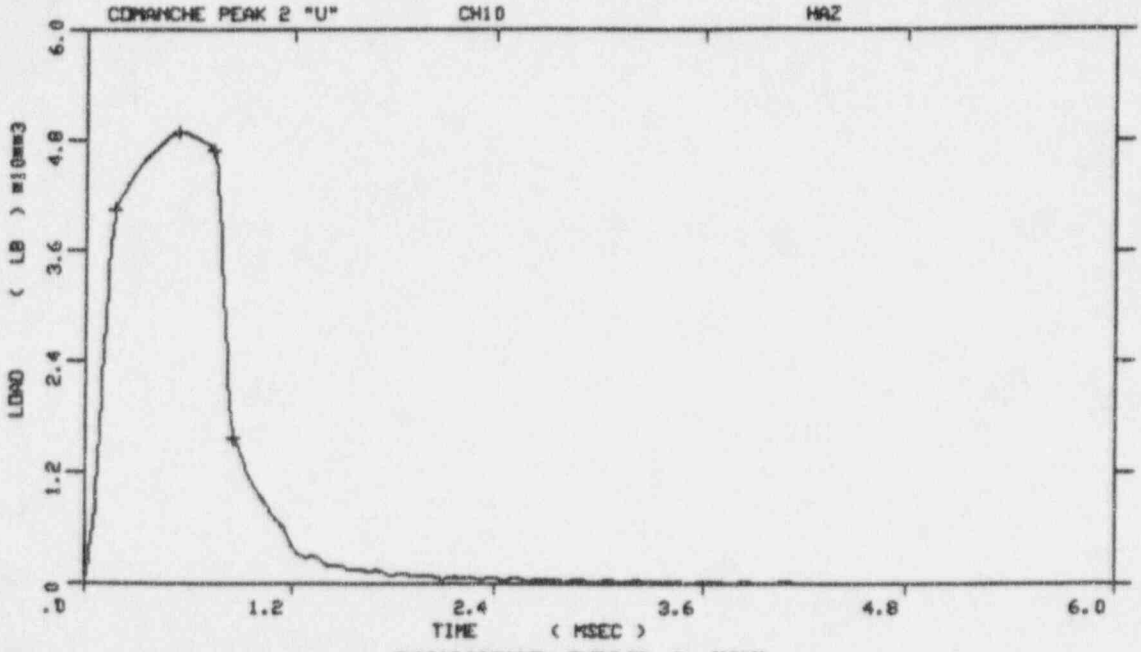

Figure A-27. Load-time records for Specimens CH5 (-75°F) and CH10 (-60°F).

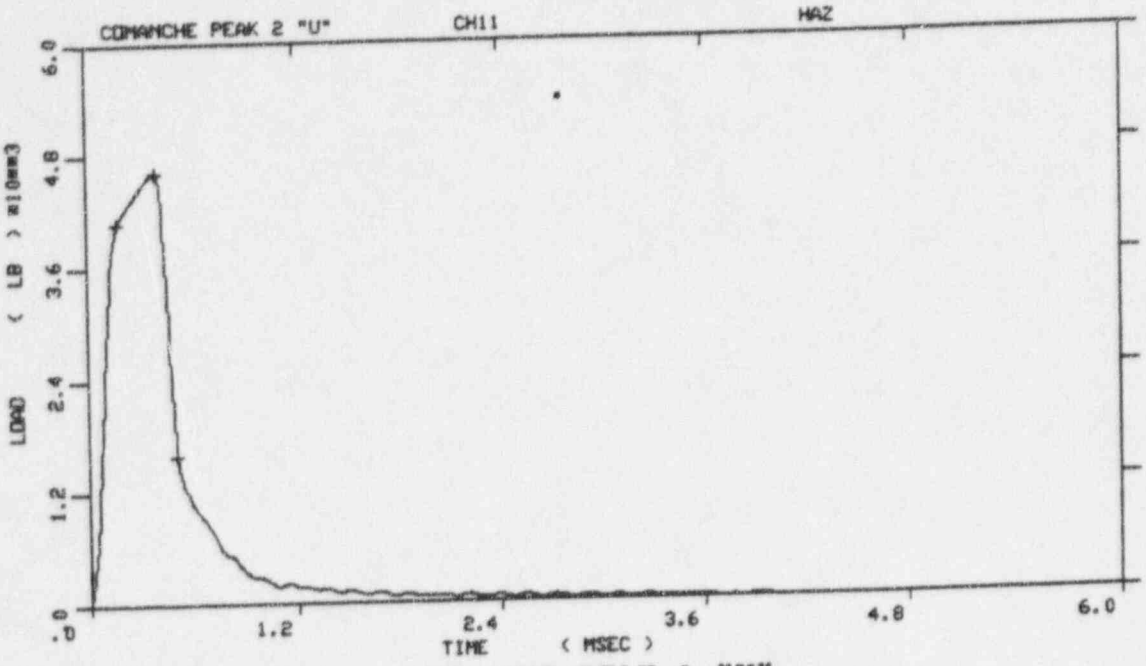

COMANCHE PEAK 2 "U"

SPECIMEN NUMBER :CH11
MATERIAL :HAZ
CAPSULE :COMANCHE PEAK 2
:"U" CAPSULE

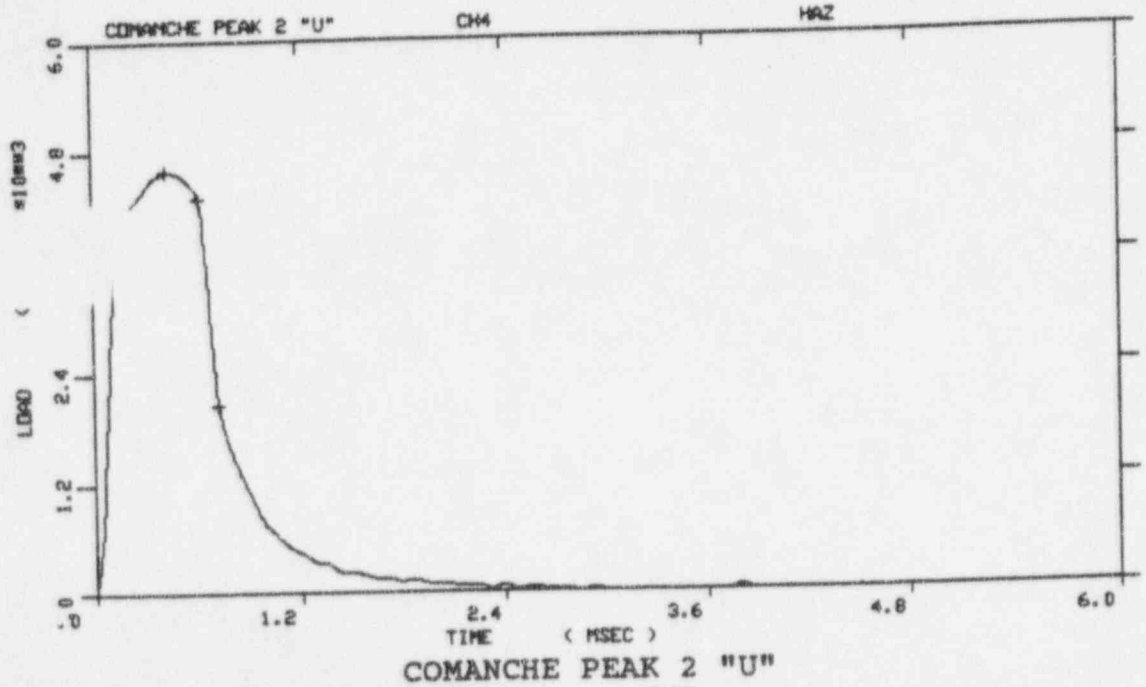

COMANCHE PEAK 2 "U"

SPECIMEN NUMBER :CH4
MATERIAL :HAZ
CAPSULE :COMANCHE PEAK 2
:"U" CAPSULE

Figure A-28. Load-time records for Specimens CH11 (-50°F) and CH4 (-25°F).

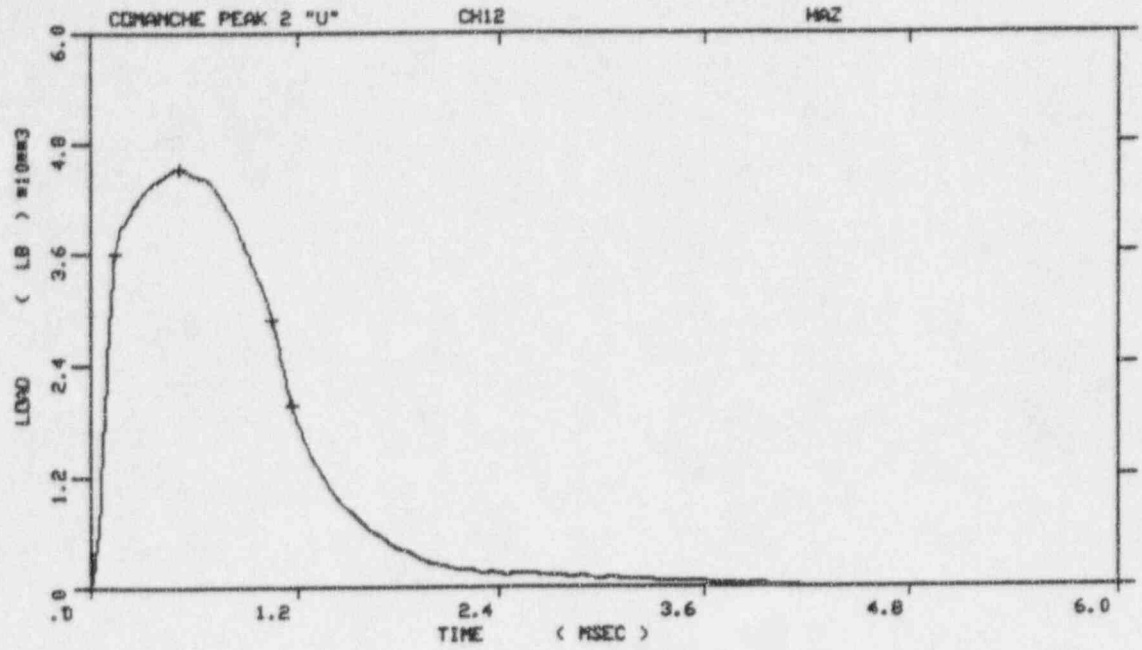

COMANCHE PEAK 2 "U"

SPECIMEN NUMBER :CH12
MATERIAL :HAZ
CAPSULE :COMANCHE PEAK 2
:"U" CAPSULE

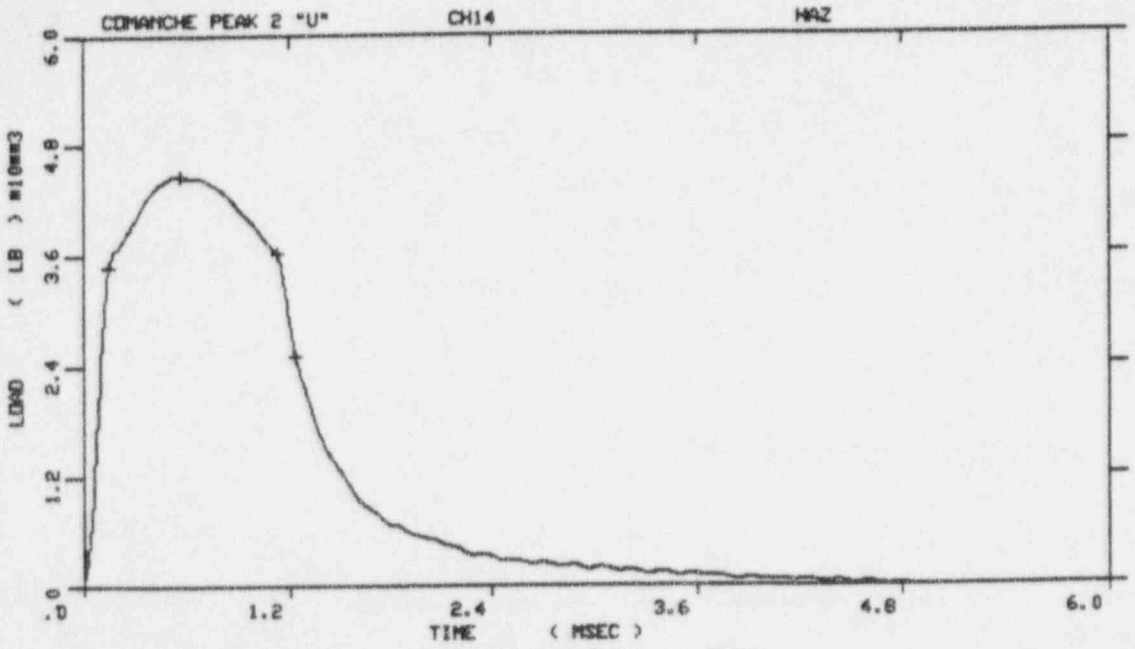

COMANCHE PEAK 2 "U"

SPECIMEN NUMBER :CH14
MATERIAL :HAZ
CAPSULE :COMANCHE PEAK 2
:"U" CAPSULE

Figure A-29. Load-time records for Specimens CH12 (0°F) and CH14 (25°F).

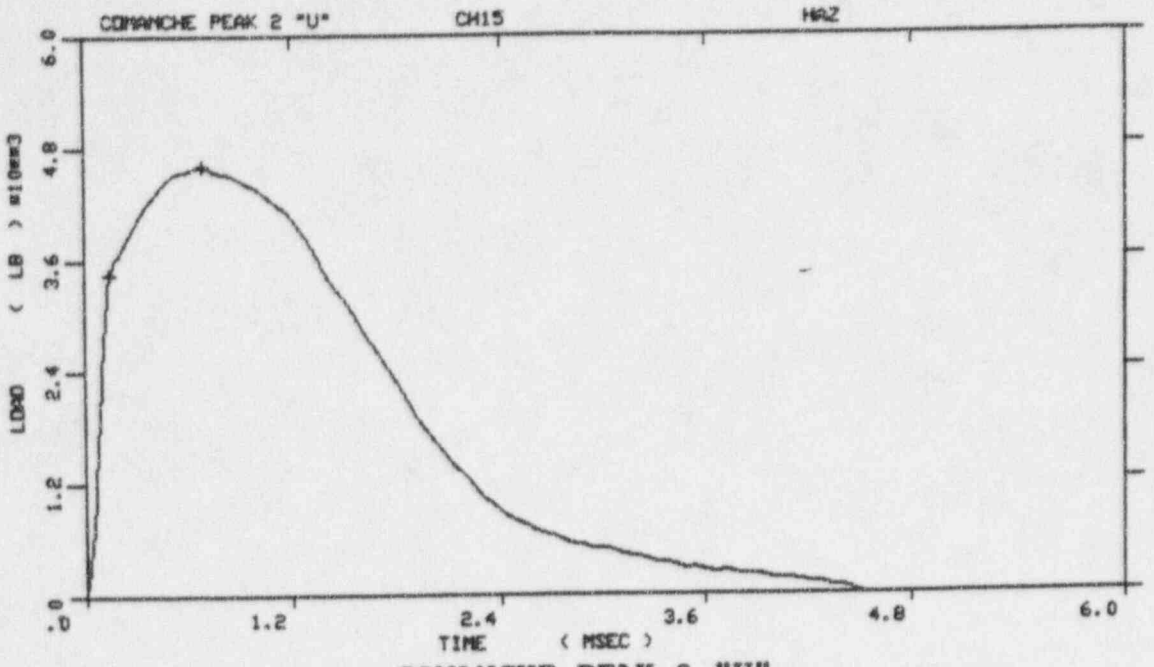

COMANCHE PEAK 2 "U"

SPECIMEN NUMBER :CH15
MATERIAL :HAZ
CAPSULE :COMANCHE PEAK 2
:"U" CAPSULE

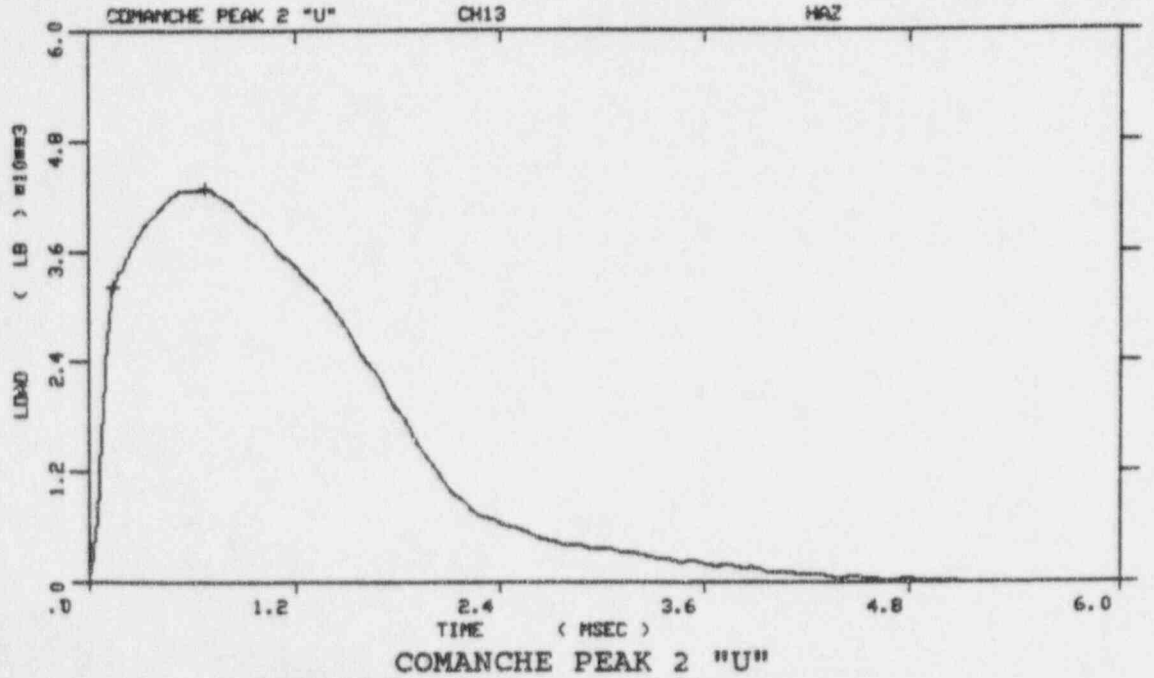

COMANCHE PEAK 2 "U"

SPECIMEN NUMBER :CH13
MATERIAL :HAZ
CAPSULE :COMANCHE PEAK 2
:"U" CAPSULE

Figure A-30. Load-time records for Specimens CH15 (72°F) and CH13 (150°F).

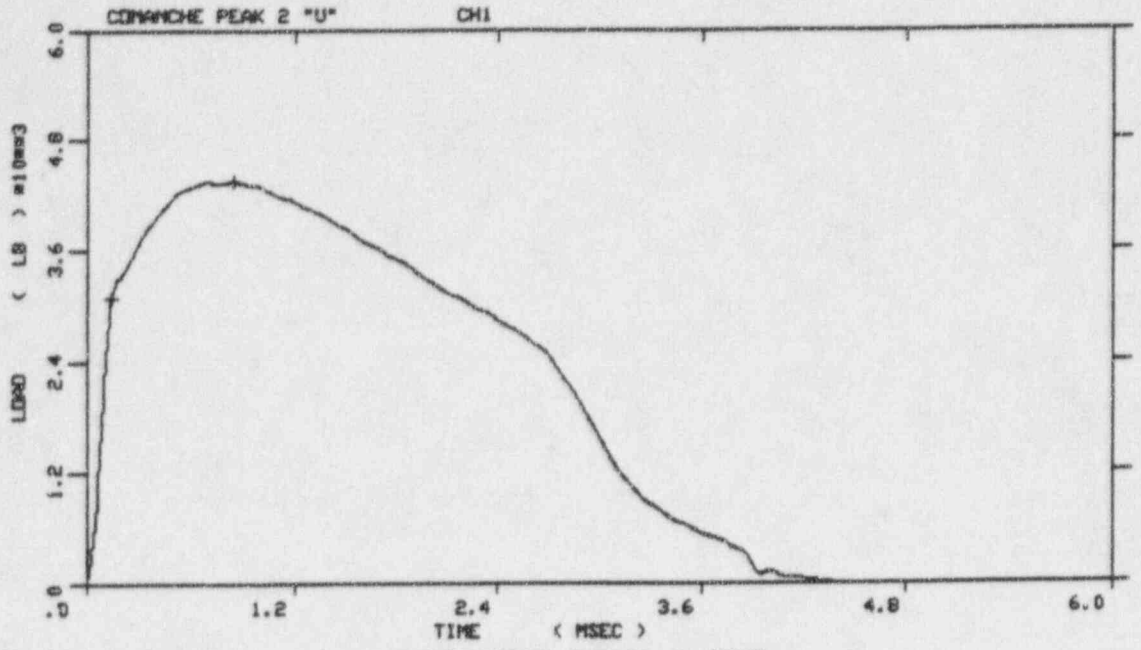

COMANCHE PEAK 2 "U"

SPECIMEN NUMBER :CH1
MATERIAL :HAZ
CAPSULE :COMANCHE PEAK 2
:"U" CAPSULE

Specimen Alignment Error - Data is not valid.

Figure A-31. Load-time records for Specimens CH1 (200°F) and CH6 (200°F).

Enclosure 2 to TXX-95243

EVALUATION OF PRESSURIZED THERMAL SHOCK FOR THE COMANCHE PEAK STEAM ELECTRIC STATION (CPSES) UNIT 2

July 1995